

Double trouble: Predicting new variant counts across two heterogeneous populations

Yunyi Shen ^{*} Lorenzo Masoero [†] Joshua G. Schraiber [‡]
Tamara Broderick [§]

March 5, 2024

Abstract

Collecting genomics data across multiple heterogeneous populations (e.g., across different cancer types) has the potential to improve our understanding of disease. Despite sequencing advances, though, resources often remain a constraint when gathering data. So it would be useful for experimental design if experimenters with access to a pilot study could predict the number of new variants they might expect to find in a follow-up study: both the number of new variants shared between the populations and the total across the populations. While many authors have developed prediction methods for the single-population case, we show that these predictions can fare poorly across multiple populations that are heterogeneous. We prove that, surprisingly, a natural extension of a state-of-the-art single-population predictor to multiple populations fails for fundamental reasons. We provide the first predictor for the number of new shared variants and new total variants that can handle heterogeneity in multiple populations. We show that our proposed method works well empirically using real cancer and population genetics data.

^{*}EECS, MIT, yshen99@mit.edu

[†]EECS, MIT, lom@mit.edu

[‡]Department of Quantitative and Computational Biology, USC, schraibe@usc.edu

[§]EECS, MIT, tbroderick@mit.edu

1 Introduction

The genomic revolution has fundamentally changed our understanding of human history (Green et al., 2010; Gravel et al., 2011; Tennessen et al., 2012; Lazaridis et al., 2014; Haak et al., 2015), the genetics of complex disease (Lek et al., 2016; Karczewski et al., 2020; Wang et al., 2021; Backman et al., 2021; Chen et al., 2023), and the development of cancer (The Cancer Genome Atlas Research Network, 2008; The Cancer Genome Atlas Research Network et al., 2013; Kandoth et al., 2013; Jayasinghe et al., 2018; Hoadley et al., 2018; Huang et al., 2018). As more and more sequencing data is gathered, novel variants continue to be discovered (Lek et al., 2016; Karczewski et al., 2020) and yield a deeper insight into the evolutionary processes that have shaped the observed patterns of genetic variation (Agarwal and Przeworski, 2021; Agarwal et al., 2023). Moreover, rare variants, which are typically detected in large samples, have become increasingly important in understanding the etiology of disease and are a key tool in development of novel therapeutics against common disease (Szustakowski et al., 2021).

Most studies of genetic variation sample from two or more groups that may share some portion of their variation, such as different human populations or different tumor types. For instance, sampling from multiple human populations is essential for discovering more variants (Karczewski et al., 2020; Chen et al., 2023) and is crucial to expanding equity and inclusion in genomic medicine (Popejoy and Fullerton, 2016; Hindorff et al., 2018; Fatumo et al., 2022). Due to the shared evolutionary history of all humans, in this setting many common variants will be shared between populations (Biddanda et al., 2020), but differences in allele frequency between populations are key to understanding adaptation (Novembre and Di Rienzo, 2009) and disease (Fu et al., 2011; Assimes et al., 2021; Roselli et al., 2018). Similarly, when collecting disease case and control samples to examine the enrichment of rare variants in cases, the vast majority of the variants will be shared. Rare variants shared across different type of diseases have drawn attention since they may be linked to common genetic bases of different diseases (Rafnar et al., 2009; Bojesen et al., 2013; Rashkin et al., 2020). On the other hand, most variation between tumors in different individuals will be private, but shared variation between tumors across samples may point to the genetic basis of cancer, and thus paths toward novel treatments (Project, 2014; Ma et al., 2015; Prior et al., 2020; Pirozzi and Yan, 2021).

Despite large decreases in the cost of sequencing (Christensen et al., 2015; Park and Kim, 2016; Schwarze et al., 2018), detecting novel variants still requires a large enough set of

samples to benefit from careful planning. This is especially true when attempting to expand our catalogue of variation across diverse human groups, because some of the most diverse human groups have been studied the least (Popejoy and Fullerton, 2016). It would therefore be of significant practical utility to have a reliable and data-informed planning method; namely, a prediction method should accurately estimate the number of novel variants in a new (follow-up) study of multiple populations, given data from a typically small, previous (pilot) study. Moreover, prediction of the number of shared or private variants seen in a follow-up study can be useful as a null model for identifying “unusual” variants or classes of variants that may indicate their role in biologically interesting processes, such as adaptation or disease. In all of these cases, it is crucial to account for novel variants that are shared between groups as opposed to those that are private to a single group.

Several researchers have developed approaches to predict the number of new variants that will be detected in a follow-up sequencing study, given information from a pilot study (Camerlenghi et al., 2022; Masoero et al., 2022; Chakraborty et al., 2019; Zou et al., 2016; Gravel and National Heart Lung & Blood Institute (NHLBI) GO Exome Sequencing Project, 2014; Ionita-Laza et al., 2009). However, all of these methods assume samples are from a single population. So these methods cannot be used directly to predict the number of new shared variants across different populations in a follow-up study. And because these methods do not model the possibility of shared variants between groups, single-population approaches can be expected to misestimate the number of novel variants in a follow-up study.

In this work, we develop an approach to predict the number of novel variants discovered in samples from multiple populations or groups. We focus on the case of two populations here, although in principle our approach can be extended to more than two. We work in the setting where a pilot study has collected genetic data in each of the two groups, and the experimenter wishes to collect additional data in a larger study. In principle, the variant prediction challenge can be tackled in two ways: (1) one could construct an explicit model of variation within and between groups based on first principles or (2) one could employ a “black box” that is agnostic to the underlying biology. This work, like the single-population approaches referenced above, adopts the latter approach. We hope that, by taking the black-box approach, our method can apply to data that arise from very different processes – ranging across tumor sequencing, case-control studies, population genetics, and other settings.

In the one-population case, Masoero et al. (2022) showed that a Bayesian nonparametric (BNP) approach can deliver strong empirical performance. However, we here prove that

a natural two-population extension to the method of [Masoero et al. \(2022\)](#) fails for fundamental reasons (Section 4). We nonetheless demonstrate how to take advantage of the flexibility of the Bayesian framework (Section 3) to develop a novel two-population BNP model (Section 5) and methodology (Section 6). We provide theory to establish the desirable power-law properties of our model in Section 7. Finally, we use both simulations and analysis of real cancer and population genetic datasets to showcase the accuracy and robustness of our model (Section 8); along the way, we highlight multi-population circumstances where using one-population approaches can be misleading.

2 Problem setup

We consider the case where we have genomic samples from a pilot study conducted in two populations, indexed by $p \in \{1, 2\}$, and are interested to predict variant numbers in a follow-up study. Let N_p be the number of pilot samples from population p ; collect the vector of pilot sample cardinalities in $\mathbf{N} := (N_1, N_2)$. We assume there is a common fixed reference genome for the two populations, and we assume for convenience that each variant is given a unique label; for instance, one might assign a random label, uniform on $[0, 1]$, to a variant upon its discovery. Take the n -th sample in the p -th population; we let $x_{p,n,\ell}$ equal 1 if the variant with label ψ_ℓ is observed in this sample and 0 otherwise. Let $J_{\mathbf{N}}$ denote the (scalar) total number of unique variants observed across the \mathbf{N} samples. Then the following measure will have a mass of size 1 at each variant label where the n -th sample in the p -th population differs from the reference genome:

$$X_{p,n} := \sum_{\ell=1}^{J_{\mathbf{N}}} x_{p,n,\ell} \delta_{\psi_\ell}, \quad (1)$$

where δ_{ψ_ℓ} is a Dirac mass at ψ_ℓ ; that is, $\delta_{\psi_\ell}(\psi)$ equals 1 if $\psi = \psi_\ell$ and 0 otherwise. Equivalently, we might let $x_{p,n,\ell} = 0$ for an imagined countable infinity of possible yet-to-be-observed variants, each assigned a new label ψ_ℓ for $\ell > J_{\mathbf{N}}$; then we have

$$X_{p,n} = \sum_{\ell=1}^{\infty} x_{p,n,\ell} \delta_{\psi_\ell}. \quad (2)$$

To represent the pilot study, we write $1:N_p$ for indices $\{1, \dots, N_p\}$. We can then write $X_{p,1:N_p}$ for the pilot samples in population p . And we let $X_{1,2,1:\mathbf{N}}$ denote the full collection of pilot

samples, across both populations.

Given the pilot study, we would like to predict (1) the total number of new variants in a follow-up study, as well as (2) the number of new variants shared between the populations. To that end, let M_p be the number of new samples from p considered for the follow-up study; collect the vector of follow-up study sample cardinalities in $\mathbf{M} = (M_1, M_2)$. First, then, we are interested in the number of variants that (a) are not present in the first \mathbf{N} pilot samples but (b) are present in at least one of the \mathbf{M} follow-up samples. We call this quantity $U_{\mathbf{N}}^{(\mathbf{M})}$, where the U stands for “unseen,” and write:

$$U_{\mathbf{N}}^{(\mathbf{M})} = \sum_{\ell=1}^{\infty} \left[\prod_{p=1}^2 \mathbf{1} \left(\sum_{n=1}^{N_p} x_{p,n,\ell} = 0 \right) \right] \mathbf{1} \left(\sum_{p=1}^2 \sum_{m=1}^{M_p} x_{p,N_p+m,\ell} > 0 \right). \quad (3)$$

We next consider the number of new variants appearing k_1 times in population 1 and k_2 times in population 2. In a single population, the variants appearing once are often called singletons, the variants appearing twice called doubletons, and so on. Analogously and collecting $\mathbf{k} := (k_1, k_2)$, we will denote the variants appearing \mathbf{k} times across the two populations as *\mathbf{k} -tons*. We can write the number of \mathbf{k} -tons in the follow-up as

$$U_{\mathbf{N}}^{(\mathbf{M}, \mathbf{k})} = \sum_{\ell=1}^{\infty} \left[\prod_{p=1}^2 \mathbf{1} \left(\sum_{n=1}^{N_p} x_{p,n,\ell} = 0 \right) \right] \left[\prod_{p=1}^2 \mathbf{1} \left(\sum_{m=1}^{M_p} x_{p,N_p+m,\ell} = k_p \right) \right]. \quad (4)$$

The total number of new variants appearing in both populations in the follow-up can be found by summing $U_{\mathbf{N}}^{(\mathbf{M}, \mathbf{k})}$ over integers $k_1, k_2 \geq 1$. And $U_{\mathbf{N}}^{(\mathbf{M})}$ can similarly be recovered by summing over \mathbf{k} such that $k_1 + k_2 \geq 1$.

Our aim in what follows is, then, to predict $U_{\mathbf{N}}^{(\mathbf{M})}$ and $U_{\mathbf{N}}^{(\mathbf{M}, \mathbf{k})}$, across \mathbf{M} and \mathbf{k} , given the pilot data $X_{1:2,1:\mathbf{N}}$.

3 A Bayesian framework for two populations

Before choosing a particular model, we describe a general Bayesian framework for predicting follow-up variant numbers given pilot data in two populations.

First, we assume that variants in a particular sample appear independently of each other; specifically, within any population p and sample n , we assume $x_{p,n,\ell}$ are independent across

ℓ . While ignoring linkage disequilibrium may seem at first to be too strong of an oversimplification, every existing work in a single population makes the same assumption (Camerlenghi et al., 2022; Masoero et al., 2022; Chakraborty et al., 2019; Zou et al., 2016; Gravel and National Heart Lung & Blood Institute (NHLBI) GO Exome Sequencing Project, 2014; Ionita-Laza et al., 2009). And importantly, our empirical results below show that our proposed method performs well despite this assumption.

Next we assume that samples within a single population are exchangeable; that is, we assume a distribution over the samples and further that the probability of the data is unchanged when the samples are observed in a different order. By de Finetti’s theorem (De Finetti, 1929), the two preceding assumptions imply the existence of an unknown parameter $\theta_{p,\ell} \in [0, 1]$ representing the frequency of variant ℓ in population p , such that $x_{p,n,\ell} \sim \text{Bernoulli}(\theta_{p,\ell})$, i.i.d. across n and independent across p and ℓ .

We will find it convenient to collect the ℓ -th variant frequencies across populations in the vector $\boldsymbol{\theta}_\ell = (\theta_{1,\ell}, \theta_{2,\ell})$. Then we can match the frequency vector $\boldsymbol{\theta}_\ell$ with its variant label in the following vector-valued measure: $\Theta := \sum_{\ell=1}^{\infty} \boldsymbol{\theta}_\ell \delta_{\psi_\ell}$.

To take a Bayesian approach, it remains to specify a prior over the frequencies. In the one-population case, Masoero et al. (2022) generate the frequencies according to a Poisson point process with a diffuse (i.e., non-atomic) rate measure, so we propose an analogous approach in the two-population case. In particular, we treat the labels ψ_ℓ as values of convenience rather than meaningful in any way; without loss of generality, we can imagine them as generated i.i.d. uniform on $[0, 1]$ in what follows, to ensure almost sure uniqueness. Then we write $\Theta \sim \text{PPP}(\nu)$ to indicate that Θ is generated by drawing $\{\boldsymbol{\theta}_\ell\}_{\ell=1}^{\infty}$ from a Poisson point process (PPP) with rate measure $\nu(d\boldsymbol{\theta})$ and drawing the ψ_ℓ i.i.d. uniform on $[0, 1]$.

We call the resulting model the *two-population model*. When we draw the $x_{p,n,\ell}$ conditional on Θ with the independent Bernoulli draws described above and collect them in the measures $X_{1:2,1:\mathbf{N}}$ as in Equation (1), we say that $X_{1:2,1:\mathbf{N}}$ is drawn according to a *multiple-population Bernoulli process* (mBeP) with measure parameter Θ and count-vector parameter \mathbf{N} . Finally, then the two population model can be written succinctly as:

$$\begin{aligned} \Theta &\sim \text{PPP}(\nu) && \text{(Prior)} \\ X_{1:2,1:\mathbf{N}} \mid \Theta &\sim \text{mBeP}(\Theta, \mathbf{N}). && \text{(Likelihood)} \end{aligned} \tag{5}$$

It remains to choose a rate measure $\nu(d\boldsymbol{\theta})$ for the two-population model.

4 A natural extension from one population fails

We here delineate desired model behaviors and then use these behaviors to rule out what might at first seem like a natural choice of the rate measure $\nu(d\theta)$, namely a factorized rate measure.

As a first desirable behavior in our present model, we know that any real-life sample can, out of necessity, exhibit only finitely many variants.

Desideratum (A). *Each sample exhibits finitely many variants. I.e., $\forall p, n$, we have $\sum_{\ell=1}^{\infty} x_{p,n,\ell} < \infty$.*

Second, while in reality there exists a fixed, finite upper bound on the number of variants, we are considering cases where the number of samples in the pilot and follow-up are small relative to that upper bound. Therefore, it is conceptually and computationally convenient to avoid modeling the upper bound entirely; instead, we assume that, if we sequence enough new samples, we will always discover new variants.

Desideratum (B). *No matter how many variants we have seen so far in any population, there are always more variants to discover in each population. That is, if we were to keep sequencing samples (no matter which population each sample is from), we would eventually encounter a new variant.*

The model of [Masoero et al. \(2022\)](#) satisfies Desiderata (A) and (B) (for a single population; i.e., $p \in \{1\}$). In particular, [Masoero et al. \(2022\)](#) generate frequencies according to a PPP with rate measure $\mu_{3BP}(d\theta) = \alpha\theta^{-\sigma-1}(1-\theta)^{c+\sigma-1}d\theta$ and hyperparameter values $\alpha > 0, \sigma \in [0, 1), c > -\sigma$. Given a particular variant label, variants appear in samples i.i.d. Bernoulli across samples, conditioned on the frequency. The resulting frequencies are said to be generated according to a *three-parameter beta process* (3BP) ([Teh and Gorur, 2009](#); [Broderick et al., 2012](#); [James, 2017](#)). Since $\int \theta \mu_{3BP}(d\theta) < \infty$, the number of variants in any sample is a.s. finite. And since $\int \mu_{3BP}(d\theta) = \infty$, the number of non-zero frequencies from the PPP is countably infinite.

Given the success of this one-population rate measure, a natural proposal for the two-population case is to choose a PPP rate measure that factorizes into two familiar one-population rate measures.

Condition (C). *The rate measure for the frequency-generating PPP in two populations factorizes across populations: $\nu(d\theta) = \mu(d\theta_1)\mu(d\theta_2)$.*

Our next result shows that a two-population model with a factorized rate measure cannot simultaneously satisfy both Desiderata (A) and (B).

Theorem 1. *Take the two-population model of Equation (5). If the Poisson point process rate measure in the prior factorizes across populations according to Condition (C), the model cannot simultaneously generate samples with finitely many variants (Desideratum (A)) and guarantee that there are always more variants to discover (Desideratum (B)).*

See Appendix A for the proof. The rough intuition is as follows. We observe that Desideratum (A) is equivalent to $\forall p \in \{1, 2\}, \int_{[0,1]^2} \theta_p \nu(d\boldsymbol{\theta}) < \infty$. To derive a contradiction, suppose that Desideratum (B) and Condition (C) hold. By Condition (C), we can factorize

$$\int_{[0,1]^2} \theta_1 \nu(d\boldsymbol{\theta}) = \int_{[0,1]} \theta_1 \nu_1(d\theta_1) \int_{[0,1]} \nu_2(d\theta_2).$$

We next show that Desideratum (B) and Condition (C) together imply that at least one of the factors in the product must be infinite and the remaining factor must be strictly positive. So the full product must be infinite, a contradiction with Desideratum (A). See Appendix A for a fuller and more detailed treatment.

5 Our Model

To achieve the desiderata in Section 4, we propose a new rate measure. We show that the resulting two-population model (Equation (5)) satisfies Desiderata (A) and (B). And we show how to make predictions using our model.

In what follows, we propose to use the two-population model with the following PPP rate measure on the variant frequencies:

$$\nu_{\text{prop}}(d\boldsymbol{\theta}) := \alpha \frac{(\theta_1 + \theta_2^{\sigma_2/\sigma_1})^{-\sigma_1} \theta_1^{\gamma_1-1} (1-\theta_1)^{c_1-1} \theta_2^{\gamma_2-1} (1-\theta_2)^{c_2-1}}{(\theta_1 + \theta_2)^{\gamma_1+\gamma_2} B(\gamma_1, c_1) B(\gamma_2, c_2)} \mathbf{1}_{[0,1]^2}(\boldsymbol{\theta}) d\boldsymbol{\theta}. \quad (6)$$

Here $B(\cdot, \cdot)$ denotes the beta function. The measure ν is characterized by seven scalar hyperparameters, which we collect in the vector $\boldsymbol{\zeta} := (\alpha, \sigma_1, \sigma_2, \gamma_1, \gamma_2, c_1, c_2)$. Before discussing their roles next, we observe that our rate measure takes the form of the product rate measure $\mu_{\text{3BP}}(d\theta_1)\mu_{\text{3BP}}(d\theta_2)$ multiplied by a term that does not factorize into components unique to frequencies in population 1 and 2.

Proposition 1. *If the hyperparameters satisfy $\alpha, c_1, c_2, \gamma_1, \gamma_2 > 0$ and $\sigma_1, \sigma_2 \in (0, 1)$, the two-population model (Equation (5)) satisfies Desiderata (A) and (B) when paired with our rate measure ν_{prop} from Equation (6).*

See Appendix B.1 for a proof.

A common challenge in BNP is computation with the countably infinite set of parameters implied by Desideratum (B). Like typical models used in practice, though, our model enjoys conjugacy. Namely, analogous to the one-population model from Masoero et al. (2022), our rate measure in Equation (6) is an exponential family conjugate prior for the Bernoulli process likelihood in the sense of Broderick et al. (2018). We thereby avoid any infinite-dimensional integrals. See Appendix C for a formal account and proof.

6 Prediction

With our model in hand, we now show how to predict the number of new variants in a follow-up study. We first consider the case where the hyperparameters are known (Section 6.1). Then we show how to choose the hyperparameters in Section 6.2.

6.1 Predicting variant numbers for fixed hyperparameters

First, suppose the model hyperparameters are fixed and known.

Proposition 2. *Take a two-population model (Equation (5)) with our proposed PPP rate measure (Equation (6)). Consider pilot data $X_{1:2, 1:N}$ for two populations, with pilot size N . Consider a follow-up study with M additional samples. Take any \mathbf{k} such that, for each $p \in \{1, 2\}$, $k_p \leq M_p$. Then the number of new variants appearing exactly \mathbf{k} times in the follow-up study satisfies*

$$U_{\mathbf{N}}^{(M, \mathbf{k})} \mid X_{1:2, 1:N} \sim \text{Poisson} \left(\lambda_{\mathbf{N}}^{(M, \mathbf{k})} \right),$$

where

$$\begin{aligned} \lambda_{\mathbf{N}}^{(M, \mathbf{k})} := & \alpha \binom{M_1}{k_1} \binom{M_2}{k_2} \frac{B(\gamma_1 + k_1, c_1 + N_1 + M_1 - k_1) B(\gamma_2 + k_2, c_2 + N_2 + M_2 - k_2)}{B(\gamma_1, c_1) B(\gamma_2, c_2)} \\ & \cdot \mathbb{E}_{Z, W} \left[\frac{(Z + W^{\sigma_2/\sigma_1})^{-\sigma_1}}{(Z + W)^{\gamma_1 + \gamma_2}} \right]. \end{aligned} \tag{7}$$

$\mathbb{E}_{Z,W}$ denotes the expectation with respect to independent random variables Z and W :

$$Z \sim \text{Beta}(\gamma_1 + k_1, c_1 + N_1 + M_1 - k_1), \quad \text{and} \quad W \sim \text{Beta}(\gamma_2 + k_2, c_2 + N_2 + M_2 - k_2).$$

The proof appears in Appendix E.1. Like the one-population case (Masoero et al., 2022), the predictive distribution is Poisson. Unlike the one-population case, the Poisson parameter here is not available in closed form (Equation (7)). In practice, we approximate the expectation in the prediction using the double exponential quadrature method (Takahasi and Mori, 1974) provided in the Python package `mpmath` (mpmath development team, 2013).²

As discussed in Section 2, the total number of new variants in the follow-up study can be recovered from the number of new variants occurring \mathbf{k} times. Relative to the separate proposal after Equation (4), the following result provides a more computationally efficient way to recover the total number of new variants after computing the distributions in Proposition 2.

Proposition 3. *Take the same assumptions as in Proposition 2. Then the total number of new variants in a follow-up study satisfies*

$$U_{\mathbf{N}}^{(\mathbf{M})} \mid X_{1:2,1:N} \sim \text{Poisson} \left(\sum_{m_1=1}^{M_1} \lambda_{(N_1+m_1-1, N_2)}^{((1,0),(1,0))} + \sum_{m_2=1}^{M_2} \lambda_{(N_1+M_1, N_2+m_2-1)}^{((0,1),(0,1))} \right), \quad (8)$$

where $\lambda_{\mathbf{N}}^{(\mathbf{M}, \mathbf{k})}$ is defined in Equation (7).

See Appendix E.2 for the proof. Intuitively, we first imagine taking a single new draw at a time from population 1 ($\mathbf{M} = (1, 0)$) and then a single new draw at a time from population 2 ($\mathbf{M} = (0, 1)$). Any variant that is new in the follow-up relative to the pilot must be new at exactly one step of this scheme.

The naive proposal in Section 2 would require summing over all possible \mathbf{k} such that $k_1 + k_2 \geq 1$. We know that, for each population, $k_p \leq M_p$. If we sum up to this bound, we would require $M_1 * M_2 - 1$ evaluations of Equation (7). By contrast, Equation (8) requires just $M_1 + M_2$ total evaluations of Equation (7). In practice, we expect that $\lambda_{\mathbf{N}}^{(\mathbf{M}, \mathbf{k})}$ becomes negligible for larger k_p , so one might employ a truncation to speed up the naive scheme. But figuring out an appropriate truncation level would require some work and involve a tradeoff between computation and accuracy.

²We opted for quadrature since naive Monte Carlo struggles with the divisor in the integrand for Z and W near 0. We expect more efficient choices are available with further work.

6.2 Empirics for Hyperparameters

In practice, the hyperparameter values are unknown, and we must learn them from the observed data. We take an analogous empirical-Bayes approach to the one-population case of [Masoero et al. \(2022\)](#).

In particular, we start by splitting the pilot data into a training set and a test set. Uniformly at random among the pilot data, we choose $\mathbf{N}_{\text{train}} = (N_{1,\text{train}}, N_{2,\text{train}})$ samples to form the training set. Here $N_{p,\text{train}}$ must satisfy $0 < N_{p,\text{train}} < N_p$. The remaining $\mathbf{N} - \mathbf{N}_{\text{train}}$ samples form the test set. We now treat our training set as a miniature pilot and our test set as a miniature follow-up. For the vector of appearance counts \mathbf{k} , let $\lambda_{\mathbf{N}_{\text{train}}}^{(\mathbf{N} - \mathbf{N}_{\text{train}}, \mathbf{k})}$ be the Poisson parameter from Proposition 2. And let $u_{\mathbf{N}_{\text{train}}}^{(\mathbf{N} - \mathbf{N}_{\text{train}}, \mathbf{k})}$ be the observed number of new variants appearing \mathbf{k} times in the two populations; we use the lower case character u to distinguish from the predictive random variable above.

Roughly, we will aim to choose hyperparameters that maximize the probability of observing $u_{\mathbf{N}_{\text{train}}}^{(\mathbf{N} - \mathbf{N}_{\text{train}}, \mathbf{k})}$. More precisely, we consider k_p in the miniature follow-up study up to a maximum count $v \in \mathbb{N}$. The log probability across the corresponding \mathbf{k} terms can be written as follows, where we emphasize the dependence on the hyperparameters $\zeta := (\alpha, \sigma_1, \sigma_2, \gamma_1, \gamma_2, c_1, c_2)$:

$$\mathcal{L}(\zeta) = \sum_{\substack{\mathbf{k}: k_1, k_2 \in 0:v \\ k_1 + k_2 \geq 1}} \log \left[\text{Poisson} \left(u_{\mathbf{N}_{\text{train}}}^{(\mathbf{N} - \mathbf{N}_{\text{train}}, \mathbf{k})} \mid \lambda_{\mathbf{N}_{\text{train}}}^{(\mathbf{N} - \mathbf{N}_{\text{train}}, \mathbf{k})}(\zeta) \right) \right] \quad (9)$$

We set v to balance our goals of accurate prediction with computational cost. Each term in the sum requires computing Equation (7), and there are $(v + 1)^2 - 1$ terms in the sum. We find empirically that setting $v = 10$ gives results comparable to larger settings of v and therefore use $v = 10$ in our experiments; see Appendix G.6 for our experimental comparison of v levels.

We choose the training set size as $N_{p,\text{train}} = \lfloor N_p/2 \rfloor$. We expect a larger training set size to more closely represent the actual pilot study. However, recall that we focus on the challenging case where the size of the pilot study is small. A larger training set size yields a smaller test size, which can yield a very noisy estimate of test error if too small. Our choice is meant to balance between these two extremes.

In our experiments, we optimize $\mathcal{L}(\zeta)$ across the hyperparameters ζ using L-BFGS in

scipy with default parameters and gradients estimated numerically. We initialize at $\zeta_{\text{init}} = (\alpha, \sigma_1, \sigma_2, \gamma_1, \gamma_2, c_1, c_2)_{\text{init}} = (10^3, 0.5, 0.5, 0.5, 0.5, 1, 1)$. Local optima and the accuracy of our gradient approximations are concerns. But our experiments suggest that our procedure is able to return useful predictions. The computational bottleneck is the many evaluations of the integral in Equation (7). Currently the overall optimization procedure can take several hours; reducing this cost is a promising area for future work.

7 Power law asymptotics for the number of new variants

Past work suggests that, in a single population, we might expect the observed number of variants to grow as a power law of the number of samples (Masoero et al., 2022). More generally, existing BNP models typically either exhibit logarithmic growth or power-law growth, each asymptotic in the number of samples.³ We here rule out logarithmic growth under our model (with fixed hyperparameters) and establish results that are suggestive of power-law growth.

Power-law behavior has widely been recognized as desirable in BNP models (Teh and Gorur, 2009; Lee et al., 2016). But past work establishing power laws in these models has focused on the single-population case (Gnedin et al., 2007; Teh and Gorur, 2009; Broderick et al., 2012; Lee et al., 2016). A number of new challenges arise when we consider two populations. A first challenge is specifying how samples are collected across the two populations. In one population, there is a single way to grow the number of samples; in two populations, there are many more possibilities. We focus on two sampling schemes:

- the *projection scheme*, where we sample from only one of the two populations
- the *proportional scheme*, where we collect samples from both populations according to some fixed proportion $\rho > 0$; in particular, after ρ is chosen, we have $N_2 = \lceil \rho N_1 \rceil$.

In what follows, $\mathbf{0} = (0, 0)$ is a vector of zeros, and $a_N \sim b_N$ indicates $\lim_{N \rightarrow \infty} a_N/b_N = 1$.

³For instance, under a 3BP with strictly positive discount parameter and Bernoulli likelihood, the number of variants grows (asymptotically) as a power law of the number of samples (Gnedin et al., 2007; Broderick et al., 2012). Under a 3BP with zero discount, the number of variants grows logarithmically in the number of samples (Broderick et al., 2012). Likewise, a Dirichlet process with categorical likelihood yields logarithmic growth in the number of observed clusters, but a Pitman-Yor Process exhibits power-law growth (Gnedin et al., 2007; Teh and Gorur, 2009).

7.1 The projection scheme

First we establish power-law bounds for the expected rate of growth of the number of variants under the projection scheme. We present symmetric results for each population, so we will find it useful to introduce the notation $\neg p$ to indicate the population that is not p ; i.e., when $p = 1$, we have $\neg p = 2$ and vice versa.

Proposition 4 (Power-law bounds under the projection scheme). *Fix hyperparameters $\alpha, c_1, c_2, \gamma_1, \gamma_2 > 0$ and $\sigma_1, \sigma_2 \in (0, 1)$. Consider data drawn from the two-population model of Equation (5) with $\nu = \nu_{\text{prop}}$ (Equation (6)). Then the number of new variants concentrates around its expectation:*

$$\text{Fix } N_{\neg p} = 0. \quad U_{\mathbf{0}}^{(N)} \sim \mathbb{E}U_{\mathbf{0}}^{(N)} \text{ a.s. as } N_p \rightarrow \infty.$$

Moreover, there exist functions $\Phi_{\text{lower}}^{\text{project}}, \Phi_{\text{upper}}^{\text{project}}$ that serve as respective upper and lower bounds on $\mathbb{E}U_{\mathbf{0}}^{(N)}$,

$$\forall \mathbf{N}, \quad \Phi_{\text{lower}}^{\text{project}}(\mathbf{N}) \leq \mathbb{E}U_{\mathbf{0}}^{(N)} \leq \Phi_{\text{upper}}^{\text{project}}(\mathbf{N}), \quad (10)$$

and that show the asymptotic behavior below.

Upper bound For either $p \in \{1, 2\}$ and for any δ such that $0 < \delta < \min\{\gamma_1, \gamma_2\}$, there exists a constant $C_{\text{upper}, p, \delta} > 0$ not depending on \mathbf{N} such that:

$$\text{Fix } N_{\neg p} = 0. \quad \Phi_{\text{upper}}^{\text{project}}(\mathbf{N}) \sim C_{\text{upper}, p, \delta} N_p^{\sigma_p + \delta} \text{ as } N_p \rightarrow \infty. \quad (11)$$

Lower bound Here let p be the population such that $\sigma_p \leq \sigma_{\neg p}$. Define $\sigma'_{\neg p} := \sigma_{\neg p} - \gamma_p(\sigma_{\neg p}/\sigma_p - 1)$. Then there exist constants $C_{\text{lower}, p}, C'_{\text{lower}, p}, C''_{\text{lower}, p} > 0$ not depending on \mathbf{N} such that:

$$\text{Fix } N_{\neg p} = 0. \quad \Phi_{\text{lower}}^{\text{project}}(\mathbf{N}) \sim C_{\text{lower}, p} N_p^{\sigma_p} \text{ as } N_p \rightarrow \infty. \quad (12)$$

and

$$\text{Fix } N_p = 0. \quad \Phi_{\text{lower}}^{\text{project}}(\mathbf{N}) \sim \max\{C'_{\text{lower}, p} N_{\neg p}^{\sigma_p}, C''_{\text{lower}, p} N_{\neg p}^{\sigma'_{\neg p}}\} \text{ as } N_{\neg p} \rightarrow \infty. \quad (13)$$

See Appendix H.1 for the proof. Note that, due to the maximum in Equation (13), the lower bound will grow (asymptotically) at least as fast as $N_{\neg p}^{\sigma_p}$ as $N_{\neg p} \rightarrow \infty$. It follows that the lower bound is (asymptotically) positive and diverging.

In the one-population 3BP, it is possible to establish almost sure power-law growth in the

number of variants as a function of the number of samples (Broderick et al., 2012; Teh and Gorur, 2009). By contrast, here we are only able to provide power-law *bounds* on the growth. Nonetheless our analysis does conclusively rule out logarithmic growth.

The gap between our upper and lower bounds depends on the population. If we take the population with lower rate parameter ($\sigma_p \leq \sigma_{-p}$), the gap between the powers in the upper and lower bounds (Equations (11) and (12)) can be made arbitrarily close by taking δ to 0. If we take the population with higher rate parameter, we generally expect a non-trivial gap between the powers in the upper and lower bounds (Equations (11) and (13)). We highlight the special case where the rate parameters are equal next.

Corollary 1. *Take the same assumptions and constants as Proposition 4. Take $\sigma_1 = \sigma_2 = \sigma$. Let $p \in \{1, 2\}$. Fix $N_{-p} = 0$. Then*

$$C_{\text{lower},p} N_p^{\sigma_p} \sim \Phi_{\text{lower}}^{\text{project}}(\mathbf{N}) \leq \mathbb{E}U_{\mathbf{0}}^{(\mathbf{N})} \leq \Phi_{\text{upper}}^{\text{project}}(\mathbf{N}) \sim C_{\text{upper},p,\delta} N_p^{\sigma_p+\delta},$$

where the asymptotic equivalences hold as $N_p \rightarrow \infty$.

Proof. The result follows from Equations (11) and (12). Equation (13) simultaneously applies – with the roles of p and $-p$ switched – and offers no contradiction. \square

Despite the asymmetry of our PPP rate measure in Equation (6), we do obtain symmetric roles for the rate parameters across the two populations when $\sigma_1 = \sigma_2$; this symmetry inspires our use of the name *rate parameter* in analogy to the one-population case.

We next simulate data from our model under the projection scheme, separately in each population (Figure 2); our simulations are compatible with power-law growth and with the bounds from our theory. For instance, when we grow population 1, we find that for larger N_1 the number of variants grows roughly as a constant times $N_1^{0.34}$. Since $\sigma_1 = 0.3 < 0.6 = \sigma_2$, our bounds suggest growth between $N_1^{0.3}$ and $N_1^{0.3+\delta}$. We expect the small discrepancy is due to the finite sample. Similarly, when we grow population 2, we find that for larger N_2 , the number of variants grows roughly as a constant times $N_2^{0.49}$. Since $\sigma'_2 = 0.6 - 0.1(0.6/0.3 - 1) = 0.5$, our bounds suggest growth between $N_1^{0.5}$ and $N_1^{0.6+\delta}$. Again, we expect the small discrepancy is due to the finite sample size.

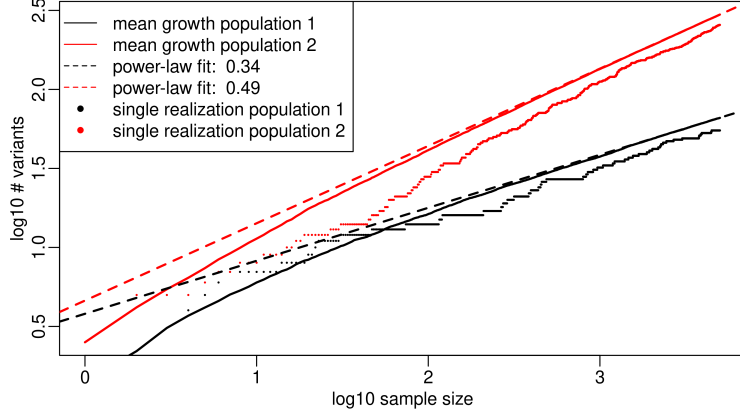


Figure 2: Illustration of simulated data from our model with $\alpha = 10, \sigma_1 = 0.3, \sigma_2 = 0.6, c_1 = c_2 = 1, \gamma_1 = \gamma_2 = 0.1$. Under the projection scheme, we take samples from only one population (population 1 in black and 2 in red). The observed number of variants for a given sample size is plotted as a point. To generate a solid curve, we take 100 independent realizations and plot the mean number of observed variants at a particular sample size (and interpolate between sample sizes). To plot the power-law fit, we make a linear least square fit of the log-log plot of the final third of the mean-growth curve and plot the resulting line. The fitted power for population 1 is 0.34 and for population 2 is 0.49.

7.2 The proportional scheme

We next establish power-law bounds for the expected rate of growth of the number of variants under the proportional scheme. Recall that under the projection scheme, the total number of samples was equal to the number of samples in one of the populations. Under the proportional scheme, the total number of samples will instead be $N_1 + N_2 = \lceil (1 + \rho)N_1 \rceil$. We will control the asymptotics by taking $N_1 \rightarrow \infty$.

Proposition 5 (Power-law bounds under the proportional scheme). *Take the model and hyperparameters as in Proposition 4. Let p be such that $\sigma_p \leq \sigma_{-p}$. For any N_1 , let $N_2 = \lceil \rho N_1 \rceil$. Then the number of new variants concentrates around its expectation:*

$$U_0^{(\mathbf{N})} \sim \mathbb{E}U_0^{(\mathbf{N})} \text{ a.s. as } N_1 \rightarrow \infty.$$

Moreover, there exist functions $\Phi_{\text{lower}}^{\text{proport}}, \Phi_{\text{upper}}^{\text{proport}}$ that serve as respective upper and lower bounds on $\mathbb{E}U_0^{(\mathbf{N})}$,

$$\forall \mathbf{N}, \quad \Phi_{\text{lower}}^{\text{proport}}(\mathbf{N}) \leq \mathbb{E}U_0^{(\mathbf{N})} \leq \Phi_{\text{upper}}^{\text{proport}}(\mathbf{N}),$$

and that exhibit the asymptotic behavior we describe next. Define σ'_{-p} as in Proposition 4.

For any δ such that $0 < \delta < \min\{\gamma_1, \gamma_2\}$, there exist constants $C, C'_\delta > 0$ not depending on \mathbf{N} such that

$$\begin{aligned} \Phi_{\text{lower}}^{\text{proport}}(\mathbf{N}) &\sim C(N_1 + N_2)^{\max\{\sigma_p, \sigma'_{-p}\}} \quad \text{as } N_1 \rightarrow \infty \\ \text{and } \Phi_{\text{upper}}^{\text{proport}}(\mathbf{N}) &\sim C'_\delta(N_1 + N_2)^{\max\{\sigma_p, \sigma_{-p}\} + \delta} \quad \text{as } N_1 \rightarrow \infty. \end{aligned}$$

See Appendix H.2 for a proof. Essentially we lower bound the total number of variants by the number seen in either population. We upper bound the total number of variants by the sum of variants seen in each population; this bound may be somewhat loose since some variants might be shared across the two populations, and hence double counted.

We next present the special case where the two rate parameters are equal; in this case, the powers in the lower and upper bounds align up to an arbitrary $\delta > 0$ difference.

Corollary 2. *Take the same assumptions and constants as Proposition 5. Take $\sigma_1 = \sigma_2 = \sigma$. Then*

$$C(N_1 + N_2)^\sigma \sim \Phi_{\text{lower}}^{\text{proport}}(\mathbf{N}) \leq \mathbb{E}U_{\mathbf{0}}^{(\mathbf{N})} \leq \Phi_{\text{upper}}^{\text{proport}}(\mathbf{N}) \sim C'_\delta(N_1 + N_2)^{\sigma + \delta} \quad \text{as } N_1 \rightarrow \infty.$$

The result follows directly from Proposition 5 and noting that, when the rate parameters are equal, we have $\sigma'_{-p} = \sigma_{-p} = \sigma$.

8 Experiments

We next check the quality of our predictions experimentally. First we check that our method performs well on well-specified synthetic data, as well as some particular forms of misspecification. Then we see that our method provides high-quality predictions on a real human cancer genetics dataset and a real human genomic dataset. Throughout, we illustrate the advantages of modeling two populations together rather than treating the two populations separately or all from a single population.

Experimental setup. In all of our experiments, we will have access to a collection of genetic samples for each of two populations (e.g., two types of cancer). Our validation procedure is reminiscent of cross-validation and analogous to the single population validation procedures of [Masoero et al. \(2022\)](#); [Zou et al. \(2016\)](#). Within each population, we uni-

formly at random choose a partition of the data into 20 equally-sized blocks.⁴ In each of 20 folds, we reserve one block (unique to this fold) to be the pilot data for its corresponding population, so the final pilot sample has size $\mathbf{N} = (N_1, N_2)$. The remaining data will serve as potential follow-up data. Each method has access only to the pilot data (across both populations), and we use the follow-up data (across both populations) to evaluate the accuracy of each method. None of the methods we consider in this paper use ordering information on the pilot data, but to generate all of our figures, we choose an ordering on the pilot data uniformly at random. Likewise, we choose an ordering on the follow-up data uniformly at random. In our figures, we present first the pilot data from population 1, then the pilot data from population 2, then the follow-up data from population 1, then the follow-up data from population 2. We can think of these figures as encapsulating a series of evaluations as follows. We train every method on the full pilot data in populations 1 and 2. Then we progressively test on follow-up sample sizes $\mathbf{M} = (M_1, M_2)$ of the following forms: $(1, 0), (2, 0), \dots, (19N_1, 0), (19N_1, 1), (19N_1, 2), \dots, (19N_1, 19N_2)$. In this way, we capture a wide range of ratios between follow-up sample sizes across the two populations: from all follow-up data in a single population to a ratio of follow-up sizes that matches the ratio in the pilot. To summarize our results across all 20 folds, we will show an empirical mean across folds, both for each prediction method as well as for the ground truth. And we will show a shaded one-standard deviation interval for the prediction methods. The ground truth showed very small variation across folds so the interval appears almost invisible.

Recall that we are also interested in predicting the number of \mathbf{k} -tons in a follow-up sample of size \mathbf{M} (Equation (4)); that is, we are interested in predicting the number of new variants appearing exactly \mathbf{k} times across the two populations. To evaluate our prediction in this case, we consider just the extreme where we use all possible data in the follow-up. For each value of \mathbf{k} with k_1, k_2 each less than a threshold, we compute the *relative residual*: namely, the signed difference between a method’s prediction and the observed value in the reserved follow-up data, normalized by the observed value. We plot an empirical average of this quantity across the folds. We also report the actual observed values and absolute (un-normalized) residuals in Appendix G, again averaged across the folds.

⁴Since the dataset size may not be a multiple of 20, block sizes in practice may vary by 1. We will elide small details of this form in the remainder of this section for clarity of exposition. Also, the population genetics data is substantially larger than our other datasets, so – to avoid a very large pilot size – we use 30-fold cross-validation in that case (Section 8.2.2).

Comparisons. To the best of our knowledge, there are no alternative methods for the prediction task we are interested in here. However, there are a number of methods that predict the number of variants in a follow-up given pilot data in a single population (Masoero et al., 2022; Chakraborty et al., 2019; Gravel and National Heart Lung & Blood Institute (NHLBI) GO Exome Sequencing Project, 2014). So we consider two natural competitors in our experiments. First, we define the *independent* two-population extension of a single-population method as follows. Given \mathbf{N} pilot samples and \mathbf{M} follow-up samples, we train the single-population method first on the N_1 pilot samples from population 1 and predict the number of variants expected in M_1 follow-up samples from population 1. We separately train the single-population method on the N_2 samples from population 2 and predict the number of variants expected in M_2 follow-up samples from population 2. We report the sum of the predicted number of variants across both populations as the final prediction. In general, we expect the independent method to overcount the number of variants when there are follow-up samples from both populations. The independent method essentially assumes each variant is unique to a single population. From that perspective, when $\mathbf{k} = (k_1, 0)$, we can take the population-1 prediction for the number of k_1 -tons and use it as the independent-method prediction for the number of \mathbf{k} -tons; an analogous prediction holds when $k_1 = 0$ and $k_2 > 0$. Whenever both elements of \mathbf{k} are strictly positive, the independent method predicts there are zero \mathbf{k} -tons. In the real data we analyze at the sizes we consider, this zero prediction is unrealistic (see Figure S10, S11, S12 for raw number of \mathbf{k} -tons in synthetic experiments and Figure S13, S14 in real data experiments).

Second, we define the *dependent* two-population extension of a single-population method. In this case, we train the single-population method on all of the $N_1 + N_2$ pilot samples, as though they are the pilot samples from a single population. To form a prediction on a follow-up sample of size \mathbf{M} , we report the prediction on a single-population follow-up of size $M_1 + M_2$. In general, we expect the dependent method to struggle when both (a) the two populations exhibit notably different variant growth rates and (b) the ratio of populations in the follow-up does not closely mirror the pilot. To predict the number of \mathbf{k} -tons, we predict the number of variants, conditional on the pilot, that we would expect to see k_1 times out of M_1 follow-up samples and also k_2 times out of M_2 distinct follow-up samples (all from the same assumed single population). For single-population methods that do not provide k -ton predictions (for scalar k), we will therefore not be able to provide \mathbf{k} -ton predictions in the dependent extension. However, we are able to provide \mathbf{k} -ton predictions for the special case of the single-population 3BP method due to Masoero et al. (2022); we provide the prediction

and its supporting theory in Appendix D.1.

Since there are many single-population methods, in general we will select just one single-population method to use when reporting the independent and dependent results. In each case, we will try to use the single-population method that is best in a relevant sense, which we make precise in each case below.

8.1 Synthetic experiments

We first confirm that our method is able to predict well on data simulated from our own model (Equation (6)), as a check on our methodology before moving to real data. To that end, we generate 500 data points in each of two populations; we describe the simulation procedure in more detail in Appendix F. So, in each of our 20 folds, the pilot data has size $\mathbf{N} = (25, 25)$.

We simulate two different datasets from our model (Equation (6)); we choose the hyperparameters to reflect a range of growth rates, sample sizes, and correlations between the two populations in each case. For the first dataset, we choose hyperparameters $\zeta := (\alpha, \sigma_1, \sigma_2, \gamma_1, \gamma_2, c_1, c_2) = (100, 0.4, 0.6, 0.5, 0.5, 1, 1)$ and $\zeta = (1, 0.8, 0.7, 0.5, 0.5, 1, 1)$ for a qualitative match of the curve form in the GnomAD for a qualitative match of the curve form in GnomAD dataset (Figure 5) and cancer dataset (Figure 4) respectively.

The results in Figure 3 demonstrate that our method outperforms two potential baselines. Since here all of our data is simulated from our two-population BNP model, we use a single-population BNP model to form our baselines; namely, we compare to the independent and dependent two-population extensions of the 3BP approach due to Masoero et al. (2022). We see in the upper left plot in Figure 3 that our method (solid red line) much more closely matches the behavior of the ground truth (dashed black line) than either the independent (dotted green line) or dependent (dash-dot blue line) extensions. As expected, the independent extension dramatically overcounts the number of variants in the second follow-up population. Also as expected, the dependent extension performs well when the pilot and follow-up proportions are in agreement (at the largest sample size) but misestimates the number of variants elsewhere. By contrast, our method is able to capture the different behaviors of the two populations and account for any shared variants. In the lower left corner, the independent extension of the 3BP performs the best; its mean line is closest to the ground truth, and its prediction exhibit the smallest variation (shaded range) across folds. Importantly, we can infer from the center and left plots that there are extremely few shared

variants in this simulation; see Appendix G.3.1 for more precise counts. That is, the assumption of the independent extension is very close to being correct. So, following Bayesian Occam’s Razor (MacKay, 2003, ch. 28 p. 343), we expect better performance from the simpler model (the independent extension) when its more stringent assumptions are true. That being said, our proposed model still performs very well here; its mean line is also very close to the ground truth, in contrast to the dependent extension. We conclude that our method is able to handle prediction of the number of new variants under a variety of two-population behaviors – while the independent extension is limited to the special cases where the two populations are known a priori to behave independently.

From the center and right plots in Figure 3, we also see that our method provides better estimates of the numbers of various k -tons. Recall that the independent extension predicts zero for anything except private k -tons, and we see that there are in fact non-trivial counts of shared k -tons in the first data set. Given this limitation of the independent extension, we focus on plotting results for our method and the dependent extension. Darker colors indicate more erroneous predictions, so we conclude in both datasets that our method is providing more accurate predictions than the dependent 3BP extension. Note that the observed numbers of k -tons vary dramatically across k values. So generally we expect more noise in the upper right of our plots of k -tons – and should therefore take care to not to treat every square in these plots equally. We can see the actual observation values for the two datasets in Figure S10; in particular, for the first dataset, the observed number of k -tons varies from an average (across folds) of 1161.2 at $(0, 1)$ to 0 at various locations, e.g. $(8, 3)$, $(10, 4)$, and $(7, 7)$ (see the gray boxes in the upper left panel of Figure S10). We see similar behavior in the real data, as we describe below.

We provide further checks that our method is able to handle datasets generated from the (mis-specified) assumptions of the independent and dependent 3BP extensions in Appendix G.1.

8.2 Real data

We next confirm that our method performs well on a real dataset in cancer genomics and semi-synthetic dataset in population genetics. In particular, we confirm that our method performs better than the independent and dependent extensions of one-population methods described above.

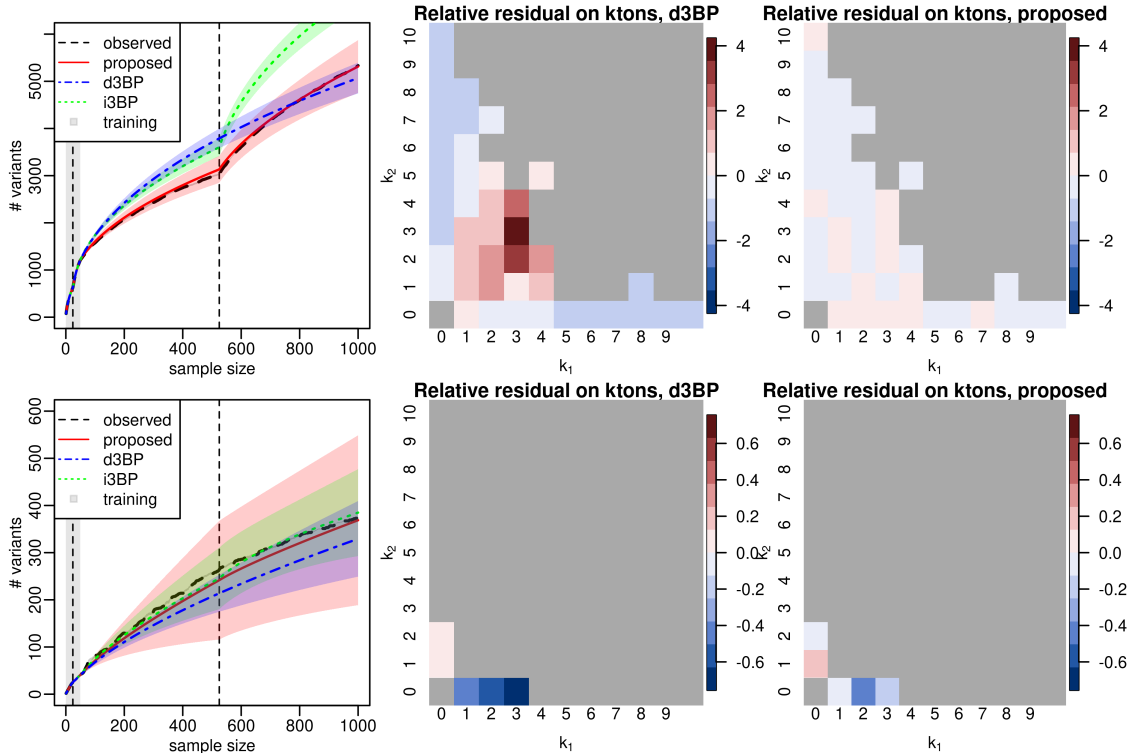


Figure 3: Predictions when data is sampled from our model (Equation (6)). Each row represents a different simulated dataset, as described in Section 8.1. *Left*: The dashed black line shows the observed number of variants as a function of the sample number. The samples appear in the following order: the pilot from population 1, the pilot from population 2, the follow-up from population 1, the follow-up from population 2. A vertical dashed gray line separates the two populations in the pilot and follow-up, respectively. The gray shading covers the pilot data. All curves agree exactly on the pilot data. In the follow-up region, we plot mean (lines) and 1 standard deviation intervals (shaded regions) from three methods: our proposed method (solid red), the dependent version of the single-population 3BP (dash-dot blue), and the independent version of the 3BP (dotted green). *Center and Right*: For each \mathbf{k} with component values up to 10, we plot the relative residual for predictions from our method (right) and the dependent 3BP (center). Note that the color scales are fixed across a row but vary across a column. A square is gray when the observed value is strictly less than 2 in at least one fold or $\mathbf{k} = (0, 0)$, where by definition having 0 observed.

Comparisons. For the real datasets, we find that different one-population methods exhibit substantially different performance for different types of data. So, for each type of data (cancer, population genetics), we test a variety of different one-population methods. We compare them on the one-population task and choose the best-performing method to serve as the comparison (via independent and dependent extensions) for our two-population method. For one-population methods, we consider the fourth-order jackknife (Burnham and Overton, 1978; Gravel and National Heart Lung & Blood Institute (NHLBI) GO Exome Sequencing Project, 2014), the Good-Toulmin estimator (Orlitsky et al., 2016; Chakraborty et al., 2019), linear programming (Zou et al., 2016), the 3BP approach of Masoero et al. (2022) and the scaled process by Camerlenghi et al. (2022) (See Appendix G.2 for this comparison).

8.2.1 Two cancer genomic datasets

In cancer genomics, biologists are actively searching for (rare) shared genetic variants across cancer types that might lend insight into common causes of different cancers (Bojesen et al., 2013; Rashkin et al., 2020). In our analysis that follows, we find that both our method and the independent extension perform well at predicting the number of new variants, while the dependent extension performs poorly. But unlike the independent extension, our method is able to predict the (non-trivial) number of shared variants across populations – and provides a better prediction than the dependent extension.

In these experiments, we use the cancer genome atlas (TCGA) and MSK-IMPACT datasets (The Cancer Genome Atlas Research Network, 2008; The Cancer Genome Atlas Research Network et al., 2013; Cheng et al., 2015). We used the same processing as in Chakraborty et al. (2019) and Masoero et al. (2022). To form our two populations, we focus on the two types of cancer with the largest numbers of samples; in each dataset, the resulting two types of cancer are lung cancer and breast cancer. In the MSK-IMPACT dataset, there are total of 749 lung cancer samples and 1532 breast cancer samples. In the TCGA dataset, there are total of 492 lung cancer samples and 811 breast cancer samples. So the pilot sizes are challenging in each case: 38, 57, 24, and 40, respectively.

For each population (lung cancer, breast cancer) within each dataset (TCGA, MSK-IMPACT), we compare performance of the one-population methods above; see Appendix G.2. For each population in each dataset, we find that the best-performing one-population method is the 3BP. So use the 3BP for the independent and dependent one-population extensions in this analysis.

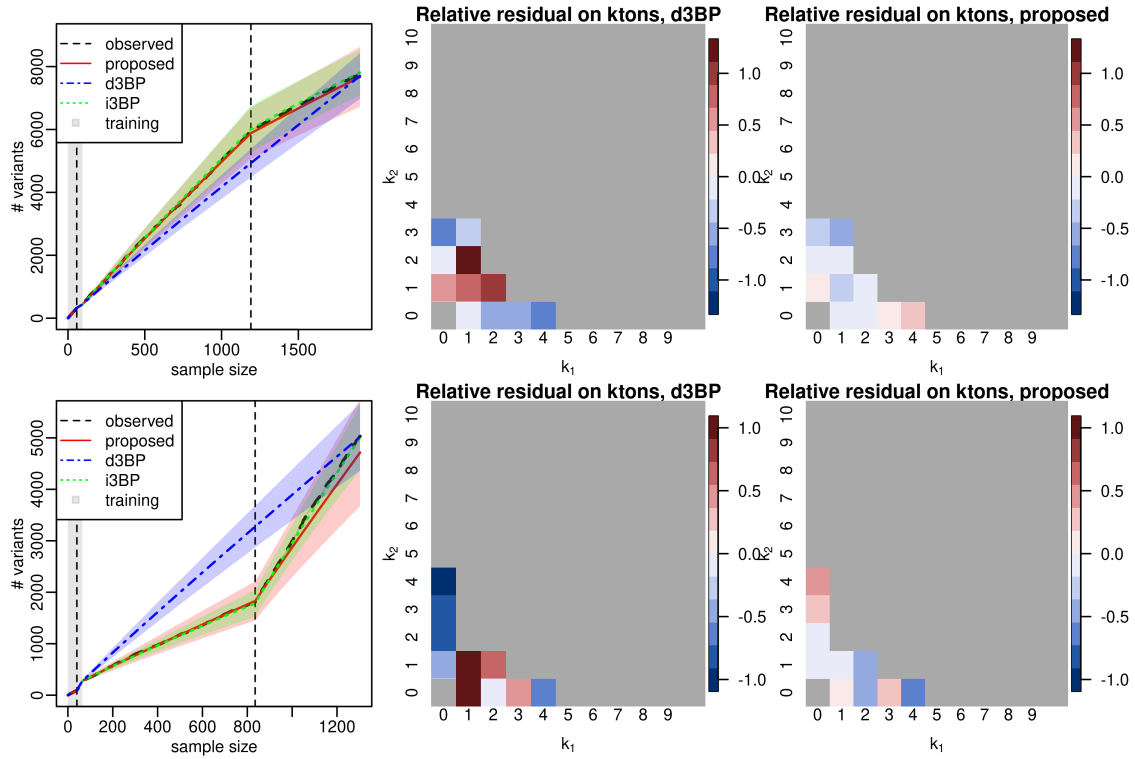


Figure 4: Predictions for the cancer genomics data. The rows correspond to datasets (upper: MSK-IMPACT, lower: TCGA). Population 1 is breast cancer, and population 2 is lung cancer. Other details of the plots are as in Figure 3.

The results in Figure 4 demonstrate that our method outperforms the two one-population baselines. In particular, both our method and the independent extension agree closely with the ground truth number of new variants across the various follow-up sizes (left panels). Indeed, we expect a low level of sharing between cancer types since most variants in cancer are *de novo* variants – not subject to the natural selection that might make variants more likely to be shared across populations. As expected the dependent extension agrees with ground truth when the composition of the follow-up matches the pilot, but its predictions can be very far from the ground truth for other follow-up sizes. In the center and right plots, we see that there are still a number of shared variants with non-trivial counts in the ground truth; see also Figure S13 for direct plots of the ground truth. The independent extension is unable to predict such counts. And while the dependent extension can predict a non-zero number in these cases, we see from the center and right plots in Figure 4 that our method’s predictions are more accurate. Overall then, our method is the only one able to provide both useful predictions of the numbers of variants in a follow-up as well as useful predictions of the number of shared variants across populations in the follow-up.

8.2.2 A semi-synthetic population genetics dataset

For population genetics, we use the GnomAD dataset [Karczewski et al. \(2020\)](#). The dataset provides variant frequencies, but it does not provide exact variant data for each sample. Therefore, we take the semi-synthetic approach of [Masoero et al. \(2022\)](#); in particular, for each individual, we randomly and independently sample the presence of each variant according to the reported frequency of that variant in the data. In general, prediction is more challenging (a) when the pilot is small in absolute terms since less data is available about the trend in variant growth and (b) when the follow-up is as large as possible since we have a priori more possibility for any observed trend to break down. To accomplish goal (b), we choose large populations, with several thousands of individuals: the Korean (1909 samples), Bulgarian (1335), and Southern European (5752) populations. With these large populations, we choose 30 folds in our evaluation to ensure the pilots are still somewhat small and similar to cancer dataset (64, 45, and 192, respectively), per goal (a).

For each population (Korean, Bulgarian, Southern European), we compare performance of the one-population methods at the start of Section 8.2; see Appendix G.2. For each population in this case, we find that the fourth-order jackknife (4JK) is either the best performer or tied for best performance. So we use the 4JK for the independent and dependent one-population extensions in this analysis.

The results in Figure 5 demonstrate that our method outperforms the two one-population methods at predicting the number of new variants in a follow-up. When the follow-up composition matches the pilot (the most favorable case for the dependent extension), our method is at least on par with the dependent one-population extension at predicting the number of shared variants in a follow-up. We see in the upper left plot that the dependent extension miscounts variants when the composition of the follow-up differs from the pilot. The independent extension predicts the first population well but seems to double count shared variants when the second population appears in the follow-up. In the lower left, the two populations are more similar, so the dependent extension performs reasonably; the independent extension, though, seems to double count shared variants in the second population in the follow-up. In both examples, our method tracks closely with ground truth.

In the upper center plot, we see that the dependent one-population extension can be over an order of magnitude off in its predictions. In the upper right plot, we see that our method is much closer to ground truth across the k values here. Unlike in the cancer data case, the ground truth at all k values in this plot is substantially greater than zero; see Figure S13 for more information about the ground-truth counts. In particular, the signed residual plot in Figure S13 shows that the dependent extension is providing an overestimate along the diagonal. Indeed, we expect that the Korean and Bulgarian populations have little overlap and thus few shared variants – whereas the dependent extension assumes they are the same population. Conversely, in the lower center and right plots, we see that our method is often farther from the ground truth than the dependent extension. We note that the magnitude of the error is smaller than in the upper plots, but it is still quite high (larger than 100%). It may be that the complex history between the related Southern European and Bulgarian populations cannot be captured by the simple models we consider here. We reiterate that the independent extension predicts zero for all k values that do not have a zero component and thus fails to predict all such values in these examples.

9 Discussion

We proposed a novel approach to estimating the number of new genetic variants that will be observed in a follow-up sequencing study of two potentially heterogeneous populations. In this setting, a researcher has already conducted a pilot sequencing study and may be interested in the best allocation of resources to maximize the detection of new genetic variants in a larger follow-up study. Given the success of the Bayesian nonparametric methodology of

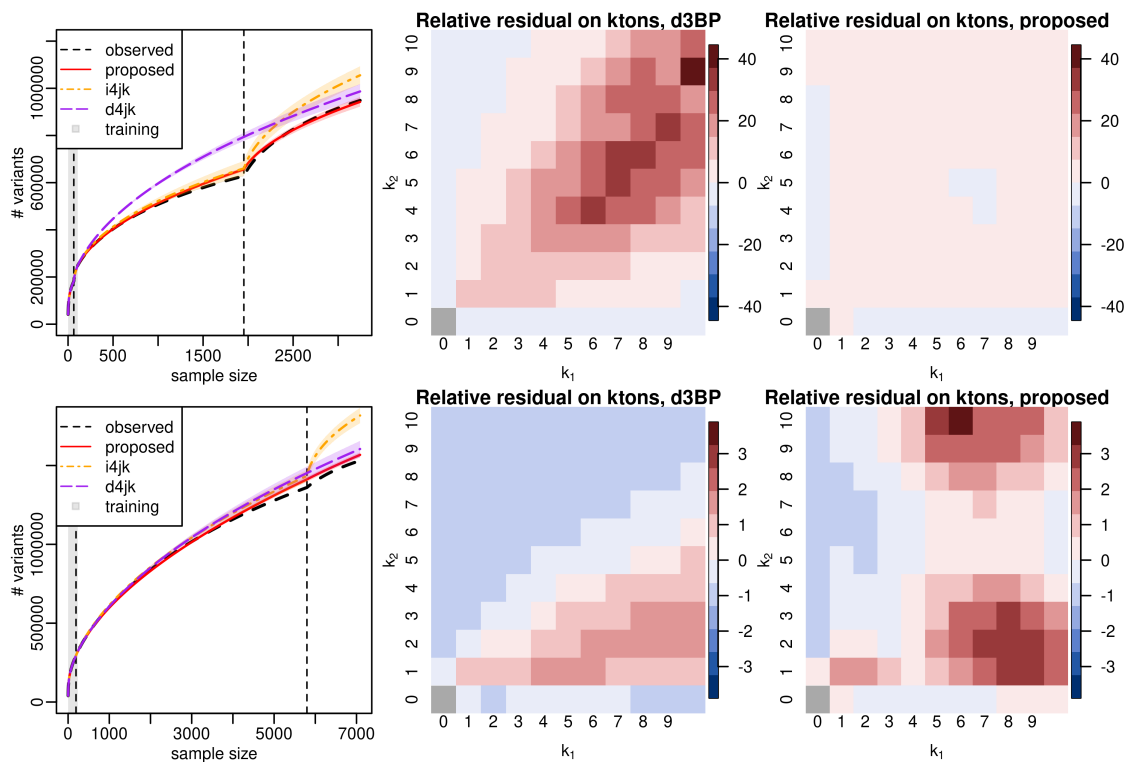


Figure 5: Predictions for the gnomAD data. The rows correspond to datasets (upper: Korean–Bulgarian, lower: Southern European–Bulgarian). In particular, in the top row, population 1 is Korean, and population 2 is Bulgarian. In the bottom row, population 1 is Southern European, and population 2 is Bulgarian. Other details of the plots are as in Figure 3. Other details of the plots are as in Figure 3. We highlight the very different color scales between the upper and lower rows.

Masoero et al. (2022) in the one-population case and the flexibility of the Bayesian framework, we chose to take a BNP approach for two populations. In particular, we decided to use a model where variant frequencies are generated according to a Poisson point process, parameterized by a rate measure.

Surprisingly, we proved that a product rate measure is incompatible with the requirements that any finite sample only obtains a finite number of variants while the number of variants will grow without bound as the sample sizes increase. This difficulty arises due to the fact that variants may be shared between groups; thus we proposed a novel conjugate measure that satisfies these desiderata. Given this incompatibility we used a Poisson point process with a novel non-product rate measure. Although the form of our new approach prohibits analytical calculations, we showed that numerical integrals still facilitate robust and practical evaluation of quantities of interest.

We provided upper and lower bounds on the growth in the number of new variants in our model, such that the bounds exhibit power laws. We checked the bounds empirically and also noted that empirically the variant-number growth from our model seems to exhibit a power law itself. Nonetheless, explicit proofs that this growth exhibits power law behavior will provide deeper understanding of this process.

Using simulations, we showed that our approach works to predict the number of novel variants from both real and simulated data. Since we are not aware of other two-population methods, we compared to simple baselines based on one-population methods: (1) treating the two populations as separate, which we call the independent extension and (2) treating all the data as from a single population, which we call the dependent extension. As expected, we find that the independent extension tends to overestimate the number of new variants when there are any shared variants, and it is not able to predict shared variants. The dependent extension is accurate when the populations appear in the same proportions in the pilot and the follow-up, but otherwise can provide poor estimates. Our method, by contrast, can correctly account for shared variants and differing population proportions between a pilot and follow-up.

Several opportunities remain for future work. First, we rely on numerical integration for our predictions. Even in the two-population case, these computations can be somewhat expensive. We expect further computational (and statistical) challenges when considering higher numbers of populations. We suspect that alternative approaches may prove fruitful. In addition, we explored only one possible option for generalizing the beta process to higher

dimensions. Although our experiments validated our approach, even better performance might be possible with an alternative model – especially one carefully aligned with biological prior knowledge.

Acknowledgments

YS and TB were supported in part by the DARPA I2O LwLL program, an NSF Career Award, and an ONR Early Career Grant. JGS was supported by NIH grant R35GM137758 to Michael D. Edge. The authors acknowledge the MIT SuperCloud and Lincoln Laboratory Supercomputing Center for providing HPC resources that have contributed to the research results reported within this paper.

References

- Agarwal, I., Fuller, Z. L., Myers, S. R., and Przeworski, M. (2023). Relating pathogenic loss-of function mutations in humans to their evolutionary fitness costs. *eLife*, 12:e83172.
- Agarwal, I. and Przeworski, M. (2021). Mutation saturation for fitness effects at human cpG sites. *Elife*, 10:e71513.
- Assimes, T., Tcheandjieu, C., Zhu, X., Hilliard, A., Clarke, S., Napolioni, V., Ma, S., Fang, H., Gorman, B. R., Lee, K. M., Chen, F., Pyarajan, S., Song, R., Plomondon, M., Maddox, T., Waldo, S., Sinnott-Armstrong, N., Ho, Y.-L., Wojcik, G., Buyske, S., Kooperberg, C., Haessler, J., Loos, R., Do, R., Verbanck, M., Chaudhary, K., North, K., Avery, C., Haiman, C., Marchand, L. L., Wilkens, L., Bis, J., Leonard, H., Shen, B., Lange, L., Giri, A., Lu, Y., Dikilitas, O., Kullo, I., Stanaway, I., Jarvik, G., Gordon, A., Hebring, S., Namjou, B., Kaufman, K., Koyama, S., Ito, K., Ishigaki, K., Kamatani, Y., Tsao, N., Verma, S., Ritchie, M., Kember, R., Baras, A., Lotta, L., Natarajan, P., Levin, M., Hauser, E., Miller, D., Vujkovic, M., Huffman, J., Raghavan, S., Klarin, D., Lee, J., Voight, B., Rader, D., Chang, K.-M., Damrauer, S., Lynch, J., Wilson, P., Tang, H., Sun, Y., Tsao, P., O'Donnell, C., Kathiresan, S., Saleheen, D., Gaziano, J. M., Reaven, P., Cho, K., Bick, A., Graff, M., and Huang, J. (2021). A large-scale multi-ethnic genome-wide association study of coronary artery disease. *Nature Medicine*.
- Backman, J. D., Li, A. H., Marcketta, A., Sun, D., Mbatchou, J., Kessler, M. D., Benner, C., Liu, D., Locke, A. E., Balasubramanian, S., Yadav, A., Banerjee, N., Gillies, C. E.,

- Damask, A., Liu, S., Bai, X., Hawes, A., Maxwell, E., Gurski, L., Watanabe, K., Kosmicki, J. A., Rajagopal, V., Mighty, J., Jones, M., Mitnaul, L., Stahl, E., Coppola, G., Jorgenson, E., Habegger, L., Salerno, W. J., Shuldiner, A. R., Lotta, L. A., Overton, J. D., Cantor, M. N., Reid, J. G., Yancopoulos, G., Kang, H. M., Marchini, J., Baras, A., Abecasis, G. R., and Ferreira, M. A. R. (2021). Exome sequencing and analysis of 454,787 uk biobank participants. *Nature*, 599(7886):628–634.
- Biddanda, A., Rice, D. P., and Novembre, J. (2020). A variant-centric perspective on geographic patterns of human allele frequency variation. *Elife*, 9:e60107.
- Bojesen, S. E., Pooley, K. A., Johnatty, S. E., Beesley, J., Michailidou, K., Tyrer, J. P., Edwards, S. L., Pickett, H. A., Shen, H. C., Smart, C. E., et al. (2013). Multiple independent variants at the TERT locus are associated with telomere length and risks of breast and ovarian cancer. *Nature Genetics*, 45(4):371–384.
- Broderick, T., Jordan, M. I., and Pitman, J. (2012). Beta processes, stick-breaking and power laws. *Bayesian Analysis*, 7(2):439–476.
- Broderick, T., Wilson, A. C., and Jordan, M. I. (2018). Posteriors, conjugacy, and exponential families for completely random measures. *Bernoulli*, 24(4B):3181–3221.
- Burnham, K. P. and Overton, W. S. (1978). Estimation of the size of a closed population when capture probabilities vary among animals. *Biometrika*, 65(3):625–633.
- Camerlenghi, F., Favaro, S., Masoero, L., and Broderick, T. (2022). Scaled process priors for bayesian nonparametric estimation of the unseen genetic variation. *Journal of the American Statistical Association*, pages 1–12.
- Campbell, T., Huggins, J. H., How, J. P., and Broderick, T. (2019). Truncated random measures. *Bernoulli*, 25(2):1256 – 1288.
- Chakraborty, S., Arora, A., Begg, C. B., and Shen, R. (2019). Using somatic variant richness to mine signals from rare variants in the cancer genome. *Nature Communications*, 10(1):1–9.
- Chen, S., Francioli, L. C., Goodrich, J. K., Collins, R. L., Kanai, M., Wang, Q., Alföldi, J., Watts, N. A., Vittal, C., Gauthier, L. D., Poterba, T., Wilson, M. W., Tarasova, Y., Phu, W., Grant, R., Yohannes, M. T., Koenig, Z., Farjoun, Y., Banks, E., Donnelly, S., Gabriel, S., Gupta, N., Ferriera, S., Tolonen, C., Novod, S., Bergelson, L., Roazen, D., Ruano-Rubio, V., Covarrubias, M., Llanwarne, C., Petrillo, N., Wade, G., Jeandet, T.,

Munshi, R., Tibbetts, K., Abreu, M., Aguilar Salinas, C. A., Ahmad, T., Albert, C. M., Ardissino, D., Armean, I. M., Atkinson, E. G., Atzmon, G., Barnard, J., Baxter, S. M., Beaugerie, L., Benjamin, E. J., Benjamin, D., Boehnke, M., Bonnycastle, L. L., Bottinger, E. P., Bowden, D. W., Bown, M. J., Brand, H., Brant, S., Brookings, T., Bryant, S., Calvo, S. E., Campos, H., Chambers, J. C., Chan, J. C., Chao, K. R., Chapman, S., Chasman, D. I., Chisholm, R., Cho, J., Chowdhury, R., Chung, M. K., Chung, W. K., Cibulskis, K., Cohen, B., Connolly, K. M., Correa, A., Cummings, B. B., Dabelea, D., Danesh, J., Darbar, D., Darnowsky, P., Denny, J., Duggirala, R., Dupuis, J., Ellinor, P. T., Elosua, R., Emery, J., England, E., Erdmann, J., Esko, T., Evangelista, E., Fatkin, D., Florez, J., Franke, A., Fu, J., Färkkilä, M., Garimella, K., Gentry, J., Getz, G., Glahn, D. C., Glaser, B., Glatt, S. J., Goldstein, D., Gonzalez, C., Groop, L., Gudmundsson, S., Haessler, A., Haiman, C., Hall, I., Hanis, C. L., Harms, M., Hiltunen, M., Holi, M. M., Hultman, C. M., Jalas, C., Kallela, M., Kaplan, D., Kaprio, J., Kathiresan, S., Kenny, E. E., Kim, B.-J., Kim, Y. J., King, D., Kirov, G., Kooner, J., Koskinen, S., Krumholz, H. M., Kugathasan, S., Kwak, S. H., Laakso, M., Lake, N., Langsford, T., Laricchia, K. M., Lehtimäki, T., Lek, M., Lipscomb, E., Loos, R. J. F., Lu, W., Lubitz, S. A., Luna, T. T., Ma, R. C. W., Marcus, G. M., Marrugat, J., Mattila, K. M., McCarroll, S., McCarthy, M. I., McCauley, J. L., McGovern, D., McPherson, R., Meigs, J. B., Melander, O., Metspalu, A., Meyers, D., Minikel, E. V., Mitchell, B. D., Mootha, V. K., Naheed, A., Nazarian, S., Nilsson, P. M., O'Donovan, M. C., Okada, Y., Ongur, D., Orozco, L., Owen, M. J., Palmer, C., Palmer, N. D., Palotie, A., Park, K. S., Pato, C., Pulver, A. E., Rader, D., Rahman, N., Reiner, A., Remes, A. M., Rhodes, D., Rich, S., Rioux, J. D., Ripatti, S., Roden, D. M., Rotter, J. I., Sahakian, N., Saleheen, D., Salomaa, V., Saltzman, A., Samani, N. J., Samocha, K. E., Sanchis-Juan, A., Scharf, J., Schleicher, M., Schunkert, H., Schönherr, S., Seaby, E. G., Shah, S. H., Shand, M., Sharpe, T., Shoemaker, M. B., Shyong, T., Silverman, E. K., Singer-Berk, M., Sklar, P., Smith, J. T., Smith, J. G., Soininen, H., Sokol, H., Son, R. G., Soto, J., Spector, T., Stevens, C., Stitzziel, N. O., Sullivan, P. F., Suvisaari, J., Tai, E. S., Taylor, K. D., Teo, Y. Y., Tsuang, M., Tuomi, T., Turner, D., Tusie-Luna, T., Vartiainen, E., Vawter, M., Wang, L., Wang, A., Ware, J. S., Watkins, H., Weersma, R. K., Weisburd, B., Wessman, M., Whiffin, N., Wilson, J. G., Xavier, R. J., O'Donnell-Luria, A., Solomonson, M., Seed, C., Martin, A. R., Talkowski, M. E., Rehm, H. L., Daly, M. J., Tiao, G., Neale, B. M., MacArthur, D. G., and Karczewski, K. J. (2023). A genomic mutational constraint map using variation in 76,156 human genomes. *Nature*, pages 1–11.

Cheng, D. T., Mitchell, T. N., Zehir, A., Shah, R. H., Benayed, R., Syed, A., Chandramohan,

- R., Liu, Z. Y., Won, H. H., Scott, S. N., Brannon, A. R., O'Reilly, C., Sadowska, J., Casanova, J., Yannes, A., Hechtman, J. F., Yao, J., Song, W., Ross, D. S., Oultache, A., Dogan, S., Borsu, L., Hameed, M., Nafa, K., Arcila, M. E., Ladanyi, M., and Berger, M. F. (2015). Memorial sloan kettering-integrated mutation profiling of actionable cancer targets (MSK-IMPACT): a hybridization capture-based next-generation sequencing clinical assay for solid tumor molecular oncology. *The Journal of Molecular Diagnostics*, 17(3):251–264.
- Christensen, K. D., Dukhovny, D., Siebert, U., and Green, R. C. (2015). Assessing the costs and cost-effectiveness of genomic sequencing. *Journal of personalized medicine*, 5(4):470–486.
- De Finetti, B. (1929). Funzione caratteristica di un fenomeno aleatorio. In *Atti del Congresso Internazionale dei Matematici: Bologna del 3 al 10 de settembre di 1928*, pages 179–190.
- Fatumo, S., Chikowore, T., Choudhury, A., Ayub, M., Martin, A. R., and Kuchenbaecker, K. (2022). A roadmap to increase diversity in genomic studies. *Nature medicine*, 28(2):243–250.
- Freedman, D. (1973). Another note on the Borel-Cantelli lemma and the strong law , with the Poisson approximation as a by-product. *The Annals of Probability*, 1(6):910–925.
- Fu, J., Festen, E. A., and Wijmenga, C. (2011). Multi-ethnic studies in complex traits. *Human molecular genetics*, 20(R2):R206–R213.
- Gnedin, A., Hansen, B., and Pitman, J. (2007). Notes on the occupancy problem with infinitely many boxes: General asymptotics and power lawss. *Probability Surveys*, 4(1):146–171.
- Gravel, S., Henn, B. M., Gutenkunst, R. N., Indap, A. R., Marth, G. T., Clark, A. G., Yu, F., Gibbs, R. A., Project, . G., Bustamante, C. D., et al. (2011). Demographic history and rare allele sharing among human populations. *Proceedings of the National Academy of Sciences*, 108(29):11983–11988.
- Gravel, S. and National Heart Lung & Blood Institute (NHLBI) GO Exome Sequencing Project (2014). Predicting discovery rates of genomic features. *Genetics*, 197(2):601–610.
- Green, R. E., Krause, J., Briggs, A. W., Maricic, T., Stenzel, U., Kircher, M., Patterson, N., Li, H., Zhai, W., Fritz, M. H.-Y., Hansen, N. F., Durand, E. Y., Malaspinas, A.-S., Jensen, J. D., Marques-Bonet, T., Alkan, C., Prüfer, K., Meyer, M., Burbano, H. A., Good, J. M., Schultz, R., Aximu-Petri, A., Butthof, A., Höber, B., Höffner, B., Siegemund,

- M., Weihmann, A., Nusbaum, C., Lander, E. S., Russ, C., Novod, N., Affourtit, J., Egholm, M., Verna, C., Rudan, P., Brajkovic, D., Kucan, v., Gušić, I., Doronichev, V. B., Golovanova, L. V., Lalueza-Fox, C., de la Rasilla, M., Fortea, J., Rosas, A., Schmitz, R. W., Johnson, P. L. F., Eichler, E. E., Falush, D., Birney, E., Mullikin, J. C., Slatkin, M., Nielsen, R., Kelso, J., Lachmann, M., Reich, D., and Pääbo, S. (2010). A draft sequence of the neandertal genome. *science*, 328(5979):710–722.
- Haak, W., Lazaridis, I., Patterson, N., Rohland, N., Mallick, S., Llamas, B., Brandt, G., Nordenfelt, S., Harney, E., Stewardson, K., Fu, Q., Mittnik, A., Bánffy, E., Economou, C., Francken, M., Friederich, S., Pena, R. G., Hallgren, F., Khartanovich, V., Khokhlov, A., Kunst, M., Kuznetsov, P., Meller, H., Mochalov, O., Moiseyev, V., Nicklisch, N., Pichler, S. L., Risch, R., Rojo Guerra, M. A., Roth, C., Szécsényi-Nagy, A., Wahl, J., Meyer, M., Krause, J., Brown, D., Anthony, D., Cooper, A., Alt, K. W., and Reich, D. (2015). Massive migration from the steppe was a source for indo-european languages in europe. *Nature*, 522(7555):207–211.
- Hindorff, L. A., Bonham, V. L., Brody, L. C., Ginoza, M. E., Hutter, C. M., Manolio, T. A., and Green, E. D. (2018). Prioritizing diversity in human genomics research. *Nature Reviews Genetics*, 19(3):175–185.
- Hoadley, K. A., Yau, C., Hinoue, T., Wolf, D. M., Lazar, A. J., Drill, E., Shen, R., Taylor, A. M., Cherniack, A. D., Thorsson, V., et al. (2018). Cell-of-origin patterns dominate the molecular classification of 10,000 tumors from 33 types of cancer. *Cell*, 173(2):291–304.
- Huang, K.-l., Mashl, R. J., Wu, Y., Ritter, D. I., Wang, J., Oh, C., Paczkowska, M., Reynolds, S., Wyczalkowski, M. A., Oak, N., et al. (2018). Pathogenic germline variants in 10,389 adult cancers. *Cell*, 173(2):355–370.
- Ionita-Laza, I., Lange, C., and M. Laird, N. (2009). Estimating the number of unseen variants in the human genome. *Proceedings of the National Academy of Sciences*, 106(13):5008–5013.
- James, L. F. (2017). Bayesian poisson calculus for latent feature modeling via generalized Indian buffet process priors. *The Annals of Statistics*, 45(5):2016–2045.
- Jayasinghe, R. G., Cao, S., Gao, Q., Wendl, M. C., Vo, N. S., Reynolds, S. M., Zhao, Y., Climente-González, H., Chai, S., Wang, F., et al. (2018). Systematic analysis of splice-site-creating mutations in cancer. *Cell reports*, 23(1):270–281.

- Kandoth, C., McLellan, M. D., Vandin, F., Ye, K., Niu, B., Lu, C., Xie, M., Zhang, Q., McMichael, J. F., Wyczalkowski, M. A., Leiserson, M. D. M., Miller, C. A., Welch, J. S., Walter, M. J., Wendl, M. C., Ley, T. J., Wilson, R. K., Raphael, B. J., and Ding, L. (2013). Mutational landscape and significance across 12 major cancer types. *Nature*, 502(7471):333–339.
- Karczewski, K. J., Francioli, L. C., Tiao, G., Cummings, B. B., Alfoldi, J., Wang, Q., Collins, R. L., Laricchia, K. M., Ganna, A., Birnbaum, D. P., Gauthier, L. D., Brand, H., Solomonson, M., Watts, N. A., Rhodes, D., Singer-Berk, M., England, E. M., Seaby, E. G., Kosmicki, J. A., Walters, R. K., Tashman, K., Farjoun, Y., Banks, E., Poterba, T., Wang, A., Seed, C., Whiffin, N., Chong, J. X., Samocha, K. E., Pierce-Hoffman, E., Zappala, Z., O'Donnell-Luria, A. H., Minikel, E. V., Weisburd, B., Lek, M., Ware, J. S., Vittal, C., Armean, I. M., Bergelson, L., Cibulskis, K., Connolly, K. M., Covarrubias, M., Donnelly, S., Ferriera, S., Gabriel, S., Gentry, J., Gupta, N., Jeandet, T., Kaplan, D., Llanwarne, C., Munshi, R., Novod, S., Petrillo, N., Roazen, D., Ruano-Rubio, V., Saltzman, A., Schleicher, M., Soto, J., Tibbetts, K., Tolonen, C., Wade, G., Talkowski, M. E., Aguilar Salinas, C. A., Ahmad, T., Albert, C. M., Ardissino, D., Atzmon, G., Barnard, J., Beaugerie, L., Benjamin, E. J., Boehnke, M., Bonnycastle, L. L., Bottinger, E. P., Bowden, D. W., Bown, M. J., Chambers, J. C., Chan, J. C., Chasman, D., Cho, J., Chung, M. K., Cohen, B., Correa, A., Dabelea, D., Daly, M. J., Darbar, D., Duggirala, R., Dupuis, J., Ellinor, P. T., Elosua, R., Erdmann, J., Esko, T., Färkkilä, M., Florez, J., Franke, A., Getz, G., Glaser, B., Glatt, S. J., Goldstein, D., Gonzalez, C., Groop, L., Haiman, C., Hanis, C., Harms, M., Hiltunen, M., Holli, M. M., Hultman, C. M., Kallela, M., Kaprio, J., Kathiresan, S., Kim, B.-J., Kim, Y. J., Kirov, G., Kooner, J., Koskinen, S., Krumholz, H. M., Kugathasan, S., Kwak, S. H., Laakso, M., Lehtimäki, T., Loos, R. J. F., Lubitz, S. A., Ma, R. C. W., MacArthur, D. G., Marrugat, J., Mattila, K. M., McCarroll, S., McCarthy, M. I., McGovern, D., McPherson, R., Meigs, J. B., Melander, O., Metspalu, A., Neale, B. M., Nilsson, P. M., O'Donovan, M. C., Ongur, D., Orozco, L., Owen, M. J., Palmer, C. N. A., Palotie, A., Park, K. S., Pato, C., Pulver, A. E., Rahman, N., Remes, A. M., Rioux, J. D., Ripatti, S., Roden, D. M., Saleheen, D., Salomaa, V., Samani, N. J., Scharf, J., Schunkert, H., Shoemaker, M. B., Sklar, P., Soininen, H., Sokol, H., Spector, T., Sullivan, P. F., Suvisaari, J., Tai, E. S., Teo, Y. Y., Tiinamaija, T., Tsuang, M., Turner, D., Tusie-Luna, T., Vartiainen, E., Vawter, M. P., Ware, J. S., Watkins, H., Weersma, R. K., Wessman, M., Wilson, J. G., Xavier, R. J., Neale, B. M., Daly, M. J., and MacArthur, D. G. (2020). The mutational constraint spectrum quantified from variation in 141,456

humans. *Nature*, 581(7809):434–443.

Kingman, J. F. C. (1992). *Poisson processes*, volume 3. Clarendon Press.

Lazaridis, I., Patterson, N., Mittnik, A., Renaud, G., Mallick, S., Kirsanow, K., Sudmant, P. H., Schraiber, J. G., Castellano, S., Lipson, M., Berger, B., Economou, C., Bollongino, R., Fu, Q., Bos, K. I., Nordenfelt, S., Li, H., de Filippo, C., Prüfer, K., Sawyer, S., Posth, C., Haak, W., Hallgren, F., Fornander, E., Rohland, N., Delsate, D., Francken, M., Guinet, J.-M., Wahl, J., Ayodo, G., Babiker, H. A., Bailliet, G., Balanovska, E., Balanovsky, O., Barrantes, R., Bedoya, G., Ben-Ami, H., Bene, J., Berrada, F., Bravi, C. M., Brisighelli, F., Busby, G. B. J., Cali, F., Churnosov, M., Cole, D. E. C., Corach, D., Damba, L., van Driem, G., Dryomov, S., Dugoujon, J.-M., Fedorova, S. A., Gallego Romero, I., Gubina, M., Hammer, M., Henn, B. M., Hervig, T., Hodoglugil, U., Jha, A. R., Karachanak-Yankova, S., Khusainova, R., Khusnutdinova, E., Kittles, R., Kivisild, T., Klitz, W., Kučinskis, V., Kushniarevich, A., Laredj, L., Litvinov, S., Loukidis, T., Mahley, R. W., Melegh, B., Metspalu, E., Molina, J., Mountain, J., Näkkäläjärvi, K., Nesheva, D., Nyambo, T., Osipova, L., Parik, J., Platonov, F., Posukh, O., Romano, V., Rothhammer, F., Rudan, I., Ruizbakiev, R., Sahakyan, H., Sajantila, A., Salas, A., Starikovskaya, E. B., Tarekegn, A., Toncheva, D., Turdikulova, S., Uktveryte, I., Utevska, O., Vasquez, R., Villena, M., Voevoda, M., Winkler, C. A., Yepiskoposyan, L., Zalloua, P., Zemunik, T., Cooper, A., Capelli, C., Thomas, M. G., Ruiz-Linares, A., Tishkoff, S. A., Singh, L., Thangaraj, K., VILLEMS, R., Comas, D., Sukernik, R., Metspalu, M., Meyer, M., Eichler, E. E., Burger, J., Slatkin, M., Pääbo, S., Kelso, J., Reich, D., and Krause, J. (2014). Ancient human genomes suggest three ancestral populations for present-day europeans. *Nature*, 513(7518):409–413.

Lee, J., James, L. F., and Choi, S. (2016). Finite-dimensional bfry priors and variational bayesian inference for power law models. In Lee, D., Sugiyama, M., Luxburg, U., Guyon, I., and Garnett, R., editors, *Advances in Neural Information Processing Systems*, volume 29. Curran Associates, Inc.

Lek, M., Karczewski, K. J., Minikel, E. V., Samocha, K. E., Banks, E., Fennell, T., O’Donnell-Luria, A. H., Ware, J. S., Hill, A. J., Cummings, B. B., Tukiainen, T., Birnbaum, D. P., Kosmicki, J. A., Duncan, L. E., Estrada, K., Zhao, F., Zou, J., Pierce-Hoffman, E., Berghout, J., Cooper, D. N., Deflaux, N., DePristo, M., Do, R., Flannick, J., Fromer, M., Gauthier, L., Goldstein, J., Gupta, N., Howrigan, D., Kiezun, A., Kurki, M. I., Moonshine, A. L., Natarajan, P., Orozco, L., Peloso, G. M., Poplin, R., Rivas, M. A.,

- Ruano-Rubio, V., Rose, S. A., Ruderfer, D. M., Shakir, K., Stenson, P. D., Stevens, C., Thomas, B. P., Tiao, G., Tusie-Luna, M. T., Weisburd, B., Won, H.-H., Yu, D., Altshuler, D. M., Ardissino, D., Boehnke, M., Danesh, J., Donnelly, S., Elosua, R., Florez, J. C., Gabriel, S. B., Getz, G., Glatt, S. J., Hultman, C. M., Kathiresan, S., Laakso, M., McCarroll, S., McCarthy, M. I., McGovern, D., McPherson, R., Neale, B. M., Palotie, A., Purcell, S. M., Saleheen, D., Scharf, J. M., Sklar, P., Sullivan, P. F., Tuomilehto, J., Tsuang, M. T., Watkins, H. C., Wilson, J. G., Daly, M. J., and MacArthur, D. G. (2016). Analysis of protein-coding genetic variation in 60,706 humans. *Nature*, 536(7616):285–291.
- Ma, X., Edmonson, M., Yergeau, D., Muzny, D. M., Hampton, O. A., Rusch, M., Song, G., Easton, J., Harvey, R. C., Wheeler, D. A., Ma, J., Doddapaneni, H., Vadodaria, B., Wu, G., Nagahawatte, P., Carroll, W. L., Chen, I.-M., Gastier-Foster, J. M., Relling, M. V., Smith, M. A., Devidas, M., Auvil, J. M. G., Downing, J. R., Loh, M. L., Willman, C. L., Gerhard, D. S., Mullighan, C. G., Hunger, S. P., and Zhang, J. (2015). Rise and fall of subclones from diagnosis to relapse in pediatric b-acute lymphoblastic leukaemia. *Nature communications*, 6(1):6604.
- MacKay, D. J. (2003). *Information theory, inference and learning algorithms*. Cambridge university press.
- Masoero, L., Camerlenghi, F., Favaro, S., and Broderick, T. (2022). More for less: Predicting and maximizing genomic variant discovery via Bayesian nonparametrics. *Biometrika*, 109(1):17–32.
- Masoero, L., Schraiber, J., and Broderick, T. (2021). Bayesian nonparametric strategies for power maximization in rare variants association studies. In *NeurIPS 2021 Workshop on Learning Meaningful Representations of Life*.
- mpmath development team, T. (2013). *mpmath: a Python library for arbitrary-precision floating-point arithmetic (version 0.18)*. <http://mpmath.org/>.
- Novembre, J. and Di Rienzo, A. (2009). Spatial patterns of variation due to natural selection in humans. *Nature Reviews Genetics*, 10(11):745–755.
- Orlitsky, A., Suresh, A. T., and Wu, Y. (2016). Optimal prediction of the number of unseen species. *Proceedings of the National Academy of Sciences*, 113(47):13283–13288.
- Park, S. T. and Kim, J. (2016). Trends in next-generation sequencing and a new era for whole genome sequencing. *International neurology journal*, 20(Suppl 2):S76.

- Pirozzi, C. J. and Yan, H. (2021). The implications of idh mutations for cancer development and therapy. *Nature Reviews Clinical Oncology*, 18(10):645–661.
- Popejoy, A. B. and Fullerton, S. M. (2016). Genomics is failing on diversity. *Nature*, 538(7624):161–164.
- Prior, I. A., Hood, F. E., and Hartley, J. L. (2020). The frequency of ras mutations in cancer. *Cancer research*, 80(14):2969–2974.
- Project, S. J. C. R. H. U. P. C. G. (2014). The genomic landscape of diffuse intrinsic pontine glioma and pediatric non-brainstem high-grade glioma. *Nature genetics*, 46(5):444–450.
- Rafnar, T., Sulem, P., Stacey, S. N., Geller, F., Gudmundsson, J., Sigurdsson, A., Jakobsdottir, M., Helgadottir, H., Thorlacius, S., Aben, K. K. H., Blöndal, T., Thorgeirsson, T. E., Thorleifsson, G., Kristjansson, K., Thorisdottir, K., Ragnarsson, R., Sigurgeirsson, B., Skuladottir, H., Gudbjartsson, T., Isaksson, H. J., Einarsson, G. V., Benediktsdottir, K. R., Agnarsson, B. A., Olafsson, K., Salvarsdottir, A., Bjarnason, H., Asgeirsdottir, M., Kristinsson, K. T., Matthiasdottir, S., Sveinsdottir, S. G., Polidoro, S., Höiom, V., Botella-Estrada, R., Hemminki, K., Rudnai, P., Bishop, D. T., Campagna, M., Kellen, E., Zeegers, M. P., de Verdier, P., Ferrer, A., Isla, D., Vidal, M. J., Andres, R., Saez, B., Juberias, P., Banzo, J., Navarrete, S., Tres, A., Kan, D., Lindblom, A., Gurzau, E., Koppova, K., de Vegt, F., Schalken, J. A., van der Heijden, H. F. M., Smit, H. J., Termeer, R. A., Oosterwijk, E., van Hooij, O., Nagore, E., Porru, S., Steineck, G., Hansson, J., Buntinx, F., Catalona, W. J., Matullo, G., Vineis, P., Kiltie, A. E., Mayordomo, J. I., Kumar, R., Kiemeny, L. A., Frigge, M. L., Jonsson, T., Saemundsson, H., Barkardottir, R. B., Jonsson, E., Jonsson, S., Olafsson, J. H., Gulcher, J. R., Masson, G., Gudbjartsson, D. F., Kong, A., Thorsteinsdottir, U., and Stefansson, K. (2009). Sequence variants at the TERT-CLPTM1L locus associate with many cancer types. *Nature Genetics*, 41(2):221–227.
- Rashkin, S. R., Graff, R. E., Kachuri, L., Thai, K. K., Alexeeff, S. E., Blatchins, M. A., Cavazos, T. B., Corley, D. A., Emami, N. C., Hoffman, J. D., Jorgenson, E., Kushi, K. H., Meyers, T. J., Van Den Eeden, S. K., Ziv, E., Habel, L. A., Hoffmann, T. J., Sakoda, L. C., and Witte, J. S. (2020). Pan-cancer study detects genetic risk variants and shared genetic basis in two large cohorts. *Nature Communications*, 11(1):1–14.
- Roselli, C., Chaffin, M. D., Weng, L.-C., Aeschbacher, S., Ahlberg, G., Albert, C. M., Almgren, P., Alonso, A., Anderson, C. D., Aragam, K. G., Arking, D. E., Barnard, J.,

Bartz, T. M., Benjamin, E. J., Bihlmeyer, N. A., Bis, J. C., Bloom, H. L., Boerwinkle, E., Bottinger, E. B., Brody, J. A., Calkins, H., Campbell, A., Cappola, T. P., Carlquist, J., Chasman, D. I., Chen, L. Y., Chen, Y.-D. I., Choi, E.-K., Choi, S. H., Christophersen, I. E., Chung, M. K., Cole, J. W., Conen, D., Cook, J., Crijns, H. J., Cutler, M. J., Damrauer, S. M., Daniels, B. R., Darbar, D., Delgado, G., Denny, J. C., Dichgans, M., Dörr, M., Dudink, E. A., Dudley, S. C., Esa, N., Esko, T., Eskola, M., Fatkin, D., Felix, S. B., Ford, I., Franco, O. H., Geelhoed, B., Grewal, R. P., Gudnason, V., Guo, X., Gupta, N., Gustafsson, S., Gutmann, R., Hamsten, A., Harris, T. B., Hayward, C., Heckbert, S. R., Hernesniemi, J., Hocking, L. J., Hofman, A., Horimoto, A. R. V. R., Huang, J., Huang, P. L., Huffman, J., Ingelsson, E., Ipek, E. G., Ito, K., Jimenez-Conde, J., Johnson, R., Jukema, J. W., Kääh, S., Kähönen, M., Kamatani, Y., Kane, J. P., Kastrati, A., Kathiresan, S., Katschnig-Winter, P., Kavousi, M., Kessler, T., Kietselaer, B. L., Kirchhof, P., Kleber, M. E., Knight, S., Krieger, J. E., Kubo, M., Launer, L. J., Laurikka, J., Lehtimäki, T., Leineweber, K., Lemaitre, R. N., Li, M., Lim, H. E., Lin, H. J., Lin, H., Lind, L., Lindgren, C. M., Lokki, M.-L., London, B., Loos, R. J. F., Low, S.-K., Lu, Y., Lyytikäinen, L.-P., Macfarlane, P. W., Magnusson, P. K., Mahajan, A., Malik, R., Mansur, A. J., Marcus, G. M., Margolin, L., Margulies, K. B., März, W., McManus, D. D., Melander, O., Mohanty, S., Montgomery, J. A., Morley, M. P., Morris, A. P., Müller-Nurasyid, M., Natale, A., Nazarian, S., Neumann, B., Newton-Cheh, C., Niemeijer, M. N., Nikus, K., Nilsson, P., Noordam, R., Oellers, H., Olesen, M. S., Orho-Melander, M., Padmanabhan, S., Pak, H.-N., Paré, G., Pedersen, N. L., Pera, J., Pereira, A., Porteous, D., Psaty, B. M., Pulit, S. L., Pullinger, C. R., Rader, D. J., Refsgaard, L., Ribasés, M., Ridker, P. M., Rienstra, M., Risch, L., Roden, D. M., Rosand, J., Rosenberg, M. A., Rost, N., Rotter, J. I., Saba, S., Sandhu, R. K., Schnabel, R. B., Schramm, K., Schunkert, H., Schurman, C., Scott, S. A., Seppälä, I., Shaffer, C., Shah, S., Shalaby, A. A., Shim, J., Shoemaker, M. B., Siland, J. E., Sinisalo, J., Sinner, M. F., Slowik, A., Smith, A. V., Smith, B. H., Smith, J. G., Smith, J. D., Smith, N. L., Soliman, E. Z., Sotoodehnia, N., Stricker, B. H., Sun, A., Sun, H., Svendsen, J. H., Tanaka, T., Tanriverdi, K., Taylor, K. D., Teder-Laving, M., Teumer, A., Thériault, S., Trompet, S., Tucker, N. R., Tveit, A., Uitterlinden, A. G., Van Der Harst, P., Van Gelder, I. C., Van Wagoner, D. R., Verweij, N., Vlachopoulou, E., Völker, U., Wang, B., Weeke, P. E., Weijs, B., Weiss, R., Weiss, S., Wells, Q. S., Wiggins, K. L., Wong, J. A., Woo, D., Worrall, B. B., Yang, P.-S., Yao, J., Yoneda, Z. T., Zeller, T., Zeng, L., Lubitz, S. A., Lunetta, K. L., and Ellinor, P. T. (2018). Multi-ethnic genome-wide association study for atrial fibrillation. *Nature genetics*,

50(9):1225–1233.

- Saltzman, E. A., Drew, J. H., Leemis, L. M., and Henderson, S. G. (2012). Simulating multivariate nonhomogeneous poisson processes using projections. *ACM Transactions on Modeling and Computer Simulation (TOMACS)*, 22(3):1–13.
- Schwarze, K., Buchanan, J., Taylor, J. C., and Wordsworth, S. (2018). Are whole-exome and whole-genome sequencing approaches cost-effective? a systematic review of the literature. *Genetics in Medicine*, 20(10):1122–1130.
- Szustakowski, J. D., Balasubramanian, S., Kvikstad, E., Khalid, S., Bronson, P. G., Sasson, A., Wong, E., Liu, D., Wade Davis, J., Haefliger, C., Katrina Loomis, A., Mikkilineni, R., Noh, H. J., Wadhawan, S., Bai, X., Hawes, A., Krasheninina, O., Ulloa, R., Lopez, A. E., Smith, E. N., Waring, J. F., Whelan, C. D., Tsai, E. A., Overton, J. D., Salerno, W. J., Jacob, H., Szalma, S., Runz, H., Hinkle, G., Nioi, P., Petrovski, S., Miller, M. R., Baras, A., Mitnaul, L. J., Reid, J. G., Moiseyenko, O., Rios, C., Saha, S., Abecasis, G., Banerjee, N., Beechert, C., Boutkov, B., Cantor, M., Coppola, G., Economides, A., Eom, G., Forsythe, C., Fuller, E. D., Gu, Z., Habegger, L., Jones, M. B., Lanche, R., Lattari, M., LeBlanc, M., Li, D., Lotta, L. A., Manoochchri, K., Mansfield, A. J., Maxwell, E. K., Mighty, J., Nafde, M., O’Keeffe, S., Orelus, M., Padilla, M. S., Panea, R., Polanco, T., Pradhan, M., Rasool, A., Schleicher, T. D., Sharma, D., Shuldiner, A., Staples, J. C., Van Hout, C. V., Widom, L., Wolf, S. E., John, S., Chen, C.-Y., Sexton, D., Kupelian, V., Marshall, E., Swan, T., Eaton, S., Liu, J. Z., Loomis, S., Jensen, M., Duraisamy, S., Tetrault, J., Merberg, D., Badola, S., Reppell, M., Grundstad, J., Zheng, X., Deaton, A. M., Parker, M. M., Ward, L. D., Flynn-Carroll, A. O., Austin, C., March, R., Pangalos, M. N., Platt, A., Snowden, M., Matakidou, A., Wasilewski, S., Wang, Q., Deevi, S., Carss, K., Smith, K., Sogaard, M., Hu, X., Chen, X., and Ye, Z. (2021). Advancing human genetics research and drug discovery through exome sequencing of the uk biobank. *Nature genetics*, 53(7):942–948.
- Takahasi, H. and Mori, M. (1974). Double exponential formulas for numerical integration. *Publications of the Research Institute for Mathematical Sciences*, 9(3):721–741.
- Teh, Y. and Gorur, D. (2009). Indian buffet processes with power-law behavior. In Bengio, Y., Schuurmans, D., Lafferty, J., Williams, C., and Culotta, A., editors, *Advances in Neural Information Processing Systems*, volume 22. Curran Associates, Inc.
- Tennessen, J. A., Bigham, A. W., O’Connor, T. D., Fu, W., Kenny, E. E., Gravel, S., McGee, S., Do, R., Liu, X., Jun, G., Kang, H. M., Jordan, D., Leal, S. M., Gabriel, S.,

- Rieder, M. J., Abecasis, G., Altshuler, D., Nickerson, D. A., Boerwinkle, E., Sunyaev, S., Bustamante, C. D., Bamshad, M. J., Akey, J. M., Broad Go, Seattle Go, and On behalf of the NHLBI Exome Sequencing Project (2012). Evolution and functional impact of rare coding variation from deep sequencing of human exomes. *Science*, 337(6090):64–69.
- The Cancer Genome Atlas Research Network (2008). Comprehensive genomic characterization defines human glioblastoma genes and core pathways. *Nature*, 455(7216):1061–1068.
- The Cancer Genome Atlas Research Network, Weinstein, J. N., Collisson, E. A., Mills, G. B., Mills Shaw, K. R., Ozenberger, B. A., Ellrot, K., Shmulevich, I., Sander, C., and Stuart, J. M. (2013). The cancer genome atlas pan-cancer analysis project. *Nature genetics*, 45(10):1113–1120.
- Wang, Q., Dhindsa, R. S., Carss, K., Harper, A. R., Nag, A., Tachmazidou, I., Vitsios, D., Deevi, S. V., Mackay, A., Muthas, D., Hühn, M., Monkley, S., Olsson, H., Angermann, B. R., Artzi, R., Barrett, C., Belvisi, M., Bohlooly-Y, M., Burren, O., Buvall, L., Challis, B., Cameron-Christie, S., Cohen, S., Davis, A., Danielson, R. F., Dougherty, B., Georgi, B., Ghazoui, Z., Hansen, P. B., Hu, F., Jeznach, M., Jiang, X., Kumar, C., Lai, Z., Lassi, G., Lewis, S. H., Linghu, B., Lythgow, K., Maccallum, P., Martins, C., Matakidou, A., Michaëlsson, E., Moosmang, S., O’Dell, S., Ohne, Y., Okae, J., O’Neill, A., Paul, D. S., Reznichenko, A., Snowden, M. A., Walentinsson, A., Zeron, J., Pangalos, M. N., Wasilewski, S., Smith, K. R., March, R., Platt, A., Haefliger, C., and Petrovski, S. (2021). Rare variant contribution to human disease in 281,104 UK Biobank exomes. *Nature*, 597(7877):527–532.
- Zou, J., Valiant, G., Valiant, P., Karczewski, K., Chan, S. O., Samocha, K., Lek, M., Sunyaev, S., Daly, M., and MacArthur, D. G. (2016). Quantifying unobserved protein-coding variants in human populations provides a roadmap for large-scale sequencing projects. *Nature Communications*, 7(1):1–5.

A Proofs of results in Section 4

In this section, we provide additional details and proofs for the results presented in Section 4 for a generic finite number of populations. We state and prove a slight generalization of Equation (5), where the number of populations can be two or greater: $P > 1$. The two-population case of Equation (5) follows as a corollary.

Before stating our result, we extend our notation to encompass any strictly positive integer number of populations $P > 0$. We let N_p denote the number of observed pilot samples in population p with $1 \leq p \leq P$. We collect all the pilot sizes in the vector $\mathbf{N} := (N_1, \dots, N_P)$. We collect the observations from the n -th sample in the p -th population in $X_{p,n}$ as in Equation (2). We write $X_{p,1:N_p}$ for the pilot samples in population p . And we write $X_{1:P,1:N}$ for the full collection of pilot samples across populations.

We collect the variant frequencies across populations as $\boldsymbol{\theta}_\ell = (\theta_{1,\ell}, \dots, \theta_{P,\ell})$. The vector-valued measure $\Theta := \sum_{\ell=1}^{\infty} \boldsymbol{\theta}_\ell \delta_{\psi_\ell}$ matches variant frequency vectors with their labels. We write $\Theta \sim \text{PPP}(\nu)$ to indicate that Θ is generated by drawing $\{\boldsymbol{\theta}_\ell\}_{\ell=1}^{\infty}$ from a Poisson point process (PPP) with rate measure $\nu(d\boldsymbol{\theta})$ and drawing the ψ_ℓ i.i.d. uniform on $[0, 1]$. We model $x_{p,n,\ell} \sim \text{Bernoulli}(\theta_{p,\ell})$, i.i.d. across n and independent across p and ℓ ; when the $x_{p,n,\ell}$ are drawn this way, we say that $X_{1:2,1:N}$ is drawn according to a *multiple-population Bernoulli process* (mBeP) with measure parameter Θ and count-vector parameter \mathbf{N} . The P -population generalization of Equation (5) is then

$$\begin{aligned} \Theta &\sim \text{PPP}(\nu) && \text{(Prior)} \\ X_{1:P,1:N} \mid \Theta &\sim \text{mBeP}(\Theta, \mathbf{N}). && \text{(Likelihood)} \end{aligned} \tag{S1}$$

In particular, the notation and development in the main text is the $P = 2$ special case of what is written above. Observe that Desideratum (A) and Desideratum (B) do not specifically reference $P = 2$ and can be applied to the general $P > 0$ case as well.

To prove our main result, we will find it useful to show that each of Desideratum (A) and Desideratum (B) is equivalent to an integral constraint on the Lévy rate measure ν of the prior distribution Θ . To that end, we state and prove the following lemma.

Lemma S1 (Integral requirements). *Take a number of populations P with $1 < P < \infty$. Take data generated according to the model in Equation (S1). Then Desideratum (A) holds*

if and only if the rate measure ν satisfies

$$\forall p \in \{1, \dots, P\}, \quad \int_{[0,1]^P} \theta_p \nu(d\boldsymbol{\theta}) < \infty. \quad (\text{S2})$$

And Desideratum (B) holds if and only if the rate measure ν satisfies

$$\forall p \in \{1, \dots, P\}, \quad \int_{(0,1]} \nu_{-p}(d\theta_p) = \infty. \quad (\text{S3})$$

Here $\nu_{-p}(d\theta_p) := \int_{[0,1]^{P-1}} \nu(d\boldsymbol{\theta}_{-p})$, where $\boldsymbol{\theta}_{-p} = [\theta_1, \dots, \theta_{p-1}, \theta_{p+1}, \dots, \theta_P]^\top$ denotes a vector containing all population indices other than p .

Proof. By construction, a point drawn from the Poisson point process with rate measure ν is of the form $\boldsymbol{\theta} = [\theta_1, \dots, \theta_P]^\top \in [0, 1]^P$. By standard properties of multivariate Poisson processes, the p -th coordinate of the multivariate Poisson process is a univariate Poisson point process with rate measure $\nu_{-p}(d\theta_p) := \int \nu(d\boldsymbol{\theta}_{-p})$ (Mapping theorem, Kingman, 1992, ch. 2.3).

In our setting, then, an individual $X_{p,n}$ in population p is drawn from a Bernoulli process, where the parameter encoding the variants with their frequency follows a Poisson point process with rate measure ν_{-p} . Following the same argument in Broderick et al. (2018, Section 2.3), $X_{p,n}$ shows finitely many variants (Desideratum (A)) with probability one if and only if the underlying rate measure has finite expectation on $[0, 1]$. In our case, population p 's frequency is from the marginal rate; thus individuals exhibit finitely many variants if and only if $\int \theta_p \nu_{-p}(d\theta_p) < \infty$. By substituting the definition of $\nu_{-p}(d\theta_p)$, $\int \theta_p \nu_{-p}(d\theta_p) < \infty$ can be rewritten as Equation (S2).

Desideratum (B) is satisfied if and only if for each population there are infinitely many variants that can be discovered. Again by Broderick et al. (2018, Section 2.3) population p has infinitely many variants to be seen if and only if $\nu_{-p}(d\theta_p)$ has infinite mass on $(0, 1]$, which is the requirement stated in Equation (S3). \square

Remark S1 (On Desideratum (B)). *A traditional requirement of one-population Bayesian nonparametric feature models is that the rate measure has infinite mass on $(0, 1]$. Desideratum (B) provides an extension of this requirement to multiple populations. If we think of Desideratum (B) as an extension from a single dimensional θ , to a multidimensional $\boldsymbol{\theta}$, there a number of other possible extensions that might a priori seem reasonable. For instance, we*

might instead require infinite mass on $(0, 1]^P$ (i.e., all vectors in the unit cube with strictly positive entries) or infinite mass on $[0, 1]^P \setminus \mathbf{0}$ where $\mathbf{0}$ is a P -long 0-vector (i.e., the unit cube without the origin).

We next observe that these alternative extensions are not equivalent to Desideratum (B). To help us construct our counterexamples, we will use P (unidimensional) measures $\mu_1(d\theta_1), \dots, \mu_P(d\theta_P)$. We assume that for $p = 1, \dots, P$, we have $\int_{(0,1]} \mu_p(d\theta_p) = \infty$ and $\int_{(0,1]} \theta_p \mu_p(d\theta_p) < \infty$. We denote the delta measure at 0 as $\delta_0(\cdot)$.

First, we construct a measure that has 0 mass on $(0, 1]^P$ but satisfies Desideratum (B). To construct our measure, we put mass only on the axes; namely, we consider the measure $\sum_{p=1}^P \mu_p(d\theta_p) \prod_{k:k \neq p} \delta_0(d\theta_k)$. This measure can be interpreted as P populations that do not share variants; each population separately draws its variant frequencies from μ_p . Since by assumption μ_p satisfies the single-population requirements, the full measure satisfies Desideratum (B). But the measure has 0 mass on $(0, 1]^P$ because its mass lies entirely along the axes.

Next, we construct a measure that has infinite mass on $[0, 1]^P \setminus \mathbf{0}$ but does not satisfy Desideratum (B). In this case, we put mass on exactly one axis. Then all but one population exhibit zero variants. In particular, we consider the measure $\mu_1(d\theta_1) \prod_{k=2}^P \delta_0(d\theta_k)$. This measure has infinite mass on $[0, 1]^P \setminus \mathbf{0}$. But when we sample from, e.g., population 2, we will not see any variants since all variants have frequency 0. Thus this measure does not satisfy Desideratum (B).

We now extend the statement of Theorem 1 of the main text to the general setting for an arbitrary number of populations P . To do so, we first restate Condition (C), now for a generic number of populations.

Condition (C’). *The rate measure for the frequency-generating PPP in P populations factorizes across populations: $\nu(d\boldsymbol{\theta}) = \prod_{p=1}^P \nu_p(d\theta_p)$.*

Notice that Condition (C) is a special case of the condition above, when $P = 2$.

We can now state the result which generalizes Theorem 1.

Theorem S1. *Take the general P population model of Equation (S1). If the Poisson point process rate measure in the prior factorizes across populations according to Condition (C’), the model cannot simultaneously generate samples with finitely many variants (Desideratum (A)) and guarantee that there are always more variants to discover (Desideratum (B)).*

Proof. We first show that if Desideratum (B) and Condition (C') hold, then Desideratum (A) cannot hold:

If Desideratum (B) and Condition (C') hold, Desideratum (A) does not hold.

By Condition (C') we have that ν is a “product measure”, i.e. $\nu(d\boldsymbol{\theta}) = \prod_p \nu_p(d\theta_p)$ and in turn we have $\nu_{-p}(d\theta_p) = \nu_p(d\theta_p) \prod_{k:k \neq p} \int_{[0,1]} \nu_k(d\theta_k)$. By Desideratum (B) and its equivalent Equation (S3), for all p , we have $\int_{(0,1]} \nu_{-p}(d\theta_p) = \infty$ thus either:

- (i) $\int_{(0,1]} \nu_p(d\theta_p) = \infty$ and all other $k \neq p$, $\int_{[0,1]} \nu_k(d\theta_k) > 0$, or
- (ii) $0 < \int_{(0,1]} \nu_p(d\theta_p) < \infty$ and there exists one $k \neq p$ for which $\int_{[0,1]} \nu_k(d\theta_k) = \infty$.

We now show that in both cases (i), (ii), Desideratum (A) does not hold.

In case (i), for $k \neq p$:

$$\int_{[0,1]^P} \theta_k \nu(d\boldsymbol{\theta}) = \int_{[0,1]} \theta_k \nu_k(d\theta_k) \int_{[0,1]} \nu_p(d\theta_p) \prod_{i:i \neq k,p} \int_{[0,1]} \nu_i(d\theta_i) = \infty.$$

Since we have $\prod_{i:i \neq k,p} \int_{[0,1]} \nu_i(d\theta_i) > 0$ and $\int_{[0,1]} \nu_p(d\theta_p) = \infty$, it remains to check $\int_{[0,1]} \theta_k \nu_k(d\theta_k) > 0$. Recall that we assumed Equation (S3) is satisfied, we must have the “projected” measure $\nu_k(d\theta_k) \int_{[0,1]} \nu_p(d\theta_p) \prod_{i:i \neq k,p} \int_{[0,1]} \nu_i(d\theta_i)$ to have mass on $(0, 1]$, which implies $\nu_k(d\theta_k)$ must have mass on $(0, 1]$. Then we must also have $\int_{[0,1]} \theta_k \nu_k(d\theta_k) > 0$, hence implying that Desideratum (A) does not hold.

In case (ii), by direct factorization of the rate measure it holds that

$$\int_{[0,1]} \theta_p \nu(d\boldsymbol{\theta}) = \int_{(0,1]} \theta_p \nu_p(d\theta_p) \prod_{k:k \neq p} \int_{[0,1]} \nu_k(d\theta_k) = \infty.$$

Hence, also in this case, Desideratum (A) does not hold. We have then showed that if Desideratum (B) and Condition (C') hold, then Desideratum (A) cannot hold.

We now show that if Condition (C') and Desideratum (A) hold, then Desideratum (B) cannot hold.

If Desideratum (A) and Condition (C') hold, Desideratum (B) does not hold.

Under Desideratum (A) and its equivalent Equation (S2) and Condition (C'), for a given p ,

$$\int_{[0,1]^P} \theta_p \nu(d\boldsymbol{\theta}) = \prod_{k \neq p} \int_{[0,1]} \nu_k(d\theta_k) \times \int_{[0,1]} \theta_p \nu_p(d\theta_p) < \infty.$$

For the condition above to be verified, one of the following two cases must hold:

- (i) $\int_{[0,1]} \theta_p \nu_p(d\theta_p) = 0$, or
- (ii) $\int_{[0,1]} \theta_p \nu_p(d\theta_p) > 0$.

We first show that when (i) holds, Desideratum (B) can't be verified. Indeed, $\int_{[0,1]} \theta_p \nu_p(d\theta_p) = 0$ only holds when $\nu_p(d\theta_p)$ is a δ measure at 0. And in this case, the marginal ν_{-p} has no support on $(0, 1]$, thus Equation (S3) cannot hold for coordinate p .

For case (ii), we have for all coordinates $k \neq p$, $\int_{[0,1]} \nu_k(d\theta_k) < \infty$. We can repeat the argument with a different coordinate and conclude also $\int_{[0,1]} \nu_p(d\theta_p) < \infty$, thus the total mass is finite, $\int \nu(d\boldsymbol{\theta}) < \infty$, and Desideratum (B) cannot hold.

Last, suppose both Desideratum (A) and Desideratum (B). Using the two results above, by contradiction it cannot be that Condition (C') holds. \square

Proof of Theorem 1. Theorem 1 is a special case of Theorem S1 when $P = 2$. \square

B Multi-population BNP models satisfying Desiderata (A) and (B)

In this section, in light of the incompatibility result stated in Theorem 1 and proved in Appendix A, we provide details on BNP models that instead satisfy Desideratum (A) and Desideratum (B).

B.1 Proposed prior satisfies Desideratum (A) and Desideratum (B)

In Equation (6), we proposed a prior distribution that is *not* a product measure factorizing across multiple populations, i.e. it does not satisfy Condition (C). We now prove in Proposition S1 that our proposed prior of Equation (6) satisfies Desideratum (A) and Desideratum (B).

Proposition S1. Consider data generated from Equation (5), where we replace the generic rate measure ν with the following rate measure defined on the unit square $[0, 1]^2$

$$\nu_{\text{prop}}(d\boldsymbol{\theta}) = \frac{\alpha}{B(\gamma_1, c_1)B(\gamma_2, c_2)} \frac{(\theta_1 + \theta_2^{\sigma_2/\sigma_1})^{-\sigma_1}}{(\theta_1 + \theta_2)^{\gamma_1 + \gamma_2}} \theta_1^{\gamma_1 - 1} \theta_2^{\gamma_2 - 1} (1 - \theta_1)^{c_1 - 1} (1 - \theta_2)^{c_2 - 1} d\theta_1 d\theta_2. \quad (\text{S4})$$

When $\alpha, c_1, c_2, \gamma_1, \gamma_2 > 0$ and $\sigma_1, \sigma_2 \in (0, 1)$, desiderata (A) and (B) hold, i.e., by virtue of Lemma S1,

$$(i) \iint_{[0,1]^2} \theta_p \nu_{\text{prop}}(d\boldsymbol{\theta}) < \infty \text{ for } p = 1, 2, \text{ and}$$

$$(ii) \iint_{(0,1]^2} \nu_{\text{prop}}(d\boldsymbol{\theta}) = \infty.$$

Note that in Remark S1 we discussed that (ii) is not equivalent to Equation (S3), but it is sufficient for Equation (S3).

Proof. To show that the desiderata (A) and (B) for our data hold, we equivalently prove the integral requirements provided in Lemma S1 are verified when using ν_{prop} , with hyperparameters $\alpha, c_1, c_2, \gamma_1, \gamma_2 > 0$ and $\sigma_1, \sigma_2 \in (0, 1)$. The crux of the proof relies on the analysis of the behavior of the integral requirements in a neighborhood of the origin $A := [0, \epsilon]^2$ and $D := (0, \epsilon]^2$ for an arbitrarily small scalar $\epsilon > 0$. In what follows, we use the notation $I_A(x) = \mathbb{1}(x \in A)$, $I_D(x) = \mathbb{1}(x \in D)$ and

$$\phi := \frac{\alpha}{B(\gamma_1, c_1)B(\gamma_2, c_2)} < \infty.$$

We start with the integral requirement (i).

Proof of the integral requirement (i) (Equation (S2) in Lemma S1). Notice that for an arbitrary $p \in \{1, 2\}$, we can rewrite Equation (S2) as follows:

$$\iint_{[0,1]^2} \theta_p \nu_{\text{prop}}(d\boldsymbol{\theta}) = \int_{A^C} \theta_p \nu_{\text{prop}}(d\boldsymbol{\theta}) + \int_A \theta_p \nu_{\text{prop}}(d\boldsymbol{\theta}).$$

We will now show that for our proposed ν_{prop} both integrals above are finite. First, consider the integral over A^C above. For $p \in \{1, 2\}$,

$$\int_{A^C} \theta_p \nu_{\text{prop}}(d\boldsymbol{\theta}) = \phi \int I_{A^C}(\boldsymbol{\theta}) \frac{(\theta_1 + \theta_2^{\sigma_2/\sigma_1})^{-\sigma_1}}{(\theta_1 + \theta_2)^{\gamma_1 + \gamma_2}} \theta_p \theta_1^{\gamma_1 - 1} \theta_2^{\gamma_2 - 1} (1 - \theta_1)^{c_1 - 1} (1 - \theta_2)^{c_2 - 1} d\boldsymbol{\theta}. \quad (\text{S5})$$

Notice that we can bound the first part of the integrand as follows:

$$I_{AC}(\boldsymbol{\theta}) \frac{(\theta_1 + \theta_2^{\sigma_2/\sigma_1})^{-\sigma_1}}{(\theta_1 + \theta_2)^{\gamma_1 + \gamma_2}} \leq \min\{\epsilon, \epsilon^{\sigma_2/\sigma_1}\}^{-\sigma_1 - \gamma_1 - \gamma_2} < \infty. \quad (\text{S6})$$

Indeed, if $\boldsymbol{\theta} \notin A^C$, then the inequality holds trivially. If instead $\boldsymbol{\theta} \in A^C$, then $\theta_1 + \theta_2 > \epsilon$. In turn,

$$(\theta_1 + \theta_2)^{-\gamma_1 - \gamma_2} < \epsilon^{-\gamma_1 - \gamma_2} \leq \min\{\epsilon, \epsilon^{\sigma_2/\sigma_1}\}^{-\gamma_1 - \gamma_2},$$

since $\epsilon < 1$. Similarly, $(\theta_1 + \theta_2^{\sigma_2/\sigma_1}) > \min\{\epsilon, \epsilon^{\sigma_2/\sigma_1}\}$ thus

$$(\theta_1 + \theta_2^{\sigma_2/\sigma_1})^{-\sigma_1} < \min\{\epsilon, \epsilon^{\sigma_2/\sigma_1}\}^{-\sigma_1}.$$

The two bounds combined yield Equation (S6). Recognizing that the remaining part of the integrand in Equation (S5) is the kernel of a beta random variable for either value of p , it holds

$$\begin{aligned} \int_{AC} \theta_p \nu_{\text{prop}}(d\boldsymbol{\theta}) &= \phi \int I_{AC}(\boldsymbol{\theta}) \frac{(\theta_1 + \theta_2^{\sigma_2/\sigma_1})^{-\sigma_1}}{(\theta_1 + \theta_2)^{\gamma_1 + \gamma_2}} \theta_1^{(\gamma_1+1)-1} \theta_2^{\gamma_2-1} (1-\theta_1)^{c_1-1} (1-\theta_2)^{c_2-1} d\boldsymbol{\theta} \\ &< \phi \min\{\epsilon, \epsilon^{\sigma_2/\sigma_1}\}^{-\sigma_1 - \gamma_1 - \gamma_2} \int_{AC} \theta_p \theta_1^{\gamma_1-1} \theta_2^{\gamma_2-1} (1-\theta_1)^{c_1-1} (1-\theta_2)^{c_2-1} d\boldsymbol{\theta} \\ &< \infty. \end{aligned} \quad (\text{S7})$$

Thus, it remains for us to check that also on the set A , around the origin, the integral is finite, i.e. $\int_A \theta_p \nu_{\text{prop}}(d\boldsymbol{\theta}) < \infty$. First, notice that on the set A , we can obtain a pointwise upper bound for the Lévy rate ν_{prop} of Equation (6) as follows:

$$\nu_{\text{prop}}(d\boldsymbol{\theta}) I_A(\boldsymbol{\theta}) \leq \eta \frac{(\theta_1 + \theta_2^{\sigma_2/\sigma_1})^{-\sigma_1}}{(\theta_1 + \theta_2)^{\gamma_1 + \gamma_2}} \theta_1^{\gamma_1-1} \theta_2^{\gamma_2-1} I_A(\boldsymbol{\theta}) d\theta_1 d\theta_2,$$

with

$$\eta := \phi \max\{1, (1-\epsilon)^{c_1-1}\} \max\{1, (1-\epsilon)^{c_2-1}\}.$$

We here consider two separate cases.

First, for $p = 1$,

$$\int_A \theta_1 \nu_{\text{prop}}(d\boldsymbol{\theta}) < \eta \int_A \frac{(\theta_1 + \theta_2^{\sigma_2/\sigma_1})^{-\sigma_1}}{(\theta_1 + \theta_2)^{\gamma_1 + \gamma_2}} \theta_1^{(1+\gamma_1)-1} \theta_2^{\gamma_2-1} d\boldsymbol{\theta}.$$

Now notice that $(\theta_1 + \theta_2^{\sigma_2/\sigma_1})^{\sigma_1} > \theta_1^{\sigma_1}$, and for $0 < \delta < \gamma_2$

$$(\theta_1 + \theta_2)^{\gamma_1 + \gamma_2} = (\theta_1 + \theta_2)^{\gamma_1 + \gamma_2 + \delta - \delta} = (\theta_1 + \theta_2)^{\gamma_1 + \delta} (\theta_1 + \theta_2)^{\gamma_2 - \delta} > (\theta_1)^{\gamma_1 + \delta} (\theta_2)^{\gamma_2 - \delta},$$

so we can further obtain the upper bound

$$\begin{aligned} \int_A \theta_1 \nu_{\text{prop}}(d\boldsymbol{\theta}) &< \eta \int_A (\theta_1)^{-\sigma_1} \theta_1^{-\gamma_1 - \delta} \theta_2^{-\gamma_2 + \delta} \theta_1^{(1 + \gamma_1) - 1} \theta_2^{\gamma_2 - 1} d\boldsymbol{\theta} \\ &= \eta \int_0^1 \theta_1^{(1 - \sigma_1 - \delta) - 1} d\theta_1 \int_0^1 \theta_2^{\delta - 1} d\theta_2 < \infty, \end{aligned} \quad (\text{S8})$$

where the last inequality holds as long as $1 - \sigma_1 - \delta > 0$, i.e. $\delta \in (0, 1 - \sigma_1)$.

For $p = 2$,

$$\int_A \theta_2 \nu_{\text{prop}}(d\boldsymbol{\theta}) < \eta \int_A \frac{(\theta_1 + \theta_2^{\sigma_2/\sigma_1})^{-\sigma_1}}{(\theta_1 + \theta_2)^{\gamma_1 + \gamma_2}} \theta_1^{\gamma_1 - 1} \theta_2^{(1 + \gamma_2) - 1} d\boldsymbol{\theta}.$$

We use symmetric bounds as the derivation above for $p = 1$ now for the case $p = 2$, i.e. $(\theta_1 + \theta_2^{\sigma_2/\sigma_1})^{\sigma_1} > (\theta_2)^{\sigma_1}$, and, for $0 < \delta < \gamma_1$, $(\theta_1 + \theta_2)^{\gamma_1 + \gamma_2} > (\theta_1)^{\gamma_1 - \delta} (\theta_2)^{\gamma_2 + \delta}$, and plugging them in we get

$$\int_A \theta_2 \nu_{\text{prop}}(d\boldsymbol{\theta}) < \eta \int_A (\theta_1)^{\delta - 1} \theta_2^{(1 - \sigma_1 - \delta) - 1} d\boldsymbol{\theta} = \eta \int_0^1 (\theta_1)^{\delta - 1} d\theta_1 \int_0^1 \theta_2^{(1 - \sigma_1 - \delta) - 1} d\theta_2 < \infty, \quad (\text{S9})$$

where the last inequality holds as long as $1 - \sigma_1 - \delta > 0$, i.e. $\delta \in (0, 1 - \sigma_1)$. Thus, Equations (S7) to (S9) combined yield requirement (i) (Equation (S2)).

This concludes the proof of integral requirement (i) (see Equation (S2) in Lemma S1).

Proof of the integral requirement (ii) which implies Equation (S3). Recall $D = (0, \epsilon]^2$. We here recur to a decomposition similar to the first part of the proof, and rewrite the integral as

$$\iint_{(0,1]^2} \nu_{\text{prop}}(d\boldsymbol{\theta}) = \int_{(0,1]^2 \setminus D} \nu_{\text{prop}}(d\boldsymbol{\theta}) + \int_D \nu_{\text{prop}}(d\boldsymbol{\theta}) > \int_D \nu_{\text{prop}}(d\boldsymbol{\theta}).$$

We now show that in any neighborhood D of the origin, the integral above diverges. First, notice that on the set D , we can pointwise (lower) bound the Lévy rate of our proposed prior

(Equation (6)) as follows:

$$\nu_{\text{prop}}(d\boldsymbol{\theta})I_D(\boldsymbol{\theta}) \geq \kappa \frac{(\theta_1 + \theta_2^{\sigma_2/\sigma_1})^{-\sigma_1}}{(\theta_1 + \theta_2)^{\gamma_1 + \gamma_2}} \theta_1^{\gamma_1 - 1} \theta_2^{\gamma_2 - 1} I_D(\boldsymbol{\theta}) d\theta_1 d\theta_2,$$

with

$$\kappa := \frac{\alpha}{B(\gamma_1, c_1)B(\gamma_2, c_2)} \min\{1, (1 - \epsilon)^{c_1 - 1}\} \min\{1, (1 - \epsilon)^{c_2 - 1}\},$$

since on D , $\theta_p < 1$. Hence,

$$\int_D \nu_{\text{prop}}(d\boldsymbol{\theta}) \geq \int_{D \cap \{\theta_1 \geq \theta_2\}} \nu(d\boldsymbol{\theta}) \geq \kappa \int_0^\epsilon \int_0^{\theta_1} \frac{(\theta_1 + \theta_2^{\sigma_2/\sigma_1})^{-\sigma_1}}{(\theta_1 + \theta_2)^{\gamma_1 + \gamma_2}} \theta_1^{\gamma_1 - 1} \theta_2^{\gamma_2 - 1} d\theta_1 d\theta_2.$$

In the case in which $\sigma_1 \leq \sigma_2$ when $0 \leq \theta_2 \leq \theta_1 \leq 1$ it is also the case that $\theta_2^{\sigma_2/\sigma_1} \leq \theta_1$ (since $\sigma_2/\sigma_1 \geq 1$). In turn, $\theta_1 + \theta_2^{\sigma_2/\sigma_1} \leq 2\theta_1$ which implies $(\theta_1 + \theta_2^{\sigma_2/\sigma_1})^{-\sigma_1} \geq (2\theta_1)^{-\sigma_1}$. Similarly, $\theta_1 + \theta_2 \leq 2\theta_1$ which implies $(\theta_1 + \theta_2)^{-\gamma_1 - \gamma_2} \geq (2\theta_1)^{-\gamma_1 - \gamma_2}$. The two observations together allow us to further bound the integral above:

$$\begin{aligned} \int_{(0,1]^2} \nu_{\text{prop}}(d\boldsymbol{\theta}) &\geq \int_D \nu_{\text{prop}}(d\boldsymbol{\theta}) \geq \kappa \int_0^\epsilon \int_0^{\theta_1} (2\theta_1)^{-\sigma_1 - \gamma_1 - \gamma_2} \theta_1^{\gamma_1 - 1} \theta_2^{\gamma_2 - 1} d\theta_1 d\theta_2 \\ &= \kappa 2^{-\sigma_1 - \gamma_1 - \gamma_2} \int_0^\epsilon \theta_1^{-\sigma_1 - \gamma_2 - 1} \left[\int_0^{\theta_1} \theta_2^{\gamma_2 - 1} d\theta_2 \right] d\theta_1 \\ &= \frac{\kappa 2^{-\sigma_1 - \gamma_1 - \gamma_2}}{\gamma_2} \int_0^\epsilon \theta_1^{-\sigma_1 - 1} d\theta_1 \\ &= +\infty, \end{aligned}$$

where the last equality holds whenever $\sigma_1 \geq 0$.

In the case in which $\sigma_1 > \sigma_2$, when $0 \leq \theta_1 \leq \theta_2 \leq 1$ it is also the case that $\theta_2^{\sigma_2/\sigma_1} \geq \theta_1$ (since $\sigma_2/\sigma_1 \leq 1$). In turn, $\theta_1 + \theta_2^{\sigma_2/\sigma_1} \leq 2\theta_2^{\sigma_2/\sigma_1}$ which implies $(\theta_1 + \theta_2^{\sigma_2/\sigma_1})^{-\sigma_1} \geq (2\theta_2^{\sigma_2/\sigma_1})^{-\sigma_1}$. Similarly, $\theta_1 + \theta_2 \leq 2\theta_2$ which implies $(\theta_1 + \theta_2)^{-\gamma_1 - \gamma_2} \geq (2\theta_2)^{-\gamma_1 - \gamma_2}$.

The two observations together allow us to further bound the integral above:

$$\begin{aligned}
\int_{(0,1]^2} \nu_{\text{prop}}(d\boldsymbol{\theta}) &\geq \int_D \nu_{\text{prop}}(d\boldsymbol{\theta}) \geq \kappa \int_0^\epsilon \int_0^{\theta_2} (2\theta_2^{\sigma_2/\sigma_1})^{-\sigma_1} (2\theta_2)^{-\gamma_1-\gamma_2} \theta_2^{\gamma_2-1} \theta_1^{\gamma_1-1} d\theta_1 d\theta_2 \\
&= \kappa 2^{-\sigma_1-\gamma_1-\gamma_2} \int_0^\epsilon \theta_2^{-\sigma_2-\gamma_1-1} \left[\int_0^{\theta_2} \theta_1^{\gamma_1-1} d\theta_1 \right] d\theta_2 \\
&= \frac{\kappa 2^{-\sigma_1-\gamma_1-\gamma_2}}{\gamma_1} \int_0^\epsilon \theta_2^{-\sigma_2-1} d\theta_2 \\
&= +\infty,
\end{aligned}$$

where the last equality holds whenever $\sigma_2 \geq 0$.

This concludes the proof of integral requirement (ii), in turn yielding the thesis. \square

B.2 Another model defines proper rate measure satisfies Desideratum (A) and Desideratum (B)

We emphasize that the prior distribution we proposed in Equation (6) is not the *only* prior that satisfies Desideratum (A) and Desideratum (B). Next, we provide another example of a prior satisfying such requirements.

Example 1 (Hierarchical-3BP (Masoero et al., 2021)). *A hierarchical Bayesian nonparametric multi-population model satisfying Desideratum (A) and Desideratum (B) was proposed by Masoero et al. (2021). The model consists of two layers: first, a latent common “super-population” of frequencies pairs drawn from a Poisson Point Process (PPP) with Lévy measure given by the three parameter beta process (3BP):*

$$\nu_{\text{3BP}}(d\theta) = \alpha \frac{\Gamma(1+c)}{\Gamma(1-\sigma)\Gamma(c+\sigma)} \theta^{-1-\sigma} (1-\theta)^{c+\sigma-1} \mathbf{1}(\theta \in [0,1]) d\theta.$$

Then, conditionally on the latent common frequencies, population specific frequencies are drawn using a fixed parametric form:

$$\begin{aligned}
\{\theta_{0,1}, \theta_{0,2}, \dots, \} &\sim \text{PPP}(\nu_{\text{3BP}}(d\theta)) \\
\theta_{1,k} \mid \theta_{0,k} &\sim \text{Beta}(\theta_1 \mid a_1\theta_{0,k}, b_1(1-\theta_{0,k})) \quad \text{and} \quad \theta_{2,k} \mid \theta_{0,k} \sim \text{Beta}(\theta_2 \mid a_2\theta_{0,k}, b_2(1-\theta_{0,k})).
\end{aligned}$$

Using the theory of marked Poisson processes, the population-specific rates are themselves

Poisson point processes with rate measure given by

$$\mu(d\boldsymbol{\theta}) = \int_0^1 \prod_{j=1}^2 \text{Beta}(\theta_j | a_j s, b_j(1-s)) \nu_{3\text{BP}}(ds) d\theta_1 d\theta_2.$$

The integral requirements (i), (ii) of Equations (S2) and (S3) can be shown analytically. For (i), we here show finiteness of the integral in the first population. The argument for the second population is symmetric and omitted.

$$\begin{aligned} \iint \theta_1 \mu(d\boldsymbol{\theta}) &= \iint \theta_1 \int_{s=0}^{s=1} \prod_{j=1}^2 \text{Beta}(\theta_j | a_j s, b_j(1-s)) \nu_{3\text{BP}}(ds) d\boldsymbol{\theta} \\ &= \int_{s=0}^{s=1} \iint \left\{ \theta_1 \prod_{j=1}^2 \text{Beta}(\theta_j | a_j s, b_j(1-s)) d\boldsymbol{\theta} \right\} \nu_{3\text{BP}}(ds) \\ &= \int_0^1 \int \theta_1 \text{Beta}(\theta_1 | a_1 s, b_1(1-s)) d\theta_1 \nu_{3\text{BP}}(ds) \\ &= \int_0^1 \frac{a_1 s}{b_1 + (a_1 - b_1)s} \nu_{3\text{BP}}(ds) \\ &< \frac{\alpha}{\Gamma(1-\sigma)\Gamma(c+\sigma) \min\{a_1, b_1\}} \int s^{(1-\sigma)-1} (1-s)^{c+\sigma-1} ds < \infty. \end{aligned}$$

For (ii),

$$\begin{aligned} \iint \mu(d\boldsymbol{\theta}) &= \iint \int_{s=0}^{s=1} \prod_{j=1}^2 \text{Beta}(\theta_j | a_j s, b_j(1-s)) \nu_{3\text{BP}}(ds) d\boldsymbol{\theta} \\ &= \int_{s=0}^{s=1} \iint \left\{ \prod_{j=1}^2 \text{Beta}(\theta_j | a_j s, b_j(1-s)) d\boldsymbol{\theta} \right\} \nu_{3\text{BP}}(ds) \\ &= \int_0^1 \nu_{3\text{BP}}(ds) = \infty. \end{aligned}$$

C Conjugacy

We now show that our proposed prior introduced in Equation (6) when paired with the two-population Bernoulli process model yields a posterior that is conjugate.

Lemma S2. *The multipopulation Bayesian nonparametric hierarchical model obtained by pairing the variants prior rate measure ν_{prop} (of Equation (6)) with independent Bernoulli*

process likelihoods within each subpopulation (i.e., $X_{p,n,\ell} \mid \theta_{p,\ell} \sim \text{Bernoulli}(\theta_{p,\ell})$, independently across p and ℓ , and i.i.d. across n for the same p, ℓ), yields a conjugate posterior distribution.

Proof. Recall that our proposed prior for variants frequencies ν_{prop} was defined in Equation (S4). Our proof technique relies on the fact that, if we condition on an observed sample of N_1 units from population 1 and N_2 units from population 2, the *posterior* distribution of the variants frequencies in our Bayesian hierarchical model can be obtained by thinning the Poisson process underlying the model. I.e., for variants ψ_ℓ , $\ell = 1, 2, \dots$, the corresponding variants' frequency (posterior) law $f_\ell(\boldsymbol{\theta})$ can be obtained by thinning the rate measure ν_{prop} by the probability of the realized sample induced by the likelihood component of our model:

$$\begin{aligned} f_\ell(\boldsymbol{\theta}) &\propto \nu_{\text{prop}}(d\boldsymbol{\theta}) \cdot \prod_{p=1,2} \prod_{n=1}^{N_p} \text{Bernoulli}(x_{p,n,\ell} \mid \theta_p) \\ &\propto \frac{(\theta_1 + \theta_2^{\sigma_2/\sigma_1})^{-\sigma_1}}{(\theta_1 + \theta_2)^{\gamma_1 + \gamma_2}} \theta_1^{\gamma_1 + \sum_{n=1}^{N_1} x_{1,\ell,n} - 1} \theta_2^{\gamma_2 + \sum_{n=1}^{N_2} x_{2,\ell,n} - 1} \\ &\quad \times (1 - \theta_1)^{c_1 + \sum_{n=1}^{N_1} (1 - x_{1,\ell,n}) - 1} (1 - \theta_2)^{c_2 + \sum_{n=1}^{N_2} (1 - x_{2,\ell,n}) - 1}. \end{aligned}$$

This distribution is within the same family as the one induced by the prior ν_{prop} in the sense that the two share the same beta form, up to the same multiplicative leading term $\frac{(\theta_1 + \theta_2^{\sigma_2/\sigma_1})^{-\sigma_1}}{(\theta_1 + \theta_2)^{\gamma_1 + \gamma_2}}$. Notice that for a given ℓ , it is either the case that ψ_ℓ has been observed in at least one sample, or that it has not yet been observed. In the former case (ψ_ℓ observed), there exists at least one pair (p, n) for which $x_{p,n,\ell} = 1$. This implies that $f_\ell(\boldsymbol{\theta}) \leq \theta_p \nu_{\text{prop}}(d\boldsymbol{\theta})$. Since by assumption we have $\int \theta_p \nu_{\text{prop}}(d\boldsymbol{\theta}) < \infty$, this further implies that the density above can be normalized. Viceversa, in the latter case (variant not yet observed), the distribution above simplifies to

$$\begin{aligned} f_\ell(\boldsymbol{\theta}) &\propto \nu_{\text{prop}}(d\boldsymbol{\theta}) \prod_{p=1,2} \prod_{n=1}^{N_p} \text{Bernoulli}(0 \mid \theta_p) \\ &= \frac{\alpha}{B(\gamma_1, c_1) B(\gamma_2, c_2)} \frac{(\theta_1 + \theta_2^{\sigma_2/\sigma_1})^{-\sigma_1}}{(\theta_1 + \theta_2)^{\gamma_1 + \gamma_2}} \theta_1^{\gamma_1 - 1} \theta_2^{\gamma_2 - 1} (1 - \theta_1)^{c_1 + N_1 - 1} (1 - \theta_2)^{c_2 + N_2 - 1} d\boldsymbol{\theta}, \end{aligned}$$

which is again within the same family of our PPP prior, satisfying Desideratum (A) and Desideratum (B). \square

D Competing Bayesian nonparametric baselines for prediction in multi-population settings

In this section we introduce in detail the two alternative Bayesian nonparametric baselines used in our experiments of Sections 8.1 and 8.2 to benchmark our novel proposed approach when forming predictions for future variant counts in the presence of multiple populations.

D.1 Dependent three parameter beta processes [d3BP]

The first competing model we consider is one where we ignore the population label, and “pool” our observations as if they were being generated from the same population. We call this (fully) dependent model because we can view it as sample one population’s variant frequency and the other fully dependent on it. We use a three parameter beta process prior to model the variants’ frequencies, and again assume that samples are drawn from Bernoulli processes conditionally given the latent variant frequencies. Formally, for P_0 an arbitrary diffuse measure on the space of variants’ labels Ψ ,

$$\begin{aligned} \Theta &\sim \text{PPP}(\nu_{3\text{BP}}(d\theta) \times P_0(d\psi)) \\ X_{p,n} \mid \Theta &\sim \text{BeP}(\Theta). \end{aligned} \tag{S10}$$

where

$$\nu_{3\text{BP}}(d\theta) = \alpha \frac{\Gamma(1+c)}{\Gamma(1-\sigma)\Gamma(c+\sigma)} \theta^{-1-\sigma} (1-\theta)^{c+\sigma-1} \mathbf{1}(\theta \in (0,1)) d\theta,$$

with $X_{p,n}$ i.i.d. across p and n . This is equivalent to adopting the approach of [Masoero et al. \(2021\)](#) after discarding information about the individuals’ population. Recall that, given a tuple of integers $\mathbf{k} = [k_1, k_2]^\top$, we call a “ \mathbf{k} -ton” any variant appearing exactly k_p times in population p .

Proposition S2 (Predicting the number of future \mathbf{k} -tons under the d3BP). *Assume to have collected N_1 samples $X_{1,1:N_1}$ from population 1, and N_2 samples $X_{2,1:N_2}$ from population 2 under the data generating process of Equation (S10). Then the number of new variants that have not been observed in any of the first $N_1 + N_2$ samples and appear exactly \mathbf{k} times in additional $\mathbf{M} = [M_1, M_2]^\top$ samples collected from population 1 and 2 respectively is given*

by:

$$U_{\mathbf{N}}^{(\mathbf{M}, \mathbf{k})} \mid X_{1,1:N_1}, X_{2,1:N_2} \sim \text{Poisson} \left(\lambda_{\text{d3BP}, \mathbf{N}}^{(\mathbf{M}, \mathbf{k})} \right),$$

where, for $(a)_{b\uparrow} := \Gamma(a+b)/\Gamma(a+1)$ the rising factorial,

$$\lambda_{\text{d3BP}, \mathbf{N}}^{(\mathbf{M}, \mathbf{k})} = \alpha \binom{M_1}{k_1} \binom{M_2}{k_2} \frac{(c+\sigma)_{(N_1+N_2+M_1+M_2-k_1-k_2)\uparrow} (1-\sigma)_{(k_1+k_2-1)\uparrow}}{(c+1)_{(N_1+N_2+M_1+M_2-1)\uparrow}}.$$

The proof largely follows [Masoero et al. \(2021\)](#), by observing that the variant frequencies not seen being a thinned Poisson point process.

Proof. Under this model, variants' frequencies follow a 3BP with rate measure $\nu_{\text{3BP}}(d\theta)$. Then, the frequencies of those variants that (i) have not been seen in the first N_1+N_2 samples $X_{1,1:N_1}$ and $X_{2,1:N_2}$ and (ii) will be seen exactly \mathbf{k} times in the subsequent \mathbf{M} samples, come from a thinned Poisson point process with rate measure $\nu_{\text{3BP}}(d\theta)\text{Bernoulli}(0|\theta)^{M_1}\text{Bernoulli}(0|\theta)^{M_2}$ and is independent of the collection of frequencies that did appear in the first N_1, N_2 samples,

$$\begin{aligned} & \nu_{\text{3BP}}(d\theta)\text{Bernoulli}(0|\theta)^{N_1}\text{Bernoulli}(0|\theta)^{N_2} \\ & \binom{M_1}{k_1} \text{Bernoulli}(1|\theta)^{k_1} \text{Bernoulli}(0|\theta)^{M_1-k_1} \\ & \binom{M_2}{k_2} \text{Bernoulli}(1|\theta)^{k_2} \text{Bernoulli}(0|\theta)^{M_2-k_2} \\ & = \binom{M_1}{k_1} \binom{M_2}{k_2} \nu(d\theta) \text{Bernoulli}(1|\theta)^{k_1+k_2} \text{Bernoulli}(0|\theta)^{M_1+M_2+N_1+N_2-k_1-k_2}. \quad (\text{S11}) \end{aligned}$$

By the properties of Poisson point processes, the number of \mathbf{k} -tons follows a Poisson distribution with expectation being the integral of the thinned rate measure. Following [Masoero et al. \(2021, Proposition 4\)](#), the integral is given by

$$\lambda_{\text{d3BP}, \mathbf{N}}^{(\mathbf{M}, \mathbf{k})} = \alpha \binom{N_1}{k_1} \binom{N_2}{k_2} \frac{(c+\sigma)_{(M_1+M_2+N_1+N_2-k_1-k_2)\uparrow} (1-\sigma)_{(k_1+k_2-1)\uparrow}}{(c+1)_{(M_1+M_2+N_1+N_2-1)\uparrow}}.$$

□

We can compute the distribution of the total number of future variants by summing across \mathbf{k} -tons, or, equivalently, by leveraging the fact that the results for the pooled population coincide with those provided in [Masoero et al. \(2021\)](#).

D.2 i3BP

The alternative baseline method we consider is one in which in each of the two populations, variants frequencies follow a three parameter beta process, independent of the other population. In each population, variants occur according to independent Bernoulli processes. In this case, the two populations are modeled as completely independent, and we therefore call this model the “independent” 3BP (i3BP):

$$\begin{aligned} \Theta_p &\stackrel{\text{ind}}{\sim} \text{PPP}(\nu_{3\text{BP}}(\text{d}\theta; \alpha_p, c_p, \sigma_p) \times P_0(\text{d}\psi)) \\ X_{p,n} \mid \Theta &\sim \text{BeP}(\Theta_p). \end{aligned} \tag{S12}$$

Here, we overload the notation $\nu_{3\text{BP}}(\text{d}\theta; \alpha_p, c_p, \sigma_p)$ to emphasize that in each population p the variants frequencies are driven by a different three-parameter beta process with its own hyperparameters. Because of independency, and the fact that we use a diffuse measure for locations, the probability that the same variant is observed in both population under this model is zero. As a consequence, under this model the total number of *shared* variants (past, present, future) is zero. Therefore, we can’t use this model to make any prediction about shared variants, but we still could use it to predict the *total* number of new future variants, by summing the predictions arising from each population and ignoring the fact that in the real data some of the past and future variants are shared.

Proposition S3 (total number in i3BP). *Assume to have collected N_1 samples $X_{1,1:N_1}$ from population 1, and N_2 samples $X_{2,1:N_2}$ from population 2 under the data generating process of the i3BP in Equation (S12). The variant frequencies in population 1 and 2 are governed by two independent 3BP, the first with hyperparameters α_1, σ_1, c_1 and the second with hyperparameters α_2, σ_2, c_2 . The total number of new variants that is going to be observed in $\mathbf{M} = [M_1, M_2]^\top$ additional samples follows a Poisson distribution with parameter $\lambda_{i3\text{BP},\mathbf{N}}^{(\mathbf{M})}$ where*

$$\lambda_{i3\text{BP},\mathbf{N}}^{(\mathbf{M})} = \alpha_1 \sum_{k_1=1}^{M_1} \frac{(c_1 + \sigma_1)_{(N_1+k_1-1)\uparrow}}{(c_1 + 1)_{(N_1+k_1-1)\uparrow}} + \alpha_2 \sum_{k_2=1}^{M_2} \frac{(c_2 + \sigma_2)_{(N_2+k_2-1)\uparrow}}{(c_2 + 1)_{(N_2+k_2-1)\uparrow}}.$$

Proof. The result is a trivial application of [Masoero et al. \(2021, Proposition 1\)](#). Indeed, by [Masoero et al. \(2021, Proposition 1\)](#), the number of new variants in population p is Poisson distributed with mean $\alpha_p \sum_{k=1}^{M_p} \frac{(c_p + \sigma_p)_{(N_p+k-1)\uparrow}}{(c_p + 1)_{(N_p+k-1)\uparrow}}$. Moreover, because the two populations are independent and the sum of two independent Poisson random variables is a Poisson random

variable with parameter given by the sum of the two parameters, the thesis follows. \square

E Proofs for the posterior predictive quantities in the two-population proposed model

In this section we provide the proofs for the results stated in Section 6.1.

E.1 Proof of Proposition 2

Proof. We assume to have collected $\mathbf{N} = [N_1, N_2]^\top$ samples $X_{1,1:N_1}, X_{2,1:N_2}$ from the model of Equation (5) where ν_{prop} is the rate measure defined in Equation (S4). It follows from the same method used in Masoero et al. (2022, Proposition 2) on thinning of a Poisson point process, that, given the data $X_{1,1:N_1}, X_{2,1:N_2}$, the frequencies corresponding to variants that (i) have not yet been observed in any of the first $N_1 + N_2$ and are going to be observed exactly $\mathbf{k} = [k_1, k_2]^\top$ times in each population when additional $\mathbf{M} = [M_1, M_2]^\top$ samples are collected, with $0 \leq k_p \leq M_p$ for $p = 1, 2$ and $k_1 + k_2 > 0$, follows a thinned Poisson point process with rate measure:

$$\begin{aligned}
& \nu_{\text{prop}}(d\boldsymbol{\theta}) \text{Bernoulli}(0 \mid \theta_1)^{N_1} \text{Bernoulli}(0 \mid \theta_2)^{N_2} \\
& \binom{M_1}{k_1} \text{Bernoulli}(1 \mid \theta_1)^{k_1} \text{Bernoulli}(0 \mid \theta_1)^{M_1 - k_1} \\
& \binom{M_2}{k_2} \text{Bernoulli}(1 \mid \theta_2)^{k_2} \text{Bernoulli}(0 \mid \theta_2)^{M_2 - k_2} \\
& = \alpha \binom{M_1}{k_1} \binom{M_2}{k_2} \frac{(\theta_1 + \theta_2^{\sigma_2/\sigma_1})^{-\sigma_1}}{(\theta_1 + \theta_2)^{\gamma_1 + \gamma_2}} \\
& \quad \times \theta_2^{\gamma_2 + k_2 - 1} (1 - \theta_2)^{c_2 + M_2 + N_2 - k_2 - 1} \theta_1^{\gamma_1 + k_1 - 1} (1 - \theta_1)^{c_1 + N_1 - k_1 - 1} \\
& \quad \times \frac{1}{B(\gamma_1, c_1) B(\gamma_2, c_2)}
\end{aligned} \tag{S13}$$

Thus this number of these variants, exist exactly \mathbf{k} times in \mathbf{M} new samples, $U_{\mathbf{N}}^{(\mathbf{M}, \mathbf{k})}$, is a Poisson distributed random variable whose parameter is the integral of the rate measure in

Equation (S13):

$$\begin{aligned} \lambda_{\mathbf{N}}^{(M, \mathbf{k})} &= \alpha \binom{M_1}{k_1} \binom{M_2}{k_2} \frac{B(\gamma_2 + k_2, c_2 + M_2 + N_2 - k_2) B(\gamma_1 + k_1, c_1 + M_1 + N_1 - k_1)}{B(\gamma_1, c_1) B(\gamma_2, c_2)} \\ &\quad \times \mathbb{E}_{Z, W} \left[\frac{(Z + W^{\sigma_2/\sigma_1})^{-\sigma_1}}{(Z + W)^{\gamma_1 + \gamma_2}} \right], \end{aligned} \tag{S14}$$

where $B(a, b)$ is the beta function, and $\mathbb{E}_{Z, W}$ is the expectation over independent beta distributed random variables Z, W :

$$Z \sim \text{Beta}(\gamma_1 + k_1, c_1 + M_1 + N_1 - k_1), \quad W \sim \text{Beta}(\gamma_2 + k_2, c_2 + M_2 + N_2 - k_2).$$

□

E.2 Total number of variants

Next, we give the proof of Proposition 3.

Proof. The proof closely resembles the proof of Masoero et al. (2022, Proposition 1). The idea is to consider the corresponding frequencies of newly appeared variants in one sample that does not appear in previous samples. These frequencies follow a (thinned) Poisson point process. Under Equation (5) where ν is the rate measure defined in Equation (S4), the frequencies θ_ℓ follow a Poisson point process with rate measure $\nu_{\text{prop}}(d\theta)$. Under independent two population Bernoulli process (where each sample is an independent Bernoulli trials), given an individual from population p , variant ℓ appears with probability $\theta_{\ell, p}$ independently across all samples of population 1 and 2. The probability a variant did not appear in those samples is $\text{Bernoulli}(0 \mid \theta_{\ell, 1})^{N_1} \text{Bernoulli}(0 \mid \theta_{\ell, 2})^{N_2}$. Therefore, the collection of variants that did not appear in the first $\mathbf{N} = (N_1, N_2)$ are characterized by a collection of frequencies whose distribution is given by a thinned multivariate Poisson point process with rate $\nu_{\text{prop}}(d\theta) \text{Bernoulli}(0 \mid \theta_1)^{N_1} \text{Bernoulli}(0 \mid \theta_2)^{N_2}$ and are independent to the collection of frequencies that did appear in the first \mathbf{N} samples.

Within this collection of variant frequencies, there are some will appear in the next sample from population 1 with probability $\text{Bernoulli}(1 \mid \theta_1)$ the collection of these variant frequencies is inturn a furthering thinning. That is, the variant frequencies whose corresponding variants did not appear in the first $\mathbf{N} = (N_1, N_2)$ samples but is going to appear if we were to collect

an additional sample from population 1 samples is characterized by a thinned Poisson point process with rate measure

$$\nu_{\text{prop}}(d\boldsymbol{\theta}) \text{Bernoulli}(0|\theta_1)^{N_1} \text{Bernoulli}(0|\theta_2)^{N_2} \text{Bernoulli}(1|\theta_1)$$

and independent of the collection of frequencies that did not appear in the first (N_1, N_2) samples.

Similarly if the first follow up sample is from population 2 the (thinned) rate measure is

$$\nu_{\text{prop}}(d\boldsymbol{\theta}) \text{Bernoulli}(0|\theta_1)^{N_1} \text{Bernoulli}(0|\theta_2)^{N_2} \text{Bernoulli}(1|\theta_2)$$

and is independent of the collection of frequencies that did not appear in the first (N_1, N_2) samples.

Recursively, suppose we first sample follow up samples from population 1, for $m_1 \geq 1$, the collection of variant frequencies corresponding to variants that did not appear in the first $(N_1 + m_1 - 1, N_2)$ samples but then did appear in the m_1 th follow-up samples of population 1 comes from a thinned Poisson point process with rate measure

$$\nu_{\text{prop}}(d\boldsymbol{\theta}) \text{Bernoulli}(0|\theta_1)^{N_1+m_1-1} \text{Bernoulli}(0|\theta_2)^{N_2} \text{Bernoulli}(1|\theta_1)$$

The number of such variants, by property of Poisson point process, is a Poisson distribution with mean being the integral of the rate measure, and by Equation (S14), it is exactly $\lambda_{(N_1+m_1-1, N_2)}^{([1,0],[1,0])}$.

Now suppose we finished all M_1 follow up of population 1 and start the follow up sample of population 2. For $m_2 \geq 1$, the collection of variant frequencies corresponding to variants that did not appear in the first $(N_1 + M_1, N_2 + m_2 - 1)$ samples but then did appear in the m_2 th follow-up samples of population 2 comes from a thinned Poisson point process with rate measure

$$\nu_{\text{prop}}(d\boldsymbol{\theta}) \text{Bernoulli}(0|\theta_1)^{N_1+M_1} \text{Bernoulli}(0|\theta_2)^{N_2+m_2-1} \text{Bernoulli}(1|\theta_2)$$

The number of such variants is a Poisson distribution with mean being the integral of the rate measure, and by Equation (S14), it is exactly $\lambda_{(N_1+M_1, N_2+m_2-1)}^{([0,1],[0,1])}$.

Each of these Poisson point processes are independent. Since the total number of new variants $U_{\mathbf{N}}^{(\mathbf{M})}$ are sum of new variants discovered at these $M_1 + M_2$ samples, which are independently Poisson distributed, the total number of new variants are also Poisson distributed with mean

$$\sum_{m_1=1}^{M_1} \lambda_{(N_1+m_1-1, N_2)}^{((1,0),(1,0))} + \sum_{m_2=1}^{M_2} \lambda_{(N_1+M_1, N_2+m_2-1)}^{((0,1),(0,1))}$$

The recursive scheme of population 2 following population 1 is not the only method to get the distribution, one can also start with population 2 then population 1 or any other recursive scheme to get $\mathbf{M} = (M_1, M_2)$. \square

F Details on simulating data

F.1 Sampling from the proposed two population model via (truncated) Poisson point processes

We here provide a practical algorithm to generate synthetic data from the proposed hierarchical model introduced in Equation (5) where the Lévy rate measure is given in Equation (S4).

At a high level, there exist two main strategies to generate data from nonparametric hierarchical models like the one in Equation (5). The first, is to devise an exact “marginal” representation, where the infinitude of latent atoms is integrated out and observations are generated by leveraging an iterative predictive “marginal” scheme (e.g., the Chinese restaurant process, the Indian buffet process and related “urn-schemes”). The other approach is to rely on an approximate “conditional” representation, in which the infinitude of latent atoms is approximated via a truncated representation of the infinite measure (Campbell et al., 2019), and observations are generated conditionally i.i.d. on this finite representation.

In principle we can derive a marginal representation of the proposed process following Broderick et al. (2018). However such marginal representation would require us to solve many numerical integrals for every sample to determine whether a pre existing variant should exist in a follow up sample. To avoid this computational overhead, we decide to adopt the approximate (truncated) approach: we draw a truncated, approximate Poisson point process and obtain a sample $X_{p,n}$ by repeatedly sample Bernoulli trials using the sampled variant frequencies.

A general approach to sample inhomogeneous Poisson point process with an arbitrary target

rate is to find a “proposal” rate measure dominating the target, and then adopt rejection sampling (Saltzman et al., 2012). For our specific proposal, we truncated the domain to be larger than 10^{-10} , variants with frequency less than this will have little probability to exist in 500 samples as in our simulation settings.

To sample this truncated measure we chose a proposal process being piecewise constant that dominates our (truncated) rate. To do so, we span a (log-scaled) mesh using $\{10^{-10}, 10^{-9}, \dots, 10^0\}$ and we sample points within each grid independently. In each grid \mathcal{G} , we sample a homogeneous Poisson point process with rate being the maximum rate in that grid ($\lambda_m = \max_{\theta \in \mathcal{G}} \nu_{\text{prop}}(\theta)$) and we accept a sample at θ_ℓ with probability $\nu_{\text{prop}}(\theta_\ell)/\lambda_m$.

These procedure will generate an approximated realization of θ_ℓ , then we sample the Bernoulli process condition on these weights.

F.2 d3BP

To obtain a d3BP-Bernoulli process of size $\mathbf{N} = [N_1, N_2]^\top$ we first obtain $N_1 + N_2$ samples from a 3BP-Bernoulli process using the Indian buffet representation (Broderick et al., 2012; Masoero et al., 2021). Then, we randomly split individuals into two groups of size N_1 and N_2 .

G Additional experiments

In this section we provide additional experimental evidence of the predictive performance on synthetic and real genomic data of our newly proposed BNP model as well as a number of preexisting competing (single population) methods. Specifically, we consider the d3BP, i3BP (as defined in Appendices D.1 and D.2), as well as the Good-Toulmin (GT) estimator — recently employed by Chakraborty et al. (2019) in the context of rare genomic variants discovery — and the fourth order Jackknife estimator (J4) Gravel and National Heart Lung & Blood Institute (NHLBI) GO Exome Sequencing Project (2014). As well as linear programming (Zou et al., 2016, lp), and the scaled process (SP) method by Camerlenghi et al. (2022). In real data experiments we choose the best performing single population methods and apply it in two different ways namely assuming populations do not share variants or are in fact from a single population.

G.1 Additional synthetic experiments

Here we generate data from i3BP and d3BP respectively to test if our model has the ability to handle data generated from these misspecified models. For i3BP, we generate data using three parameter Indian buffet process, (Broderick et al., 2012; Masoero et al., 2022), assuming there is no shared variants. For d3BP, we generate variants from a single Indian buffet process then randomly split individuals as two populations.

Data from i3BP For i3BP, we sample from parameter $(\alpha_1, c_1, \sigma_1, \alpha_2, c_2, \sigma_2) = (20, 1, .6, 20, 1, .3)$, and $(40, 1, .1, 40, 1, .3)$ where $(\alpha_p, c_p, \sigma_p)$ are the corresponding 3BP’s mass, concentration and discount parameters in population p .

Figure S6 visualize the ground truth growth curve and predicted growth curve by all three models we tested when data is from i3BP, as well as the heat map of relative residual on the number of k-tons. In this setting our proposed method works as well as the correctly specified i3BP model on average and had larger variance, potentially due to the wrong assumption that all variants will eventually become shared. Meanwhile d3BP vastly underestimate number of ktons especially for $k_1, k_2 > 1$ as it assumes variants share the same frequencies. The overestimating of singletons in d3BP methods is not surprising since singletons are more compatible with the assumptions of all variants share the same variants and by chance we discovers it in one population.

d3BP data We sample d3BP with parameter $(\alpha, c, \sigma) = (20, 1, .5), (40, 1, .1)$ respectively.

Figure S7 visualize the ground truth growth curve and predicted growth curve by all three models we tested when data is from d3BP, as well as the heat map of relative residual on the number of k-tons. The data has relatively large amount of sharing thus we see a strong double counting problem faced by i3BP method that assumes no sharing. Our proposed method also struggle when the power law rate is small with perfect correlation. This is understandable since our method restrict the form of correlation and does not put mass perfectly along the diagonal especially for relatively common variants (Figure 1, third panel). Specifically when the power-law rate is low, the total number of variants are not dominated by extremely rare singletons and our method’s misspecification for relatively common variants could struggle.

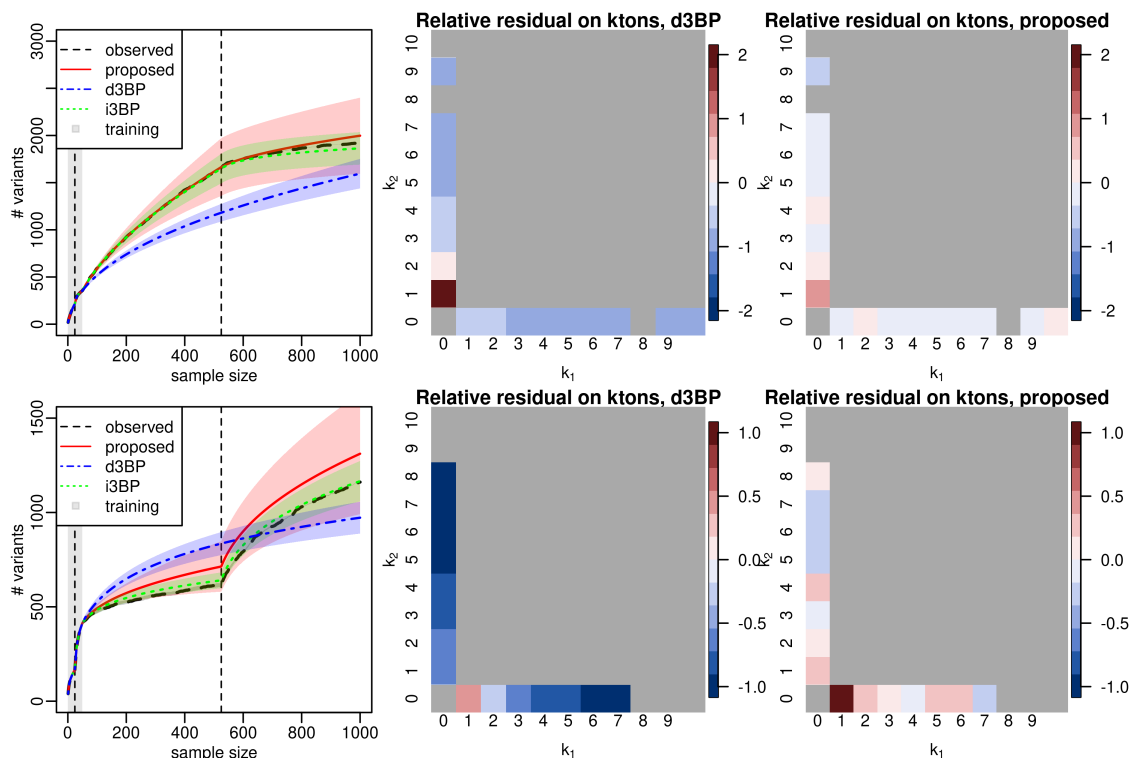


Figure S6: Prediction when data is sampled from i3BP. Each row represents a different simulated dataset, as described in Section 8.1. *Left*: The dashed black line shows the observed number of variants as a function of the sample number. The samples appear in the following order: the pilot from population 1, the pilot from population 2, the follow-up from population 1, the follow-up from population 2. A vertical dashed gray line separates the two populations in the pilot and follow-up, respectively. The gray shading covers the pilot data. All curves agree exactly on the pilot data. In the follow-up region, we plot mean (lines) and 1 standard deviation intervals (shaded regions) from three methods: our proposed method (solid red), the dependent version of the single-population 3BP (dash-dot blue), and the independent version of the 3BP (dotted green). *Center and Right*: For each \mathbf{k} with component values up to 10, we plot the relative residual for predictions from our method (right) and the dependent 3BP (center). Note that the color scales are fixed across a row but vary across a column. A square is gray when the observed value is strictly less than 2 in at least one fold and black for $\mathbf{k} = (0, 0)$.

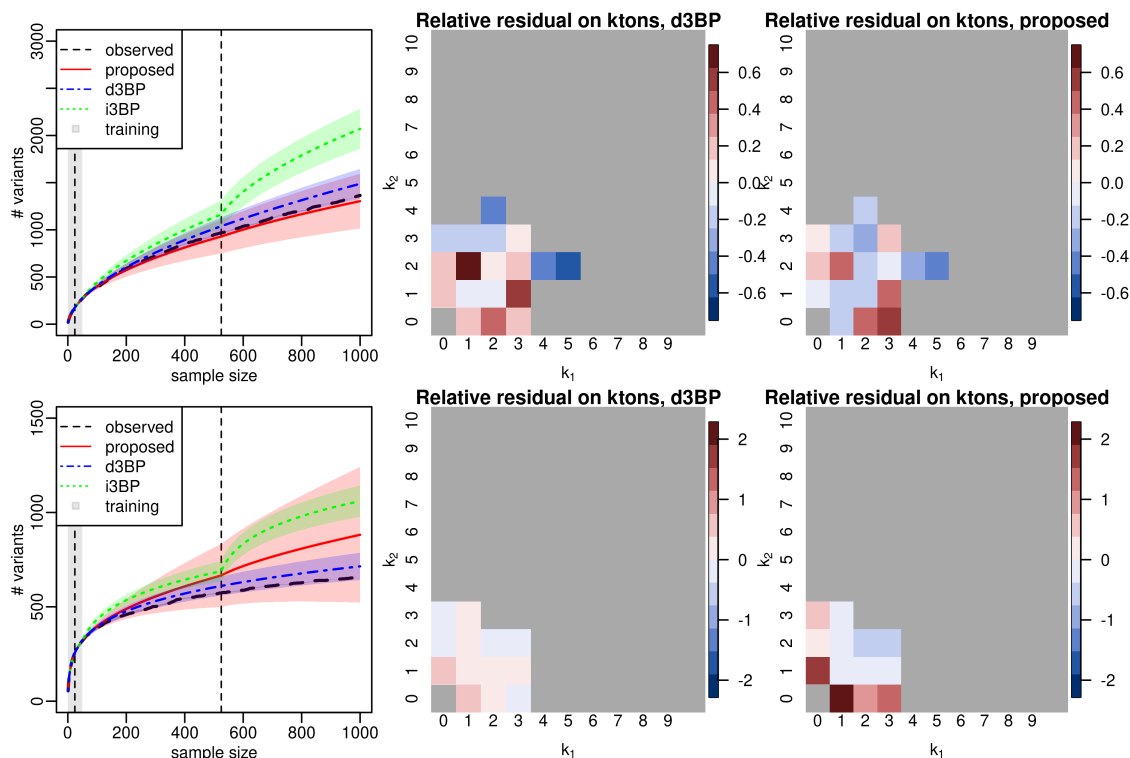


Figure S7: Prediction when data is sampled from d3BP. Each row represents a different simulated dataset, as described in Section 8.1. *Left*: The dashed black line shows the observed number of variants as a function of the sample number. The samples appear in the following order: the pilot from population 1, the pilot from population 2, the follow-up from population 1, the follow-up from population 2. A vertical dashed gray line separates the two populations in the pilot and follow-up, respectively. The gray shading covers the pilot data. All curves agree exactly on the pilot data. In the follow-up region, we plot mean (lines) and 1 standard deviation intervals (shaded regions) from three methods: our proposed method (solid red), the dependent version of the single-population 3BP (dash-dot blue), and the independent version of the 3BP (dotted green). *Center and Right*: For each \mathbf{k} with component values up to 10, we plot the relative residual for predictions from our method (right) and the dependent 3BP (center). Note that the color scales are fixed across a row but vary across a column. A square is gray when the observed value is strictly less than 2 in at least one fold and black for $\mathbf{k} = (0, 0)$.

G.2 Performance of single-population models on real data

We start by providing additional results on the performance of the array of model considered at the task of predicting the total number of genomic variance on real data when a single population is present. For these comparisons, we tested fourth-order jackknife ([Gravel and National Heart Lung & Blood Institute \(NHLBI\) GO Exome Sequencing Project, 2014, 4jk](#)), the Good-Toulmin estimator ([Orlitsky et al., 2016](#); [Chakraborty et al., 2019](#), GT), linear programming ([Zou et al., 2016](#), lp), and the 3BP approach of [Masoero et al. \(2022\)](#) as well as the scaled process (SP) method by [Camerlenghi et al. \(2022\)](#). We consider both data coming from the GnomAD dataset ([Karczewski et al., 2020](#)), as well as cancer data from the cancer genome atlas (TCGA) and the MSK-impact dataset ([Cheng et al., 2015](#)). We observe that 3BP outperforms jackknife GT, and linear programming method in cancer datasets and perform very similarly with scaled process method which has larger variance. Jackknife performs better than other competing methods in GnomAD datasets.

We provide a summary of our findings with results on a few cancer types in [Figure S8](#) and for a few subpopulations in the GnomAD dataset in [Figure S9](#).

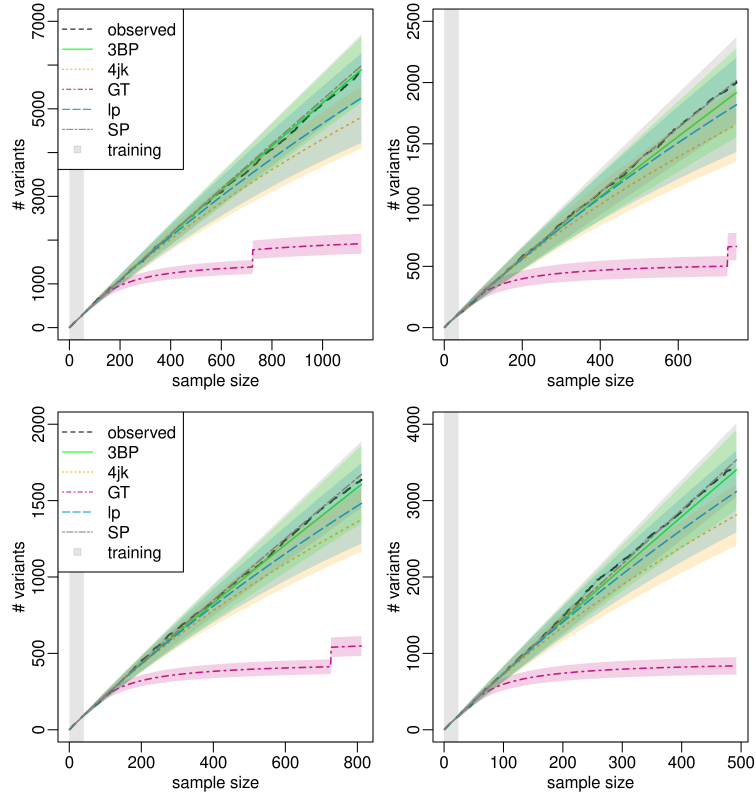


Figure S8: Prediction for the variant counts in, breast (left column) and lung cancer (right column). For MSK-IMPACT dataset (first row) and TCGA dataset (second row) respectively. Shaded area being mean \pm sd. The 3BP method outperforms alternatives in this dataset.

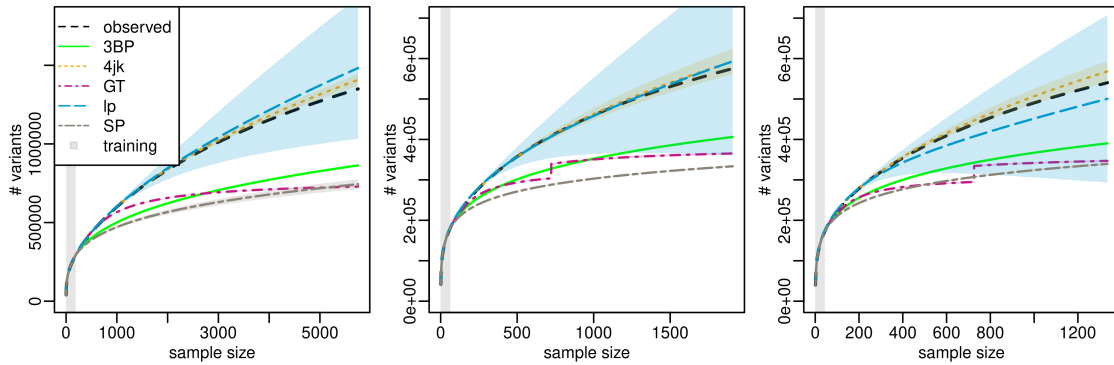


Figure S9: Prediction for the GnomAD dataset, Left column: Southern European, Middle column: Korean, Right column: Bulgarian, shaded area being mean \pm sd. The fourth order Jackknife outperforms competing alternatives in this dataset.

G.3 Raw number of shared variants and residuals in simulation and real data experiments

In this section we report raw number of shared variants and raw magnitude of residuals without normalization as in the main text. The general observations are similar to that of normalized residuals and our proposed methods performs well overall.

G.3.1 Simulations

Figure S10 to Figure S12 showed the raw number of k-tons and residuals with simulated data. The observations are similar to those of normalized results that our model could do as well as well specified i3BP and may struggle when d3BP with low power law rate was used to simulate data.

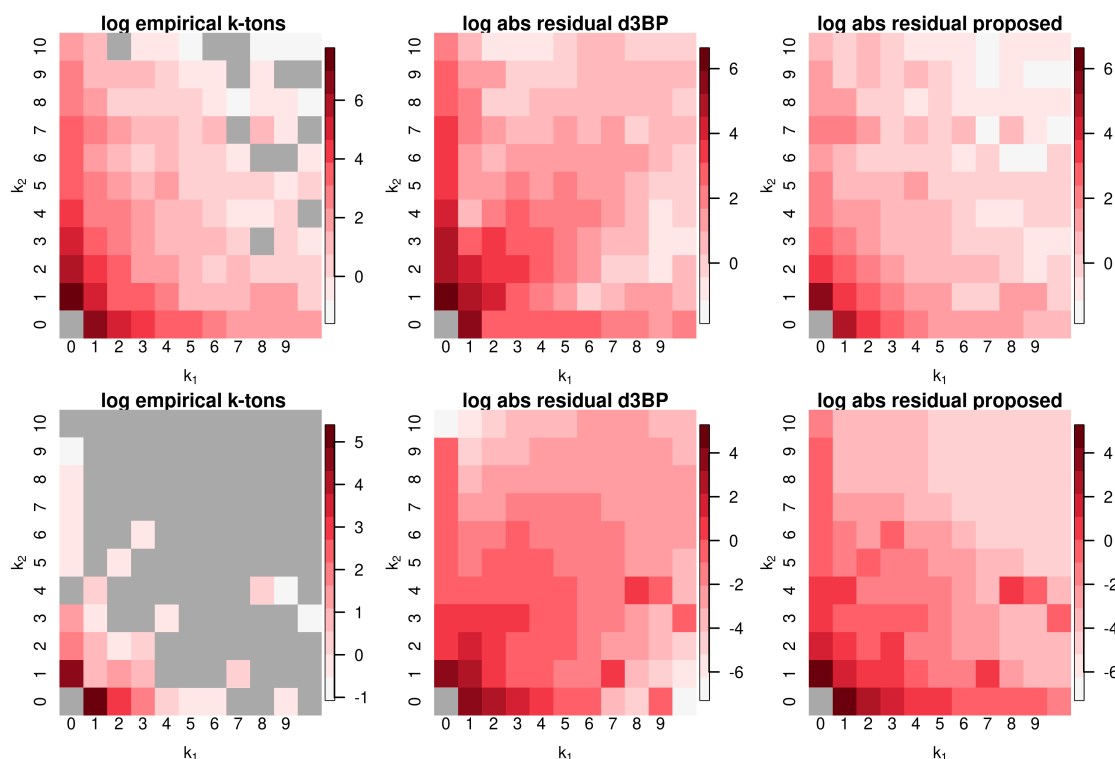


Figure S10: Ground truth of ktons and model prediction when the data sampled from the proposed model. Left most: log over average observed ktons. A square is gray when it the observed value is 0 for all folds or $\mathbf{k} = (0, 0)$. Middle and right: Log average absolute residual in d3BP and proposed model.

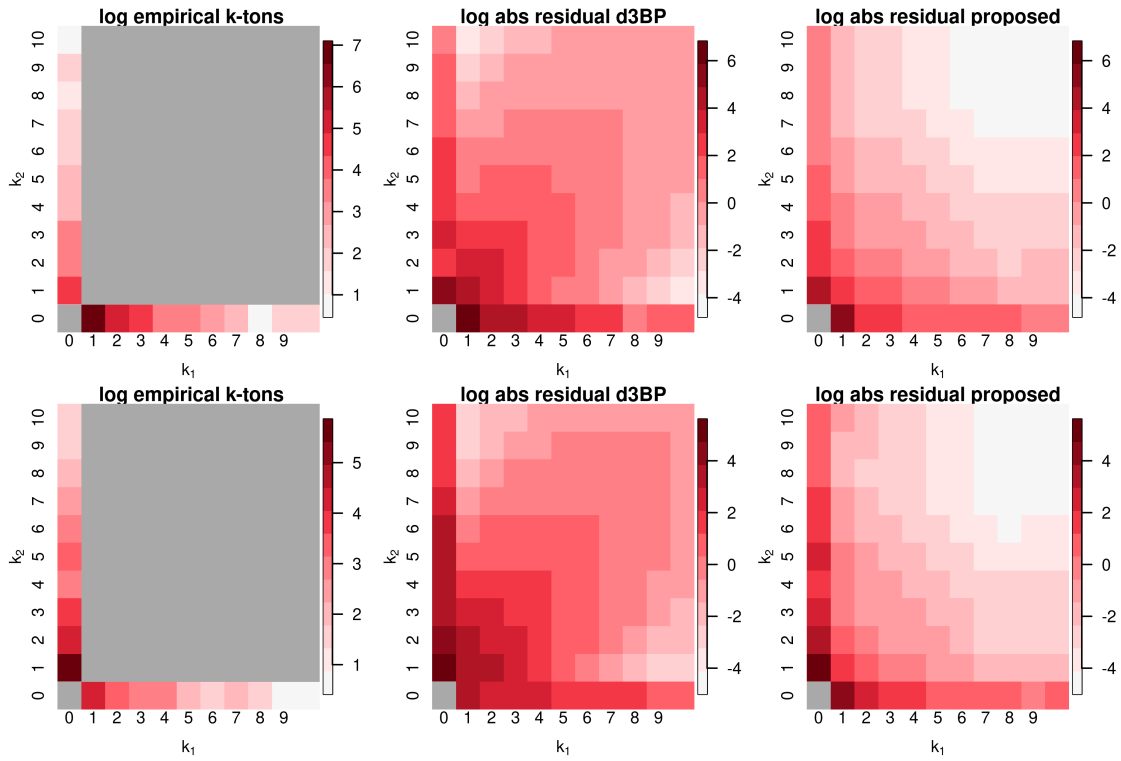


Figure S11: Ground truth of ktons and model prediction when the data sampled from i3BP. Left most: log over average observed ktons. A square is gray when it the observed value is 0 for all folds or $\mathbf{k} = (0, 0)$. Middle and right: Log average absolute residual in d3BP and proposed model.

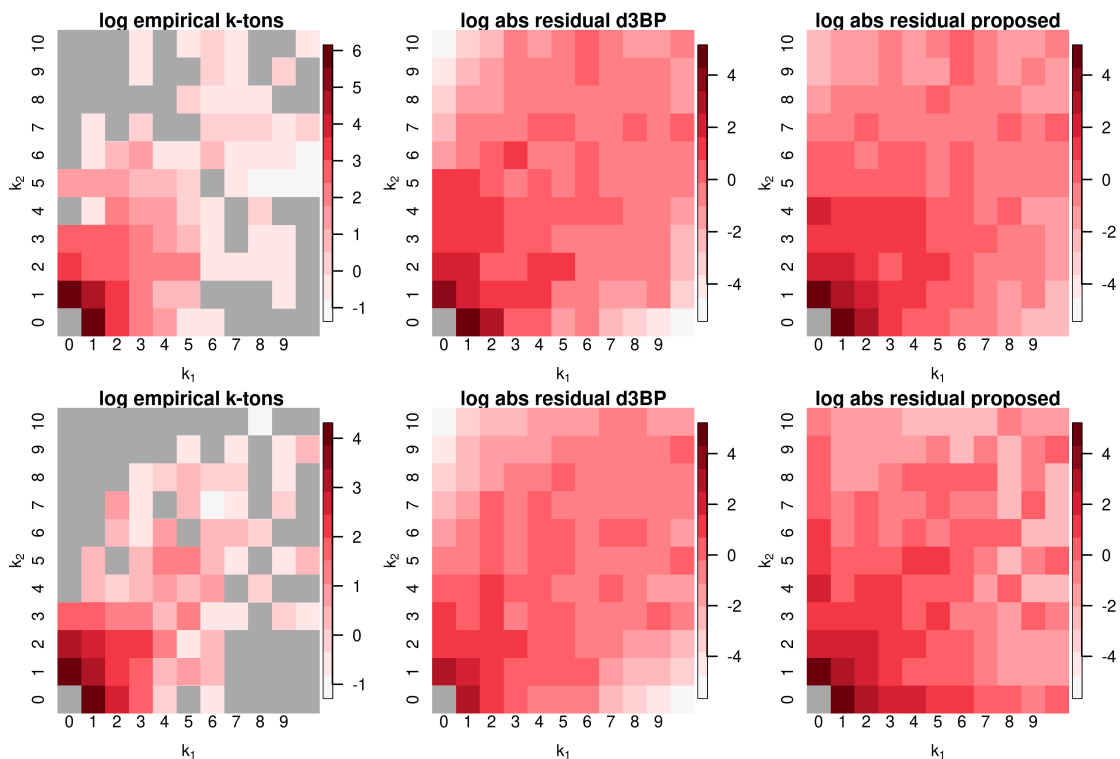


Figure S12: Ground truth of ktons and model prediction when the data sampled from d3BP. Left most:log over average observed ktons. A square is gray when it the observed value is 0 for all folds or $\mathbf{k} = (0,0)$. Middle and right: Log average absolute residual in d3BP and proposed model.

G.4 Real data experiment

Figure S13 to Figure S14 showed the raw number of k-tons that exists more than twice in all samples and magnitude of raw residuals with simulated data. We have the similar observation as normalized version that d3BP methods tend to have larger residual around the diagonal since by assumption of d3BP all variants are shared with the same frequencies.

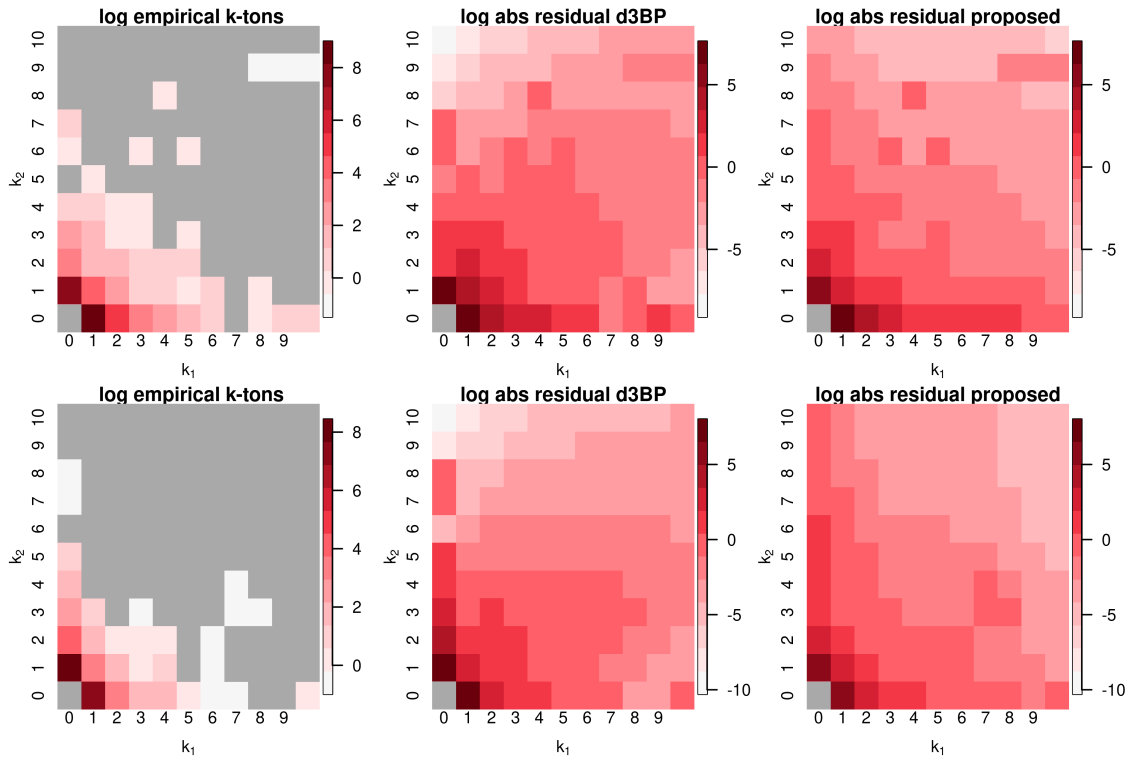


Figure S13: Ground truth of ktons and model prediction using cancer genome dataset. Left most: log over average observed ktons. A square is gray when it the observed value is 0 for all folds or $\mathbf{k} = (0, 0)$. Middle and right: Log average absolute residual in d3BP and proposed model.

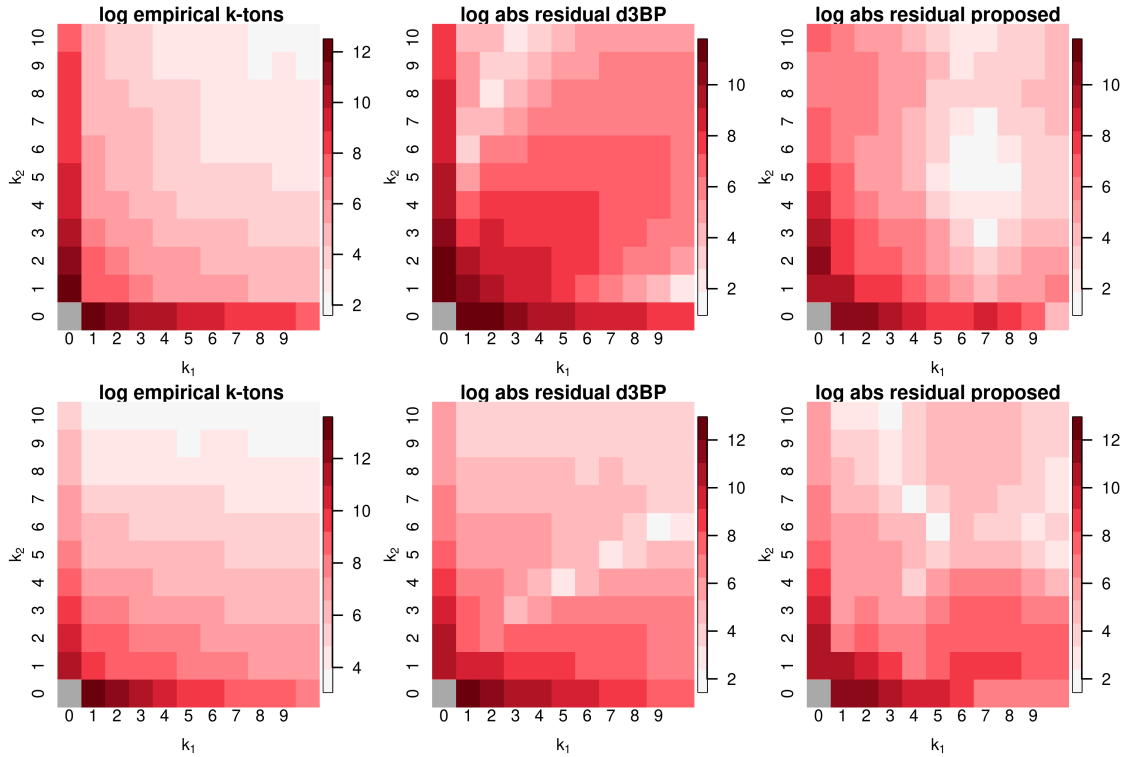


Figure S14: Ground truth of ktons and model prediction using GnomAD dataset. Left most: log over average observed ktons. A square is gray when it the observed value is 0 for all folds or $\mathbf{k} = (0, 0)$. Middle and right: Log average absolute residual in d3BP and proposed model.

G.5 Our method avoids double counting when variants grow slowly

Here we show our model's behavior when fit to data with low power law rate of d3bp and from our proposed model. Our proposed method could handle both dependency models when the growth is slow while i3bp encounters sever double counting problems.

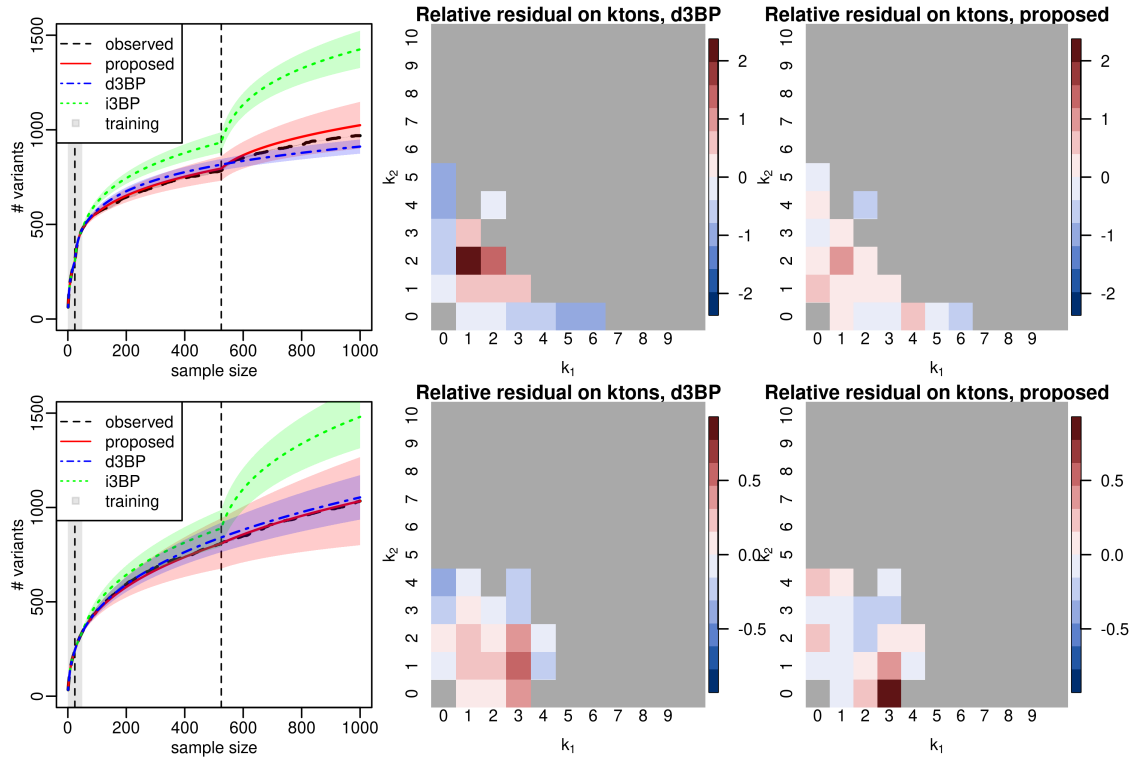


Figure S15: Prediction for slow growth correlated models. Top: proposed model $(\alpha, \sigma_1, \sigma_2, \gamma_1, \gamma_2, \sigma_1, \sigma_2) = (100, 0.4, 0.6, 0.5, 0.5, 1, 1)$. Bottom: d3bp $(\alpha, c, \sigma) = (40, 1, .3)$.

G.6 Larger trimming during training

Determine of the hyperparameters of our model involving maximizing likelihood over trimmed k-tons. We present additional results here with larger trimming in dataset with enough training data to allow $k = 15, 20$ namely the GnomAD and MSK-IMPACT dataset. The results was not influenced by the trimming (Fig. S16 S17 S18).

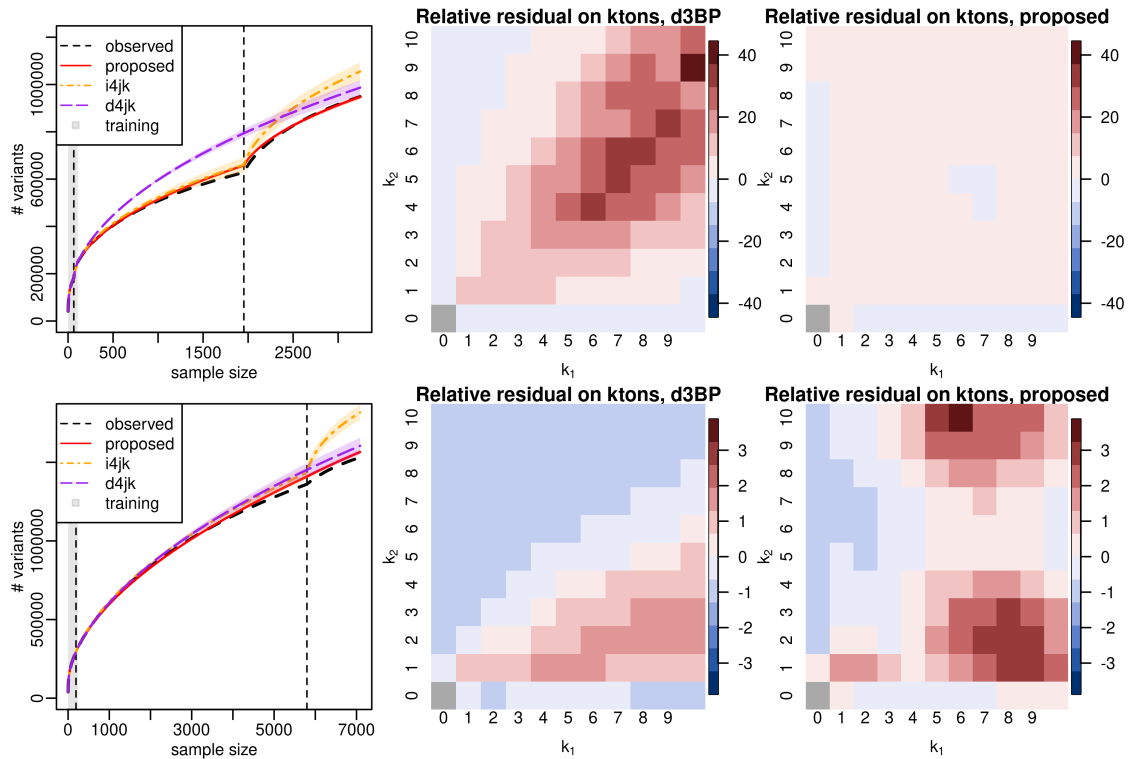


Figure S16: Prediction for the GnomAD dataset, Korean–Bulgarian and Southern European–Bulgarian respectively. The trimming here are set to 15. The results are the same as trimming at 10 in the main text Figure 5.

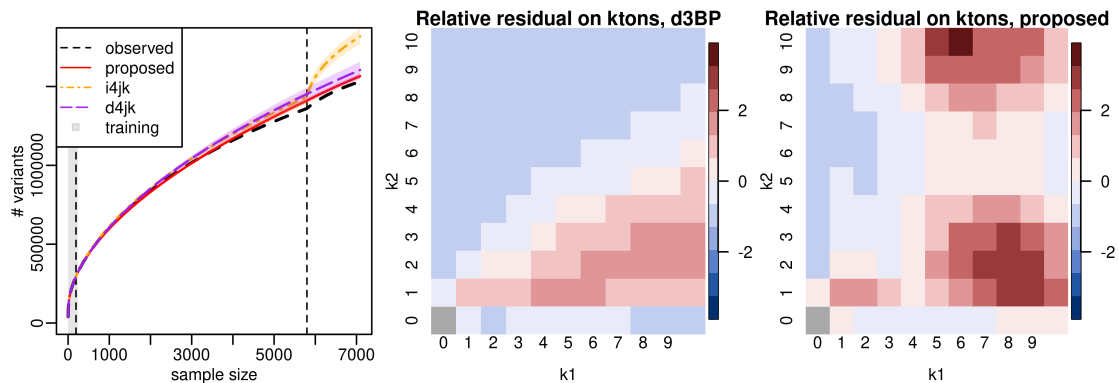


Figure S17: Prediction for the GnomAD dataset Southern European–Bulgarian respectively. The trimming here are set to 20. The results are the same as trimming at 10 in the main text Figure 5. The Korean population does not have enough training sample to allow a 20 trimming.

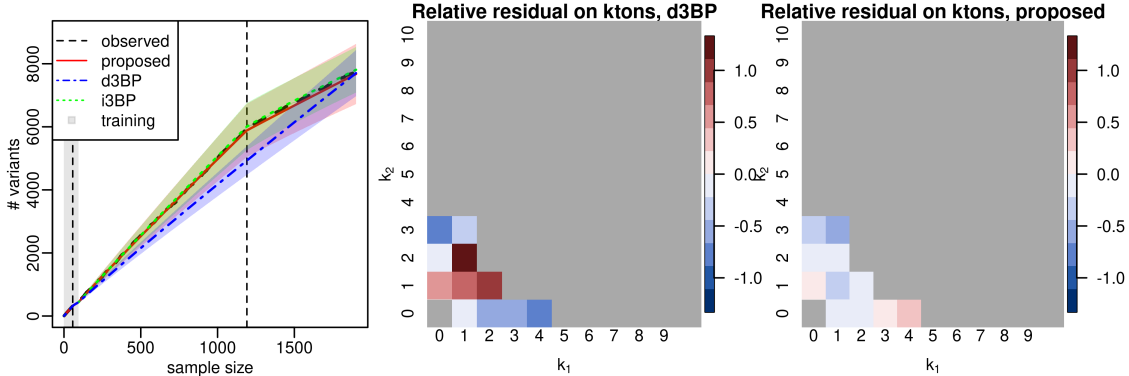


Figure S18: Prediction for the variant counts in, breast and lung cancer. For MSK-IMPACT dataset. This experiment used trimming of 15 during training and the results are not influenced.

H Power law behavior

H.1 Power law bounds in projection scheme

In this section we provide details and proofs on the asymptotic properties of number of variants seen. Here the asymptotics are obtained as more samples are being collected, as introduced in Section 7.1. Specifically we prove that the expected number of variants seen can be both upper and lower bounded by (deterministic) functions whose asymptotic behavior is that of a power-law, i.e. behave like some function $K(N)$ which, as the sample size N increases, satisfies $K(N) \sim CN^\alpha$ for a constant C and $\alpha \in (0, 1)$, where we are using the notation $f(t) \sim g(t) \iff \lim_{t \rightarrow \infty} f(t)/g(t) = 1$.

The main tool we use in our proof is an existing result for power-law asymptotics, developed for the case of single-population models (Broderick et al., 2012, Proposition 6.1). We here first restate Broderick et al. (2012, Proposition 6.1). This result explains, under the assumption that we have a single population, and the data is drawn from a Bayesian nonparametric model like the one in Equation (S10), the relationship between the rate of growth of the total number of observed variants and the tail behavior of the underlying Poisson point process rate measure. In what follows, we use the following asymptotic relation notation: $f(t) \sim g(t) \iff \lim_{t \rightarrow \infty} f(t)/g(t) = 1$.

A useful tool in our asymptotic analysis is the Laplace transformation of the rate measure’s tail, or “Poissonized” expectation $\Phi(t)$. In particular, Proposition 6.1, Lemma 6.3 and Lemma 6.4 in Broderick et al. (2012) (i) established the asymptotic behavior of the (deter-

ministic) Laplace transform Φ , and (ii) linked this asymptotic behavior to the asymptotic number of variants observed from the model. These results will play a crucial role in our analysis, so we here re-state them for completeness.

Lemma S3 connects tail of the rate measure to “Poissonized” expectation

Lemma S3 (Proposition 6.1 of Broderick et al. (2012)). *Let $\nu(d\theta)$ be a (univariate) rate measure such that for $x > 0$ there exists $\alpha \in (0, 1)$ such that:*

$$\int_0^x \nu(d\theta) \sim \frac{\alpha}{1-\alpha} x^{1-\alpha} l\left(\frac{1}{x}\right), \quad (\text{S15})$$

for a slowly varying function $l(\cdot)$. Define $\bar{\nu}(x) = \int_x^\infty \nu(d\theta)$ and $\Phi(t) = t \int_0^\infty e^{-tx} \bar{\nu}(dx)$. Then it holds

$$\Phi(t) \sim \Gamma(1-\alpha)t^\alpha l(t).$$

Lemma S4 established that “Poissonization” error vanishes as number of samples grows

Lemma S4 (Lemma 6.3 of Broderick et al. (2012)). *Assume variant frequencies are from PPP with rate measure $\nu(d\theta)$ such that $\int \nu(d\theta) = \infty$, $\int \theta \nu(d\theta) < \infty$, and variants are independent Bernoulli random variables with variant frequencies. Define $\bar{\nu}(x) = \int_x^\infty \nu(d\theta)$ and $\Phi(t) = t \int_0^\infty e^{-tx} \bar{\nu}(dx)$. Denote the number of variants seen with sample size N as U_0^N , then for $N \rightarrow \infty$*

$$|\mathbb{E}U_0^N - \Phi(N)| \rightarrow 0$$

Lemma S5 showed that number of variants seen concentrates around the expectation

Lemma S5 (Lemma 6.4 of Broderick et al. (2012)). *For the same assumption as Lemma S4, we have*

$$U_0^N \sim \mathbb{E}U_0^N \text{ a.s.}$$

We are now ready to prove Proposition 4. Recall that Proposition 4 deals with the “projection scheme”, in which we are sampling from one population only. In this case, the problem can be reduced to the corresponding single population case: we can indeed bound the rate of

growth of the number of variants with the corresponding rate of growth arising from the population from which we are sampling. This can be accomplished by adopting known techniques developed for the the single-population setting.

Proof of Proposition 4. Reduction to one population. We start by considering the “projection scheme”, in which we sample only from one population. In this case, given a two dimensional rate measure $\nu(d\theta_1 d\theta_2)$, the variants’ frequencies when sampling e.g. only from population 1 are obtained using the mapping theorem, by “projecting” ν onto the first axis indexed by θ_1 by integrating the measure ν with respect to θ_2 (from which the name “projection” scheme).

Following the approach of [Broderick et al. \(2012\)](#), we define the “projected” single population rate measures, i.e.,

$$\nu_1(d\theta_1) = \int_{s=0}^{s=1} \nu_{\text{prop}}(d\theta_1 ds), \quad \text{and} \quad \nu_2(d\theta_2) = \int_{s=0}^{s=1} \nu_{\text{prop}}(ds d\theta_2).$$

These measures are responsible for the generation of variant frequencies for each population respectively. In principle, we could directly apply Lemma [S3](#) to evaluate the growth of the number of variants. One practical difficulty is that directly checking Equation [\(S15\)](#) in conditions of Lemma [S3](#) is difficult. Therefore, due to this difficulty, instead of directly proving that the process leads to a power law behavior for the number of variants under the projection scheme, we will provide a bound for the expected number of variants seen. We accomplish so by bounding the rate measure and showing that the expected number of variants arising when adopting such bounds grow like a power law in the asymptotic regime.

To proceed, we first connect the expected number of variants in the projection scheme with the underlying projected rate measure. Intuitively, variants observed for the first time when the sample grows arbitrarily large have to be arbitrarily rare (otherwise they would have been seen in pervious samples). Therefore, it is intuitive to link the growth in the number of (rare new) variants with the tail of the (projected) rate measure. To formalize this, define:

$$\bar{\nu}_1(x) := \int_x^1 \int_{\theta_2=0}^{\theta_2=1} \nu_{\text{prop}}(d\theta_1 d\theta_2), \quad \text{and} \quad \bar{\nu}_2(x) := \int_x^1 \int_{\theta_1=0}^{\theta_1=1} \nu_{\text{prop}}(d\theta_1 d\theta_2). \quad (\text{S16})$$

Denote with $\Phi((t_1, 0))$ and $\Phi((0, t_2))$ the Laplace transforms of the tail function introduced

in Equation (S16):

$$\Phi((t_1, 0)) = t_1 \int_0^1 e^{-t_1 x} \bar{v}_1(x) dx, \quad \text{and} \quad \Phi((0, t_2)) = t_2 \int_0^1 e^{-t_2 x} \bar{v}_2(x) dx. \quad (\text{S17})$$

By applying Lemma S4, it follows that $\Phi((t_1, 0))$ and $\Phi((0, t_2))$ coincide with the asymptotic mean of the number of variants seen when total sample size is 0 in one population, and t_p in the other population p :

$$\lim_{N_1 \rightarrow \infty} \left| \Phi((N_1, 0)) - \mathbb{E}U_{\mathbf{0}}^{((N_1, 0))} \right| = 0, \quad \text{and} \quad \lim_{N_2 \rightarrow \infty} \left| \Phi((0, N_2)) - \mathbb{E}U_{\mathbf{0}}^{((0, N_2))} \right| = 0. \quad (\text{S18})$$

Then applying Lemma S5, we have $U_{\mathbf{0}}^{(N)} \sim \mathbb{E}U_{\mathbf{0}}^{(N)}$ a.s..

With Equation (S18), we can study the expected number of variants $\mathbb{E}U_{\mathbf{0}}^{((N_1, 0))}$ by studying the asymptotic behavior of the so-called ‘‘Poissonized’’ version $\Phi((t_1, 0))$, $\Phi((0, t_2))$. By using the Laplace transformation form in Equation (S17), we can then apply Lemma S3 to connect the asymptotic rate of growth of the number of new variants to the tail of the rate measures.

Power law upper bound, population 1 We here derive the asymptotic upper bound $\Phi_{\text{upper}}^{\text{project}}(\mathbf{N})$ given in Equation (11). In particular, $\Phi_{\text{upper}}^{\text{project}}(\mathbf{N})$ is an upper bound for $\Phi((t_1, 0))$ as $t_1 \rightarrow \infty$. Since $\Phi((t_1, 0))$ is what determines the rate of growth of rare variants in the projection scheme (when growing only population 1, as showed in Broderick et al. (2012, Lemma 6.3)), by bounding $\Phi((t_1, 0))$ we effectively bound the expectation $\mathbb{E}U_{\mathbf{0}}^{((N_1, 0))}$, which is our stated goal (see Equation (10)).

The idea underlying our proof is similar to the one used to prove that the proposed prior satisfies the integral requirements in Desiderata (A) and (B). Namely, we upper bound the rate measure using the two following observations:

$$\theta_1 + \theta_2^{\sigma_2/\sigma_1} \geq \max \left\{ \theta_1, \theta_2^{\sigma_2/\sigma_1} \right\} \quad \text{and} \quad \theta_1 + \theta_2 \geq \max \left\{ \theta_1, \theta_2 \right\}. \quad (\text{S19})$$

In light of these two simple observations, for a positive $\delta > 0$ it holds

$$\begin{aligned} \frac{(\theta_1 + \theta_2^{\sigma_2/\sigma_1})^{-\sigma_1}}{(\theta_1 + \theta_2)^{\gamma_1 + \gamma_2}} &= (\theta_1 + \theta_2^{\sigma_2/\sigma_1})^{-\sigma_1} (\theta_1 + \theta_2)^{-\gamma_1 - \delta} (\theta_1 + \theta_2)^{-\gamma_2 + \delta} \\ &\leq \theta_1^{-\sigma_1} \theta_1^{-\gamma_1 - \delta} \theta_2^{-\gamma_2 + \delta}. \end{aligned}$$

Thus, letting

$$\mu_{\text{upper},1}(\mathrm{d}\boldsymbol{\theta}) := \frac{\alpha}{B(\gamma_1, c_1)B(\gamma_2, c_2)} \theta_1^{-\sigma_1 - \gamma_1 - \delta} \theta_1^{\gamma_1 - 1} \theta_2^{-\gamma_2 + \delta} \theta_2^{\gamma_2 - 1} (1 - \theta_1)^{c_1 - 1} (1 - \theta_2)^{c_2 - 1} \mathrm{d}\boldsymbol{\theta},$$

it holds

$$\nu_{\text{prop}}(\mathrm{d}\boldsymbol{\theta}) \leq \mu_{\text{upper},1}(\mathrm{d}\boldsymbol{\theta}).$$

Further letting

$$\bar{\mu}_{\text{upper},1}(x) := \int_x^1 \int_0^1 \mu_{\text{upper},1}(\mathrm{d}\boldsymbol{\theta}),$$

it holds that

$$\bar{\nu}_1(\mathrm{d}\boldsymbol{\theta}) \leq \bar{\mu}_{\text{upper},1}.$$

Thus we have

$$\Phi((t_1, 0)) \leq \Phi_{\text{upper}}((t_1, 0)) := t_1 \int_0^1 e^{-t_1 x} \bar{\mu}_{\text{upper},1}(x) \mathrm{d}x.$$

The asymptotic behavior of right hand side as $t_1 \rightarrow \infty$ can be connected to the tail of $\mu_{\text{upper},1}$ using Lemma S3. We check the conditions of Lemma S3 for $\mu_{\text{upper},1}(\mathrm{d}\boldsymbol{\theta})$.

$$\begin{aligned} & \int_0^x \theta_1 \int_0^1 \mu_{\text{upper},1}(\mathrm{d}\theta_1 \mathrm{d}\theta_2) \\ &= \frac{\alpha}{B(\gamma_1, c_1)B(\gamma_2, c_2)} \int_0^x \theta_1 \theta_1^{-\sigma_1 - \gamma_1 - \delta} \theta_1^{\gamma_1 - 1} (1 - \theta_1)^{c_1 - 1} \mathrm{d}\theta_1 \int_0^1 \theta_2^{-\gamma_2 + \delta} \theta_2^{\gamma_2 - 1} (1 - \theta_2)^{c_2 - 1} \mathrm{d}\theta_2 \\ &= \frac{\alpha B(\delta, c_2)}{B(\gamma_1, c_1)B(\gamma_2, c_2)} \int_0^x \theta_1^{-\sigma_1 - \delta} (1 - \theta_1)^{c_1 - 1} \mathrm{d}\theta_1 \\ &\sim \frac{\alpha B(\delta, c_2)}{B(\gamma_1, c_1)B(\gamma_2, c_2)} \frac{1}{(1 - \sigma_1 - \delta)} x^{1 - \sigma_1 - \delta} \end{aligned}$$

Thus we have by Lemma S3 that for all $\delta \leq \min\{\gamma_1, \gamma_2\}/2$, there exists a constant $C_{\text{upper},1,\delta} > 0$, independent of t_1 , for which

$$\Phi((t_1, 0)) \leq \Phi_{\text{upper}}((t_1, 0)) \sim C_{\text{upper},1,\delta} t_1^{\sigma_1 + \delta}$$

We have by Equation (S18) the approximation error of $\Phi((N_1, 0))$ to $\mathbb{E} \left[U_{\mathbf{0}}^{((N_1, 0))} \right]$ goes to 0, and in turn

$$\mathbb{E} \left[U_{\mathbf{0}}^{((N_1, 0))} \right] \leq \Phi_{\text{upper}}((N_1, 0)) \sim C_{\text{upper}, 1, \delta} N_1^{\sigma_1 + \delta}$$

Power law upper bound, population 2 Now we derive the upper bound for population 2, again under the projection scheme. To do so, we construct a bound for $\Phi((0, t_2))$ using a similar argument to the one used for $\Phi((t_1, 0))$.

For $\delta > 0$, in light of the bounds of Equation (S19),

$$\begin{aligned} \frac{(\theta_1 + \theta_2^{\sigma_2/\sigma_1})^{-\sigma_1}}{(\theta_1 + \theta_2)^{\gamma_1 + \gamma_2}} &= (\theta_1 + \theta_2^{\sigma_2/\sigma_1})^{-\sigma_1} (\theta_1 + \theta_2)^{-\gamma_1 - \delta} (\theta_1 + \theta_2)^{-\gamma_2 + \delta} \\ &\leq \theta_2^{-\sigma_2} \theta_2^{-\gamma_2 - \delta} \theta_1^{-\gamma_1 + \delta}, \end{aligned}$$

and in turn letting

$$\mu_{\text{upper}, 2}(d\boldsymbol{\theta}) := \frac{\alpha}{B(\gamma_1, c_1)B(\gamma_2, c_2)} \theta_1^{-\gamma_1 + \delta} \theta_1^{\gamma_1 - 1} \theta_2^{-\sigma_2 - \gamma_2 - \delta} \theta_2^{\gamma_2 - 1} (1 - \theta_1)^{c_1 - 1} (1 - \theta_2)^{c_2 - 1} d\boldsymbol{\theta},$$

it holds that

$$\nu_{\text{prop}}(d\boldsymbol{\theta}) \leq \mu_{\text{upper}, 2}(d\boldsymbol{\theta}).$$

Denote with $\bar{\mu}_{\text{upper}, 2}(x) = \int_x^1 \int_0^1 \mu_{\text{upper}, 2}(d\boldsymbol{\theta})$, we have $\bar{\nu}_2(d\boldsymbol{\theta}) \leq \bar{\mu}_{\text{upper}, 2}$. Thus we have

$$\Phi((0, t_2)) \leq \Phi_{\text{upper}}((0, t_2)) := t_2 \int_0^1 e^{-t_2 x} \bar{\mu}_{\text{upper}, 2}(x) dx.$$

We again check that the conditions of Lemma S3 hold for $\mu_{\text{upper},2}(d\boldsymbol{\theta})$.

$$\begin{aligned}
& \int_0^x \theta_2 \int_0^1 \mu_{\text{upper},2}(d\theta_1 d\theta_2) \\
&= \frac{\alpha}{B(\gamma_1, c_1)B(\gamma_2, c_2)} \int_0^x \theta_2 \theta_2^{-\sigma_2 - \gamma_2 - \delta} \theta_2^{\gamma_2 - 1} (1 - \theta_2)^{c_2 - 1} d\theta_2 \int_0^1 \theta_1^{-\gamma_1 + \delta} \theta_1^{\gamma_1 - 1} (1 - \theta_1)^{c_1 - 1} d\theta_1 \\
&= \frac{\alpha B(\delta, c_2)}{B(\gamma_1, c_1)B(\gamma_2, c_2)} \int_0^x \theta_2^{-\sigma_2 - \delta} (1 - \theta_2)^{c_2 - 1} d\theta_2 \\
&\sim \frac{\alpha B(\delta, c_2)}{B(\gamma_1, c_1)B(\gamma_2, c_2)} \frac{1}{(1 - \sigma_2 - \delta)} x^{1 - \sigma_2 - \delta}
\end{aligned}$$

Thus for all δ , there exists a constant $C_{\text{upper},2,\delta}$ which does not depend on t_2 such that:

$$\Phi((0, t_2)) \leq \Phi_{\text{upper}}((0, t_2)) \sim C_{\text{upper},2,\delta} t_2^{\sigma_2 + \delta}.$$

In turn,

$$\mathbb{E} \left[U_{\mathbf{0}}^{((0, N_2))} \right] \leq \Phi_{\text{lower}}((0, N_2)) \sim C_{\text{upper},2,\delta} N_2^{\sigma_2 + \delta}.$$

Power law lower bound

To derive the asymptotic lower bound for the expected number of new variants we adopt a similar idea to the one used to derive the upper bound. Specifically, we find a lower bound for the model's rate measure, check that the lower bound satisfies the conditions in Lemma S3, and use that rate as a lower bound.

To find this lower bound, we leverage the observation that

$$\theta_1 + \theta_2 \leq 2 \max\{\theta_1, \theta_2\} \quad \text{and} \quad \theta_1 + \theta_2^{\sigma_2/\sigma_1} \leq 2 \max\{\theta_1, \theta_2^{\sigma_2/\sigma_1}\}. \quad (\text{S20})$$

We start with $\sigma_2/\sigma_1 \geq 1$. For $\Phi((t_1, 0))$, we use the fact that $\theta_1 + \theta_2 \leq 2 \max\{\theta_1, \theta_2\}$. We first consider subset of the unit square that $1/2 \geq \theta_1 \geq \theta_2$, where we also have $\theta_1 \geq \theta_2^{\sigma_2/\sigma_1}$ and $(1 - \theta_2) \leq \min\{1, 2^{1-c_2}\}$. We have in this region, $\theta_1 = \max\{\theta_1, \theta_2\} = \max\{\theta_1, \theta_2^{\sigma_2/\sigma_1}\}$. To construct a lower bound of the rate measure, we could use a rate measure whose density

is 0 outside this range and within the range we used the bounds found, concretely we have:

$$\begin{aligned} \frac{(\theta_1 + \theta_2^{\sigma_2/\sigma_1})^{-\sigma_1}}{(\theta_1 + \theta_2)^{\gamma_1 + \gamma_2}} &= (\theta_1 + \theta_2^{\sigma_2/\sigma_1})^{-\sigma_1} (\theta_1 + \theta_2)^{-\gamma_1 - \gamma_2} \\ &\geq \{(2\theta_1)^{-\sigma_1}\} \{(2\theta_1)^{-\gamma_1 - \gamma_2}\} \mathbf{1}_{1/2 \geq \theta_1 \geq \theta_2} \end{aligned}$$

To slightly simplify the integral we have when $\theta_2 \leq 1/2$, $(1 - \theta_2)^{c_2 - 1} \geq \min\{1, 2^{1 - c_2}\}$, combine the bounds, we can bound our proposed rate measure by

$$\nu_{\text{prop}}(d\boldsymbol{\theta}) \geq \mu_{s,1}(d\boldsymbol{\theta}) := \frac{\alpha 2^{-\sigma_1 - \gamma_1 - \gamma_2} \min\{1, 2^{1 - c_2}\}}{B(\gamma_1, c_1)B(\gamma_2, c_2)} \theta_1^{-\sigma_1 - \gamma_1 - \gamma_2} \theta_1^{\gamma_1 - 1} \theta_2^{\gamma_2 - 1} (1 - \theta_1)^{c_1 - 1} \mathbf{1}_{1/2 \geq \theta_1 \geq \theta_2}$$

Use the same arguments as before, it remains to check $\mu_{s,1}(d\boldsymbol{\theta})$ satisfy requirements of Lemma S1. Since we take $x \rightarrow 0$ we can focus on $x < 1/2$.

$$\begin{aligned} &\int_0^x \theta_1 \int_0^1 \mu_{s,1}(d\boldsymbol{\theta}) \\ &= \frac{\alpha 2^{-\sigma_1 - \gamma_1 - \gamma_2} \min\{1, 2^{1 - c_2}\}}{B(\gamma_1, c_1)B(\gamma_2, c_2)} \int_0^x \theta_1 \int_0^{\theta_1} \theta_1^{-\sigma_1 - \gamma_1 - \gamma_2} \theta_1^{\gamma_1 - 1} \theta_2^{\gamma_2 - 1} (1 - \theta_1)^{c_1 - 1} d\boldsymbol{\theta} \\ &= \frac{\alpha 2^{-\sigma_1 - \gamma_1 - \gamma_2} \min\{1, 2^{1 - c_2}\}}{B(\gamma_1, c_1)B(\gamma_2, c_2)} \int_0^x \theta_1^{-\sigma_1 - \gamma_1 - \gamma_2} \theta_1^{\gamma_1} (1 - \theta_1)^{c_1 - 1} \int_0^{\theta_1} \theta_2^{\gamma_2 - 1} d\boldsymbol{\theta} \\ &= \frac{\alpha 2^{-\sigma_1 - \gamma_1 - \gamma_2} \min\{1, 2^{1 - c_2}\}}{B(\gamma_1, c_1)B(\gamma_2, c_2)\gamma_2} \int_0^x \theta_1^{-\sigma_1 - \gamma_1 - \gamma_2} \theta_1^{\gamma_1} (1 - \theta_1)^{c_1 - 1} \theta_1^{\gamma_2} d\theta_1 \\ &\sim \frac{\alpha 2^{-\sigma_1 - \gamma_1 - \gamma_2} \min\{1, 2^{1 - c_2}\}}{B(\gamma_1, c_1)B(\gamma_2, c_2)\gamma_2} \int_0^x \theta_1^{-\sigma_1} d\theta_1 \\ &= \frac{\alpha 2^{-\sigma_1 - \gamma_1 - \gamma_2} \min\{1, 2^{1 - c_2}\}}{B(\gamma_1, c_1)B(\gamma_2, c_2)\gamma_2} \frac{1}{1 - \sigma_1} x^{1 - \sigma_1} \end{aligned}$$

we have then by Lemma S3 and Equation (S18), similar to upper bounds

$$\mathbb{E} \left[U_{\mathbf{0}}^{((N_1, 0))} \right] \geq \Phi_{\text{lower}}((N_1, 0)) \sim C_{\text{lower}, 1} N_1^{\sigma_1}$$

For $\Phi((0, t_2))$, first consider the region that $1/2 \geq \theta_2 \geq \theta_2^{\sigma_2/\sigma_1} \geq \theta_1$, where we also have $(1 - \theta_1) \leq \min\{1, 2^{1 - c_1}\}$. In this region, $\theta_2 = \max\{\theta_1, \theta_2\}$, $\theta_2^{\sigma_2/\sigma_1} = \max\{\theta_1, \theta_2^{\sigma_2/\sigma_1}\}$. Same as before, we lower bound our proposed rate measure with a rate whose density is 0 outside

this region, concretely we have

$$\begin{aligned}
\frac{(\theta_1 + \theta_2^{\sigma_2/\sigma_1})^{-\sigma_1}}{(\theta_1 + \theta_2)^{\gamma_1 + \gamma_2}} &= (\theta_1 + \theta_2^{\sigma_2/\sigma_1})^{-\sigma_1} (\theta_1 + \theta_2)^{-\gamma_1 - \gamma_2} \\
&\geq \left\{ (2\theta_2^{\sigma_2/\sigma_1})^{-\sigma_1} \right\} \left\{ (2\theta_2)^{-\gamma_1 - \gamma_2} \right\} \mathbf{1}_{1/2 \geq \theta_2 \geq \theta_2^{\sigma_2/\sigma_1} \geq \theta_1} \\
&= 2^{-\sigma_1 - \gamma_1 - \gamma_2} \theta_2^{-\sigma_2 - \gamma_1 - \gamma_2} \mathbf{1}_{1/2 \geq \theta_2 \geq \theta_2^{\sigma_2/\sigma_1} \geq \theta_1}.
\end{aligned}$$

Similarly we have when $\theta_1 \leq 1/2$, $(1 - \theta_1)^{c_1 - 1} \geq \min\{1, 2^{1 - c_1}\}$, combine the bounds, we have

$$\nu_{\text{prop}}(\mathbf{d}\boldsymbol{\theta}) \geq \mu_{s,2}(\mathbf{d}\boldsymbol{\theta}) := \frac{\alpha 2^{-\sigma_1 - \gamma_1 - \gamma_2} \min\{1, 2^{1 - c_1}\}}{B(\gamma_1, c_1) B(\gamma_2, c_2)} \theta_2^{-\sigma_2 - \gamma_1 - \gamma_2} \theta_2^{\gamma_2 - 1} \theta_1^{\gamma_1 - 1} (1 - \theta_2)^{c_2 - 1} \mathbf{1}_{1/2 \geq \theta_2 \geq \theta_2^{\sigma_2/\sigma_1} \geq \theta_1}$$

Use the same arguments as before, it remains to check conditions of Lemma S3 for $\mu_{s,2}(\mathbf{d}\boldsymbol{\theta})$.

We can focus on $x \leq 1/2$ since we take $x \rightarrow 0$.

$$\begin{aligned}
&\int_0^x \theta_2 \int_0^1 \mu_{s,2}(\mathbf{d}\boldsymbol{\theta}) \\
&= \frac{\alpha 2^{-\sigma_1 - \gamma_1 - \gamma_2} \min\{1, 2^{1 - c_1}\}}{B(\gamma_1, c_1) B(\gamma_2, c_2)} \int_0^x \theta_2 \int_0^{\theta_2^{\sigma_2/\sigma_1}} \theta_2^{-\sigma_2 - \gamma_1 - \gamma_2} \theta_2^{\gamma_2 - 1} \theta_1^{\gamma_1 - 1} (1 - \theta_2)^{c_2 - 1} \mathbf{d}\boldsymbol{\theta} \\
&= \frac{\alpha 2^{-\sigma_1 - \gamma_1 - \gamma_2} \min\{1, 2^{1 - c_1}\}}{B(\gamma_1, c_1) B(\gamma_2, c_2)} \int_0^x \theta_2^{-\sigma_2 - \gamma_1 - \gamma_2} \theta_2^{\gamma_2} (1 - \theta_2)^{c_2 - 1} \int_0^{\theta_2^{\sigma_2/\sigma_1}} \theta_1^{\gamma_1 - 1} \mathbf{d}\boldsymbol{\theta} \\
&= \frac{\alpha 2^{-\sigma_1 - \gamma_1 - \gamma_2} \min\{1, 2^{1 - c_1}\}}{B(\gamma_1, c_1) B(\gamma_2, c_2) \gamma_1} \int_0^x \theta_2^{-\sigma_2 - \gamma_1 - \gamma_2} \theta_2^{\gamma_2} (1 - \theta_2)^{c_2 - 1} \theta_2^{\gamma_1 \frac{\sigma_2}{\sigma_1}} \mathbf{d}\theta_2 \\
&\sim \frac{\alpha 2^{-\sigma_1 - \gamma_1 - \gamma_2} \min\{1, 2^{1 - c_1}\}}{B(\gamma_1, c_1) B(\gamma_2, c_2) \gamma_1} \int_0^x \theta_2^{-(\sigma_2 - \gamma_1(\frac{\sigma_2}{\sigma_1} - 1))} \mathbf{d}\theta_2 \\
&= \frac{\alpha 2^{-\sigma_1 - \gamma_1 - \gamma_2} \min\{1, 2^{1 - c_1}\}}{B(\gamma_1, c_1) B(\gamma_2, c_2) \gamma_1} \frac{1}{1 - (\sigma_2 - \gamma_1(\frac{\sigma_2}{\sigma_1} - 1))} x^{1 - (\sigma_2 - \gamma_1(\frac{\sigma_2}{\sigma_1} - 1))}
\end{aligned}$$

we have by Lemma S3 and Equation (S18)

$$\mathbb{E}U_{\mathbf{0}}^{((0, N_2))} \geq \Phi_{\text{lower}}((0, N_2)) \sim C''_{\text{lower},1} N_2^{\sigma_2 - \gamma_1(\frac{\sigma_2}{\sigma_1} - 1)}$$

Alternatively we observe that $(\theta_1 + \theta_2^{\sigma_2/\sigma_1})^{-\sigma_1} \geq (\theta_1 + \theta_2)^{-\sigma_1}$ in the range of $\theta_2 \geq \theta_1$ and

$$\begin{aligned} \frac{(\theta_1 + \theta_2^{\sigma_2/\sigma_1})^{-\sigma_1}}{(\theta_1 + \theta_2)^{\gamma_1 + \gamma_2}} &= (\theta_1 + \theta_2^{\sigma_2/\sigma_1})^{-\sigma_1} (\theta_1 + \theta_2)^{-\gamma_1 - \gamma_2} \\ &\geq (\theta_1 + \theta_2)^{-\gamma_1 - \gamma_2 - \sigma_1} \mathbf{1}_{1/2 \geq \theta_2 \geq \theta_1} \\ &\geq \theta_2^{-\gamma_1 - \gamma_2 - \sigma_1} \mathbf{1}_{1/2 \geq \theta_2 \geq \theta_1} \end{aligned}$$

Similarly we use that when $\theta_1 \leq 1/2$, $(1 - \theta_1)^{c_1 - 1} \geq \min\{1, 2^{1 - c_1}\}$, combine the bounds, we have

$$\nu_{\text{prop}}(d\boldsymbol{\theta}) \geq \mu'_{s,2}(d\boldsymbol{\theta}) := \frac{\alpha 2^{-\sigma_1 - \gamma_1 - \gamma_2} \min\{1, 2^{1 - c_1}\}}{B(\gamma_1, c_1)B(\gamma_2, c_2)} \theta_2^{-\sigma_1 - \gamma_1 - \gamma_2} \theta_2^{\gamma_2 - 1} \theta_1^{\gamma_1 - 1} (1 - \theta_2)^{c_2 - 1} \mathbf{1}_{1/2 \geq \theta_2 \geq \theta_1}$$

We check the conditions in Lemma S3

$$\begin{aligned} &\int_0^x \theta_2 \int_0^1 \mu'_{s,2}(d\boldsymbol{\theta}) \\ &= \frac{\alpha 2^{-\sigma_1 - \gamma_1 - \gamma_2} \min\{1, 2^{1 - c_1}\}}{B(\gamma_1, c_1)B(\gamma_2, c_2)} \int_0^x \theta_2 \int_0^{\theta_2} \theta_2^{-\sigma_1 - \gamma_1 - \gamma_2} \theta_2^{\gamma_2 - 1} \theta_1^{\gamma_1 - 1} (1 - \theta_2)^{c_2 - 1} d\boldsymbol{\theta} \\ &= \frac{\alpha 2^{-\sigma_1 - \gamma_1 - \gamma_2} \min\{1, 2^{1 - c_1}\}}{B(\gamma_1, c_1)B(\gamma_2, c_2)} \int_0^x \theta_2^{-\sigma_1 - \gamma_1 - \gamma_2} \theta_2^{\gamma_2} (1 - \theta_2)^{c_2 - 1} \int_0^{\theta_2} \theta_1^{\gamma_1 - 1} d\boldsymbol{\theta} \\ &= \frac{\alpha 2^{-\sigma_1 - \gamma_1 - \gamma_2} \min\{1, 2^{1 - c_1}\}}{B(\gamma_1, c_1)B(\gamma_2, c_2)\gamma_1} \int_0^x \theta_2^{-\sigma_1 - \gamma_1 - \gamma_2} \theta_2^{\gamma_2} (1 - \theta_2)^{c_2 - 1} \theta_2^{\gamma_1} d\theta_2 \\ &\sim \frac{\alpha 2^{-\sigma_1 - \gamma_1 - \gamma_2} \min\{1, 2^{1 - c_1}\}}{B(\gamma_1, c_1)B(\gamma_2, c_2)\gamma_1} \int_0^x \theta_2^{-\sigma_1} d\theta_2 \\ &= \frac{\alpha 2^{-\sigma_1 - \gamma_1 - \gamma_2} \min\{1, 2^{1 - c_1}\}}{B(\gamma_1, c_1)B(\gamma_2, c_2)\gamma_1} \frac{1}{1 - \sigma_1} x^{1 - \sigma_1} \end{aligned}$$

we have by Lemma S3 and Equation (S18)

$$\mathbb{E} \left[U_{\mathbf{0}}^{((0, N_2))} \right] \geq \Phi_{\text{lower}}((0, N_2)) \sim C'_{\text{lower},1} N_2^{\sigma_1}$$

Combining the two bounds we can also conclude that

$$\mathbb{E} \left[U_{\mathbf{0}}^{((0, N_2))} \right] \geq \Phi_{\text{lower}}((0, N_2, 0)) \sim \max\{C'_{\text{lower},1} N_2^{\sigma_1}, C''_{\text{lower},1} N_2^{\sigma'_2}\}$$

When $\sigma_2/\sigma_1 \leq 1$ the proof essentially switched the role of population 1 and population 2 in previous proofs.

We start with $\Phi((t_1, 0))$.

Consider the range $1/2 \geq \theta_1 \geq \theta_2^{\sigma_2/\sigma_1} \geq \theta_2$, where $\theta_1 + \theta_2^{\sigma_2/\sigma_1} \leq 2\theta_1$ and $\theta_1 + \theta_2 \leq 2\theta_1$

We have

$$\begin{aligned} \frac{(\theta_1 + \theta_2^{\sigma_2/\sigma_1})^{-\sigma_1}}{(\theta_1 + \theta_2)^{\gamma_1 + \gamma_2}} &= (\theta_1 + \theta_2^{\sigma_2/\sigma_1})^{-\sigma_1} (\theta_1 + \theta_2)^{-\gamma_1 - \gamma_2} \\ &\geq \{(2\theta_1)^{-\sigma_1}\} \{(2\theta_1)^{-\gamma_1 - \gamma_2}\} \mathbf{1}_{1/2 \geq \theta_1 \geq \theta_2^{\sigma_2/\sigma_1} \geq \theta_2} \\ &= 2^{-\sigma_1 - \gamma_1 - \gamma_2} \theta_1^{-\sigma_1 - \gamma_1 - \gamma_2} \mathbf{1}_{1/2 \geq \theta_1 \geq \theta_2^{\sigma_2/\sigma_1} \geq \theta_2}. \end{aligned}$$

Combining with $(1 - \theta_2)^{c_2 - 1} \leq \min\{1, 2^{1 - c_2}\}$ when $\theta_2 \leq 1/2$ we have

$$\nu_{\text{prop}}(\mathbf{d}\theta) \geq \mu_{s,1}(\mathbf{d}\theta) := \frac{\alpha 2^{-\sigma_1 - \gamma_1 - \gamma_2} \min\{1, 2^{1 - c_2}\}}{B(\gamma_1, c_1)B(\gamma_2, c_2)} \theta_1^{-\sigma_1 - \gamma_1 - \gamma_2} \theta_2^{\gamma_2 - 1} \theta_1^{\gamma_1 - 1} (1 - \theta_1)^{c_1 - 1} \mathbf{1}_{1/2 \geq \theta_1 \geq \theta_2^{\sigma_2/\sigma_1} \geq \theta_2}$$

Use the same arguments as before, it remains to check whether $\mu_{s,1}(\mathbf{d}\theta)$ satisfy conditions in Lemma S3. We can focus on $x \leq 1/2$ since we will want $x \rightarrow 0$.

$$\begin{aligned} &\int_0^x \theta_1 \int_0^1 \mu_{s,2}(\mathbf{d}\theta) \\ &= \frac{\alpha 2^{-\sigma_1 - \gamma_1 - \gamma_2} \min\{1, 2^{1 - c_2}\}}{B(\gamma_1, c_1)B(\gamma_2, c_2)} \int_0^x \theta_1 \int_0^{\theta_1^{\sigma_1/\sigma_2}} \theta_1^{-\sigma_1 - \gamma_1 - \gamma_2} \theta_1^{\gamma_2 - 1} \theta_2^{\gamma_1 - 1} (1 - \theta_1)^{c_1 - 1} \mathbf{d}\theta \\ &= \frac{\alpha 2^{-\sigma_1 - \gamma_1 - \gamma_2} \min\{1, 2^{1 - c_2}\}}{B(\gamma_1, c_1)B(\gamma_2, c_2)} \int_0^x \theta_1^{-\sigma_1 - \gamma_1 - \gamma_2} \theta_1^{\gamma_2} (1 - \theta_1)^{c_1 - 1} \int_0^{\theta_1^{\sigma_1/\sigma_2}} \theta_2^{\gamma_2 - 1} \mathbf{d}\theta \\ &= \frac{\alpha 2^{-\sigma_1 - \gamma_1 - \gamma_2} \min\{1, 2^{1 - c_2}\}}{B(\gamma_1, c_1)B(\gamma_2, c_2)\gamma_2} \int_0^x \theta_1^{-\sigma_1 - \gamma_1 - \gamma_2} \theta_1^{\gamma_2} (1 - \theta_1)^{c_1 - 1} \theta_1^{\gamma_2 \frac{\sigma_1}{\sigma_2}} \mathbf{d}\theta_1 \\ &\sim \frac{\alpha 2^{-\sigma_1 - \gamma_1 - \gamma_2} \min\{1, 2^{1 - c_2}\}}{B(\gamma_1, c_1)B(\gamma_2, c_2)\gamma_2} \int_0^x \theta_1^{-(\sigma_1 - \gamma_2(\frac{\sigma_1}{\sigma_2} - 1))} \mathbf{d}\theta_1 \\ &= \frac{\alpha 2^{-\sigma_1 - \gamma_1 - \gamma_2} \min\{1, 2^{1 - c_2}\}}{B(\gamma_1, c_1)B(\gamma_2, c_2)\gamma_2} \frac{1}{1 - (\sigma_1 - \gamma_2(\frac{\sigma_1}{\sigma_2} - 1))} x^{1 - (\sigma_1 - \gamma_2(\frac{\sigma_1}{\sigma_2} - 1))} \end{aligned}$$

we have by Lemma S3 and Equation (S18)

$$\mathbb{E} \left[U_{\mathbf{0}}^{((N_1, 0))} \right] \geq \Phi_{\text{lower}}((N_1, 0)) \sim C_{\text{lower}, 2}'' N_1^{\sigma_1 - \gamma_2(\frac{\sigma_1}{\sigma_2} - 1)}$$

Alternatively we observe that $(\theta_1 + \theta_2^{\sigma_2/\sigma_1})^{-\sigma_1} \geq (\theta_1^{\sigma_2/\sigma_1} + \theta_2^{\sigma_2/\sigma_1})^{-\sigma_1}$ in the range of $1/2 \geq \theta_1 \geq \theta_2$ and $\theta_1^{\sigma_2/\sigma_1} + \theta_2^{\sigma_2/\sigma_1} \leq 2\theta_1^{\sigma_2/\sigma_1}$

We have

$$\begin{aligned}
\frac{(\theta_1 + \theta_2^{\sigma_2/\sigma_1})^{-\sigma_1}}{(\theta_1 + \theta_2)^{\gamma_1 + \gamma_2}} &= (\theta_1 + \theta_2^{\sigma_2/\sigma_1})^{-\sigma_1} (\theta_1 + \theta_2)^{-\gamma_1 - \gamma_2} \\
&\geq (\theta_1^{\sigma_2/\sigma_1} + \theta_2^{\sigma_2/\sigma_1})^{-\sigma_1} (\theta_1 + \theta_2)^{-\gamma_1 - \gamma_2} \mathbf{1}_{1/2 \geq \theta_1 \geq \theta_2} \\
&\geq \left\{ (2\theta_1^{\sigma_2/\sigma_1})^{-\sigma_1} \right\} \left\{ (2\theta_1)^{-\gamma_1 - \gamma_2} \right\} \mathbf{1}_{1/2 \geq \theta_1 \geq \theta_2} \\
&= 2^{-\sigma_1 - \gamma_1 - \gamma_2} \theta_1^{-\sigma_2 - \gamma_1 - \gamma_2} \mathbf{1}_{1/2 \geq \theta_1 \geq \theta_2}.
\end{aligned}$$

Combining with $(1 - \theta_2)^{c_2 - 1} \leq \min\{1, 2^{1-c_2}\}$ as $\theta_2 \leq 1/2$, we have

$$\nu_{\text{prop}}(d\boldsymbol{\theta}) \geq \mu'_{s,1}(d\boldsymbol{\theta}) := \frac{\alpha 2^{-\sigma_2 - \gamma_1 - \gamma_2} \min\{1, 2^{1-c_2}\}}{B(\gamma_1, c_1)B(\gamma_2, c_2)} \theta_1^{-\sigma_2 - \gamma_1 - \gamma_2} \theta_1^{\gamma_2 - 1} \theta_2^{\gamma_2 - 1} (1 - \theta_1)^{c_1 - 1} \mathbf{1}_{1/2 \geq \theta_1 \geq \theta_2}$$

We check the conditions in Lemma S3

$$\begin{aligned}
&\int_0^x \theta_2 \int_0^1 \mu'_{s,1}(d\boldsymbol{\theta}) \\
&= \frac{\alpha 2^{-\sigma_2 - \gamma_1 - \gamma_2} \min\{1, 2^{1-c_2}\}}{B(\gamma_1, c_1)B(\gamma_2, c_2)} \int_0^x \theta_1 \int_0^{\theta_1} \theta_1^{-\sigma_2 - \gamma_1 - \gamma_2} \theta_1^{\gamma_1 - 1} \theta_2^{\gamma_2 - 1} (1 - \theta_1)^{c_1 - 1} d\boldsymbol{\theta} \\
&= \frac{\alpha 2^{-\sigma_2 - \gamma_1 - \gamma_2} \min\{1, 2^{1-c_2}\}}{B(\gamma_1, c_1)B(\gamma_2, c_2)} \int_0^x \theta_1^{-\sigma_2 - \gamma_1 - \gamma_2} \theta_1^{\gamma_1} (1 - \theta_1)^{c_1 - 1} \int_0^{\theta_1} \theta_2^{\gamma_2 - 1} d\boldsymbol{\theta} \\
&= \frac{\alpha 2^{-\sigma_2 - \gamma_1 - \gamma_2} \min\{1, 2^{1-c_2}\}}{B(\gamma_1, c_1)B(\gamma_2, c_2)\gamma_2} \int_0^x \theta_1^{-\sigma_2 - \gamma_1 - \gamma_2} \theta_1^{\gamma_1} (1 - \theta_1)^{c_1 - 1} \theta_1^{\gamma_2} d\theta_1 \\
&\sim \frac{\alpha 2^{-\sigma_2 - \gamma_1 - \gamma_2} \min\{1, 2^{1-c_2}\}}{B(\gamma_1, c_1)B(\gamma_2, c_2)\gamma_2} \int_0^x \theta_1^{-\sigma_2} d\theta_1 \\
&= \frac{\alpha 2^{-\sigma_2 - \gamma_1 - \gamma_2} \min\{1, 2^{1-c_2}\}}{B(\gamma_1, c_1)B(\gamma_2, c_2)\gamma_2} \frac{1}{1 - \sigma_2} x^{1 - \sigma_2}
\end{aligned}$$

we have by Lemma S3 and Equation (S18)

$$\mathbb{E} \left[U_{\mathbf{0}}^{((N_1, 0))} \right] \geq \Phi'_{\text{lower}}((N_1, 0)) \sim C'_{\text{lower}, 2} N_1^{\sigma_2}$$

Combine the two bounds we can also conclude that

$$\mathbb{E} \left[U_{\mathbf{0}}^{((N_1, 0))} \right] \geq \Phi_{\text{lower}}((N_1, 0)) \sim \max\{C'_{\text{lower}, 2} N_1^{\sigma_2}, C''_{\text{lower}, 2} N_1^{\sigma'_1}\}$$

For $\Phi((0, t_2))$, we consider the range $1/2 \geq \theta_2 \geq \theta_1$, where we also have $\theta_2^{\sigma_2/\sigma_1} \geq \theta_1$, therefore we have

$$\begin{aligned} \frac{(\theta_1 + \theta_2^{\sigma_2/\sigma_1})^{-\sigma_1}}{(\theta_1 + \theta_2)^{\gamma_1 + \gamma_2}} &= (\theta_1 + \theta_2^{\sigma_2/\sigma_1})^{-\sigma_1} (\theta_1 + \theta_2)^{-\gamma_1 - \gamma_2} \\ &\geq \left\{ (2\theta_2^{\sigma_2/\sigma_1})^{-\sigma_1} \right\} \left\{ (2\theta_2)^{-\gamma_1 - \gamma_2} \right\} \mathbf{1}_{1/2 \geq \theta_2 \geq \theta_1} \\ &= 2^{-\sigma_1 - \gamma_1 - \gamma_2} \theta_2^{-\sigma_2 - \gamma_1 - \gamma_2} \mathbf{1}_{1/2 \geq \theta_2 \geq \theta_1}. \end{aligned}$$

Combining with $(1 - \theta_1)^{c_1} \leq \min\{1, 2^{1-c_1}\}$ when $\theta_1 \leq 1/2$ We have

$$\nu_{\text{prop}}(d\boldsymbol{\theta}) \geq \mu_{s,1}(d\boldsymbol{\theta}) := \frac{\alpha 2^{-\sigma_1 - \gamma_1 - \gamma_2} \min\{1, 2^{1-c_1}\}}{B(\gamma_1, c_1)B(\gamma_2, c_2)} \theta_2^{-\sigma_2 - \gamma_1 - \gamma_2} \theta_2^{\gamma_2 - 1} \theta_1^{\gamma_1 - 1} (1 - \theta_2)^{c_2 - 1} \mathbf{1}_{1/2 \geq \theta_2 \geq \theta_1}$$

We then check the condition of Lemma S3. We can focus on $x \leq 1/2$ since we will want $x \rightarrow 0$.

$$\begin{aligned} &\int_0^x \theta_1 \int_0^1 \mu_{s,1}(d\boldsymbol{\theta}) \\ &= \frac{\alpha 2^{-\sigma_1 - \gamma_1 - \gamma_2} \min\{1, 2^{1-c_1}\}}{B(\gamma_1, c_1)B(\gamma_2, c_2)} \int_0^x \theta_2 \int_0^{\theta_2} \theta_2^{-\sigma_2 - \gamma_1 - \gamma_2} \theta_2^{\gamma_2 - 1} \theta_1^{\gamma_1 - 1} (1 - \theta_2)^{c_2 - 1} d\boldsymbol{\theta} \\ &= \frac{\alpha 2^{-\sigma_1 - \gamma_1 - \gamma_2} \min\{1, 2^{1-c_1}\}}{B(\gamma_1, c_1)B(\gamma_2, c_2)} \int_0^x \theta_2^{-\sigma_2 - \gamma_1 - \gamma_2} \theta_2^{\gamma_2} (1 - \theta_2)^{c_2 - 1} \int_0^{\theta_2} \theta_1^{\gamma_1 - 1} d\boldsymbol{\theta} \\ &= \frac{\alpha 2^{-\sigma_1 - \gamma_1 - \gamma_2} \min\{1, 2^{1-c_1}\}}{B(\gamma_1, c_1)B(\gamma_2, c_2)\gamma_1} \int_0^x \theta_2^{-\sigma_2 - \gamma_1 - \gamma_2} \theta_2^{\gamma_2} (1 - \theta_2)^{c_2 - 1} \theta_2^{\gamma_1} d\theta_2 \\ &\sim \frac{\alpha 2^{-\sigma_1 - \gamma_1 - \gamma_2} \min\{1, 2^{1-c_1}\}}{B(\gamma_1, c_1)B(\gamma_2, c_2)\gamma_1} \int_0^x \theta_2^{-\sigma_2} d\theta_2 \\ &= \frac{\alpha 2^{-\sigma_1 - \gamma_1 - \gamma_2} \min\{1, 2^{1-c_1}\}}{B(\gamma_1, c_1)B(\gamma_2, c_2)\gamma_1} \frac{1}{1 - \sigma_2} x^{1 - \sigma_2} \end{aligned}$$

we have by Lemma S3 and Equation (S18)

$$\mathbb{E} \left[U_{\mathbf{0}}^{((0, N_2))} \right] \geq \Phi_{\text{lower}}((0, N_2)) \sim C_{\text{lower}, 2} N_2^{\sigma_2}.$$

Combine the two bounds, we get the expectation part of the theorem.

Law of large number results are established by directly apply Proposition 6.4 of Broderick et al. (2012). We have $U_{\mathbf{0}}^{((0, N_2))} \sim \mathbb{E} \left[U_{\mathbf{0}}^{((0, N_2))} \right]$ a.s. and $U_{\mathbf{0}}^{((N_1, 0))} \sim \mathbb{E} \left[U_{\mathbf{0}}^{((N_1, 0))} \right]$ a.s..

□

H.2 Power law bounds in proportional scheme

Here we give the proof of Proposition 5. The key observation is that total number of variants seen can be upper bounded by the sum of variants seen in each population (the “double counting”) and lower bounded by variants seen in either population.

Proof. For a proportional sample $(N_1, N_2) = (N, \lceil \rho N \rceil)$ with $\rho > 0$ and $N_p \rightarrow \infty$ being integers. We first observe that by assumptions on sample size, we have $N_2/N_1 \rightarrow \rho$

We can bound the number of new variants $U_{\mathbf{0}}^{(N)}$ by

$$\max\{U_{\mathbf{0}}^{((N,0))}, U_{\mathbf{0}}^{(0, \frac{N_2}{N_1}N)}\} \leq U_{\mathbf{0}}^{((N,aN))} \leq U_{\mathbf{0}}^{((N,0))} + U_{\mathbf{0}}^{((0,aN))} \leq 2 \max\{U_{\mathbf{0}}^{((N,0))}, U_{\mathbf{0}}^{(0,aN)}\}$$

Use the result in projection scheme. For $\sigma_2/\sigma_1 \geq 1$, we have

$$\begin{aligned} \mathbb{E} \left[U_{\mathbf{0}}^{((N, \frac{N_2}{N_1}N))} \right] &\geq \max\{\Phi_{\text{lower}}((N_1, 0)), \Phi_{\text{lower}}((0, N_2))\} \\ &\sim \max\{C_{\text{lower},1} N_1^{\sigma_1}, C'_{\text{lower},1} N_2^{\sigma_2 - \gamma_1 (\frac{\sigma_2}{\sigma_1} - 1)}, C'_{\text{lower},1} N_2^{\sigma_1}\} \\ &= \max\{C_{\text{lower},1} (1 + \frac{N_2}{N_1})^{\sigma_1} (N_1 + N_2)^{\sigma_1}, \\ &\quad C'_{\text{lower},1} [(1 + \frac{N_2}{N_1}) / \frac{N_2}{N_1}]^{\sigma_2 - \gamma_1 (\frac{\sigma_2}{\sigma_1} - 1)} (N_1 + N_2)^{\sigma_2 - \gamma_1 (\frac{\sigma_2}{\sigma_1} - 1)}, \\ &\quad C'_{\text{lower},1} [(1 + \frac{N_2}{N_1}) / \frac{N_2}{N_1}]^{\sigma_1} (N_1 + N_2)^{\sigma_1}\} \\ &\geq \min\{C_{\text{lower},1} (1 + \frac{N_2}{N_1})^{\sigma_1}, C'_{\text{lower},1} [(1 + \frac{N_2}{N_1}) / \frac{N_2}{N_1}]^{\sigma_2 - \gamma_1 (\frac{\sigma_2}{\sigma_1} - 1)}, C'_{\text{lower},1} [(1 + \frac{N_2}{N_1}) / \frac{N_2}{N_1}]^{\sigma_1}\} \times \\ &\quad (N_1 + N_2)^{\max\{\sigma_1, \sigma_2 - \gamma_1 (\frac{\sigma_2}{\sigma_1} - 1)\}} \\ &\rightarrow \min\{C_{\text{lower},1} (1 + \rho)^{\sigma_1}, C'_{\text{lower},1} [(1 + \rho) / \rho]^{\sigma_2 - \gamma_1 (\frac{\sigma_2}{\sigma_1} - 1)}, C'_{\text{lower},1} [(1 + \rho) / \rho]^{\sigma_1}\} \times \\ &\quad (N_1 + N_2)^{\max\{\sigma_1, \sigma_2 - \gamma_1 (\frac{\sigma_2}{\sigma_1} - 1)\}} \end{aligned}$$

For $\sigma_2/\sigma_1 \leq 1$, we have

$$\begin{aligned}
\mathbb{E} \left[U_{\mathbf{0}}^{((N, \frac{N_2}{N_1} N))} \right] &\geq \max\{\Phi_{\text{lower}}((N_1, 0)), \Phi_{\text{lower}}((0, N_2))\} \\
&\sim \max\{C''_{\text{lower},2} N_1^{\sigma_2}, C_{\text{lower},2} N_2^{\sigma_2}, C'_{\text{lower},2} N_1^{\sigma_2}\} \\
&= \max\{C''_{\text{lower},2} (1 + \frac{N_2}{N_1})^{\sigma_2} (N_1 + N_2)^{\sigma_2}, \\
&\quad C_{\text{lower},2} [(1 + \frac{N_2}{N_1}) / \frac{N_2}{N_1}]^{\sigma_2} (N_1 + N_2)^{\sigma_2}, \\
&\quad C'_{\text{lower},2} (1 + \frac{N_2}{N_1})^{\sigma_1 - \gamma_2 (\frac{\sigma_1}{\sigma_2} - 1)} (N_1 + N_2)^{\sigma_1 - \gamma_2 (\frac{\sigma_1}{\sigma_2} - 1)}\} \\
&\geq \min\{C''_{\text{lower},2} (1 + \frac{N_2}{N_1})^{\sigma_2}, C_{\text{lower},2} [(1 + \frac{N_2}{N_1}) / \frac{N_2}{N_1}]^{\sigma_2}, C'_{\text{lower},2} (1 + \frac{N_2}{N_1})^{\sigma_1 - \gamma_2 (\frac{\sigma_1}{\sigma_2} - 1)}\} \times \\
&\quad (N_1 + N_2)^{\max\{\sigma_2, \sigma_1 - \gamma_2 (\frac{\sigma_1}{\sigma_2} - 1)\}} \\
&\rightarrow \min\{C''_{\text{lower},2} (1 + \rho)^{\sigma_2}, C_{\text{lower},2} [(1 + \rho) / \rho]^{\sigma_2}, C'_{\text{lower},2} (1 + \rho)^{\sigma_1 - \gamma_2 (\frac{\sigma_1}{\sigma_2} - 1)}\} \times \\
&\quad (N_1 + N_2)^{\max\{\sigma_2, \sigma_1 - \gamma_2 (\frac{\sigma_1}{\sigma_2} - 1)\}}
\end{aligned}$$

Now we can have the upper bound, for any $\delta > 0$, we have

$$\begin{aligned}
\mathbb{E} \left[U_{\mathbf{0}}^{((N, \frac{N_2}{N_1} N))} \right] &\leq 2 \max\{\Phi_{\text{upper}}((N_1, 0)), \Phi_{\text{lower}}((0, N_2))\} \\
&\sim 2 \max\{C_{\text{upper},1,\delta} N_1^{\sigma_1 + \delta}, C_{\text{upper},2,\delta} N_2^{\sigma_2 + \delta}\} \\
&= 2 \max\{C_{\text{upper},1,\delta} (1 + \frac{N_2}{N_1})^{\sigma_1 + \delta} (N_1 + N_2)^{\sigma_1 + \delta}, C_{\text{upper},2,\delta} [(1 + \frac{N_2}{N_1}) / \frac{N_2}{N_1}]^{\sigma_2 + \delta} (N_1 + N_2)^{\sigma_2 + \delta}\} \\
&\leq 2 \max\{C_{\text{upper},1,\delta} (1 + \frac{N_2}{N_1})^{\sigma_1 + \delta}, C_{\text{upper},2,\delta} [(1 + \frac{N_2}{N_1}) / \frac{N_2}{N_1}]^{\sigma_2 + \delta}\} (N_1 + N_2)^{\max\{\sigma_1, \sigma_2\} + \delta} \\
&\rightarrow 2 \max\{C_{\text{upper},1,\delta} (1 + \rho)^{\sigma_1 + \delta}, C_{\text{upper},2,\delta} [(1 + \rho) / \rho]^{\sigma_2 + \delta}\} (N_1 + N_2)^{\max\{\sigma_1, \sigma_2\} + \delta}
\end{aligned}$$

Law of large number results are established by same method of [Broderick et al. \(2012\)](#) and [Gnedin et al. \(2007\)](#), by applying the large deviation bounds in [Freedman \(1973, pp.911, Theorem 4\)](#), i.e., we have for any $\epsilon > 0$, there exists an ϵ' only depends on ϵ and some c such

that

$$P \left(\left| \frac{U_{\mathbf{0}}^{((N, \frac{N_2}{N_1} N))}}{\mathbb{E} \left[U_{\mathbf{0}}^{((N, \frac{N_2}{N_1} N))} \right]} - 1 \right| \geq \epsilon \right) < c e^{-\epsilon' \mathbb{E} \left[U_{\mathbf{0}}^{((N, \frac{N_2}{N_1} N))} \right]}$$

Using the derived upper bound on $\mathbb{E} \left[U_{\mathbf{0}}^{((N, \frac{N_2}{N_1} N))} \right]$, the right hand side is summable, thus by Borrel Cantelli we have $U_{\mathbf{0}}^{((N, \frac{N_2}{N_1} N))} \sim \mathbb{E} \left[U_{\mathbf{0}}^{((N, \frac{N_2}{N_1} N))} \right]$ a.s..

□

H.3 Power law bounds when $\sigma_1 = \sigma_2 = \sigma$

We give proof of Corollary 2 when $\sigma_1 = \sigma_2 = \sigma$.

Proof. We use the same bound from proportional scheme with $\sigma_1 = \sigma_2 = \sigma$

$$\max\{\mathbb{E}U_{\mathbf{0}}^{(N_1,0)}, \mathbb{E}U_{\mathbf{0}}^{(0,N_2)}\} \leq \mathbb{E}U_{\mathbf{0}}^{(N_1,N_2)} \leq \mathbb{E}U_{\mathbf{0}}^{(N_1,0)} + \mathbb{E}U_{\mathbf{0}}^{(0,N_2)} \leq 2 \max\{\mathbb{E}U_{\mathbf{0}}^{(N_1,0)}, \mathbb{E}U_{\mathbf{0}}^{(0,N_2)}\}$$

We can lower bound the left hand side, with any $\min\{\gamma_1, \gamma_2\} > \delta > 0$ by

$$\begin{aligned} \max\{\mathbb{E}U_{\mathbf{0}}^{(N_1,0)}, \mathbb{E}U_{\mathbf{0}}^{(0,N_2)}\} &\geq \max\{C_{\text{lower},1} N_1^\sigma, C'_{\text{lower},1} N_2^\sigma\} \\ &\geq \min\{C_{\text{lower},1}, C'_{\text{lower},1}\} \max\{N_1, N_2\}^\sigma \\ &\geq 2^{-\sigma} \min\{C_{\text{lower},1}, C'_{\text{lower},1}\} (N_1 + N_2)^\sigma \end{aligned}$$

And the right hand side can be upper bounded in a similar manner, for any $\delta > 0$:

$$\begin{aligned} 2 \max\{\mathbb{E}U_{\mathbf{0}}^{(N_1,0)}, \mathbb{E}U_{\mathbf{0}}^{(0,N_2)}\} &\leq 2 \max\{C_{\text{upper},1,\delta}, C_{\text{upper},2,\delta}\} \max\{N_1, N_2\}^\sigma \\ &\leq 2 \max\{C_{\text{upper},1,\delta}, C_{\text{upper},2,\delta}\} (N_1 + N_2)^{\sigma+\delta} \end{aligned}$$

□

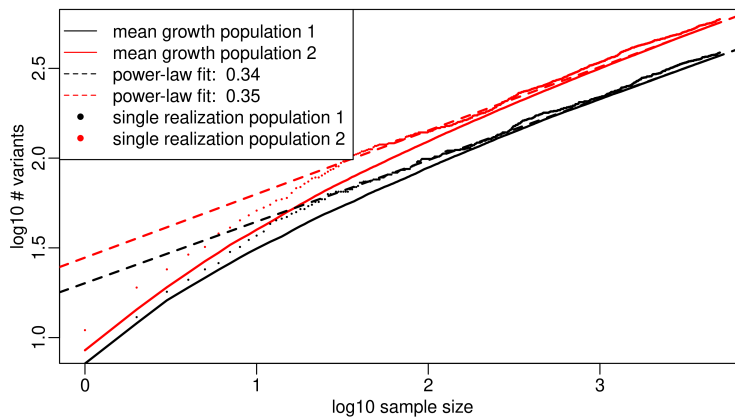


Figure S19: Simulated sampling curve with $\alpha = 10, \sigma_1 = 0.3, \sigma_2 = 0.6, c_1 = c_2 = 1, \gamma_1 = \gamma_2 = 0.5$ in the projection scheme, i.e. sampling population 1 or population 2 only. The mean growth curves (shown in lines) were calculated using 100 independent realizations and a single realization is shown as dots. The bound for population 2 is 0.3 and 0.6 and the predicted power law rate for population 1 is 0.3. We fit the line using the last 1/3 of the mean growth curve. The fitted powerlaw align well with our theoretical prediction.